THE JOURNAL of the Acoustical Society of America

VOL. 11 NO. 2

Physics Library
QC
1
.A185
VOL. 11
NO. 2

OCTOBER, 1939

Published for the

ACOUSTICAL SOCIETY OF AMERICA

by the

AMERICAN INSTITUTE OF PHYSICS
Incorporated

LANCASTER, PA., AND NEW YORK, N. Y.

ACOUSTICAL SOCIETY OF AMERICA

FOUNDED 1929

OFFICERS

F. R. WATSON, *President*
University of Illinois
Urbana, Illinois

WALLACE WATERFALL, *Secretary*
The Celotex Corporation
Chicago, Illinois

F. A. FIRESTONE, *Vice President*
University of Michigan
Ann Arbor, Michigan

G. T. STANTON, *Treasurer*
Electrical Research Products, Inc.
New York, New York

F. A. FIRESTONE, *Editor*
University of Michigan
Ann Arbor, Michigan

EXECUTIVE COUNCIL

FREDERICK V. HUNT
Harvard University
Cambridge, Massachusetts

H. F. OLSON
R.C.A. Victor Company, Inc.
Camden, New Jersey

D. A. LAIRD
Colgate University
Hamilton, New York

L. J. SIVIAN
Bell Telephone Laboratories, Inc.
New York, New York

DON LEWIS
University of Iowa
Iowa City, Iowa

W. F. SNYDER
National Bureau of Standards
Washington, D. C.

The officers are also members of the Executive Council

EDITORIAL BOARD

F. A. FIRESTONE, *Editor*

JOHN S. PARKINSON
WALLACE WATERFALL

E. C. WENTE

IRVING WOLFF
F. R. WATSON, *Ex officio*

Manuscripts for publication should be submitted to F. A. Firestone, 147 East Physics Building, University of Michigan, Ann Arbor, Michigan.

Proof and all correspondence concerning papers in the process of publication should be addressed to the Publications Manager, American Institute of Physics, 175 Fifth Avenue, New York, New York.

Subscription price to members $4 per year. To non-members: Domestic rate $6 per year; Foreign rate $6.60 per year.

Changes of address and complaints of failure to receive the Journal should be addressed to the Publications Manager. New copies can be sent free only if notice of non-delivery is received within three months of date of issue.

The Journal of the Acoustical Society of America is published quarterly at Prince and Lemon Streets, Lancaster, Pennsylvania.

Entered as second-class matter at the Post Office at Lancaster, Pennsylvania.

Copyright, 1939, by the Acoustical Society of America.

THE JOURNAL of the Acoustical Society of America

• CONTENTS •

Remaking Speech	HOMER DUDLEY	169
Filtration of Oblique Elastic Waves in Stratified Media	R. B. LINDSAY	178
Normal Modes of Vibration in Room Acoustics: Experimental Investigations in Nonrectangular Enclosures	RICHARD H. BOLT	184
Effect of Rotatory and Lateral Inertia on Flexural Vibration of Prismatic Bars	WILLIAM T. THOMSON	198
Transmission of Sound Inside Pipes	PHILIP M. MORSE	205
Sound Insulation Characteristics for Ideal Partitions	KERON C. MORRICAL	211
Design for a Keyboard Instrument in Just Intonation	CHAS. WILLIAMSON	216
Sound Source for Investigating Microphone Distortion	WILLIAM D. PHELPS	219
Microphone Efficiency: A Discussion and Proposed Definition	FRANK MASSA	222
Degenerative Sound Analyzer	H. H. SCOTT	225
Propagation of Shock Waves in Air. I	L. THOMPSON AND N. RIFFOLT	233
Propagation of Shock Waves in Air. II	L. THOMPSON	245
News of the Society		254
Book Reviews		255
Current Publications on Acoustics		257
References to Contemporary Papers on Acoustics		263

Vol. 11 OCTOBER, 1939 No. 2

Physics
Physics-LSA
Anaheim
10-22-62
Repl.

THE JOURNAL
OF THE
ACOUSTICAL SOCIETY OF AMERICA

Volume 11 Number 2

OCTOBER • 1939

Remaking Speech

HOMER DUDLEY
Bell Telephone Laboratories, New York, New York

(Received July 28, 1939)

Speech has been remade automatically from a buzzer-like tone and a hiss-like noise corresponding to the cord-tone and the breath-tone of normal speech. Control of pitch and spectrum obtained from a talker's speech are applied to make the synthetic speech copy the original speech sufficiently for good intelligibility although the currents used in such controls contain only low syllabic frequencies of the order of 10 cycles per second as contrasted with frequencies of 100 to 3000 cycles in the remade speech. The isolation of these speech-defining signals of pitch and spectrum makes it possible to reconstruct the speech to a wide variety of specifications. Striking demonstrations upon altering the pitch of the remade speech stress the contribution of the pitch to the emotional content of speech. Similarly the spectrum is shown to contribute most of the intelligibility to the speech.

INTRODUCTION

SPEECH has been remade, as shown in the oscillograms of Fig. 1 for the words "Showing speech remade," by analyzing a talker's speech for the fundamental speech information and then using this information to remake the speech with a synthesizing device, the entire process being carried out automatically and almost instantaneously by electrical circuits.[1] The apparatus used has been called a "vocoder" because it operates on the principle of coding the voice and then reconstructing the voice in accordance with this code. The process consists of a speech analysis followed by a speech synthesis and these have separately been subjects of study by many workers[2] in a wide variety of fields; for example, philologists, phoneticians, linguists, elocutionists, psychologists, physiologists, laryngologists, physicists, communication engineers, etc.

[1] U. S. Patent 2,151,091.

GENERAL PLAN FOR REMAKING SPEECH

A portable form of the vocoder is pictured in Fig. 2. The underlying plan followed in the design of this equipment was that of building an

[2] The list of publications on speech analysis is so large that no attempt has been made to provide references. Serious attempts at speech synthesis started with von Kempelen's manually operated speaking machine which he described in his book published in 1791. The generation of vowel sounds has been studied by Willis, Wheatstone, Helmholtz, Scripture and many others. Stewart (Nature, Sept. 2, 1922) built a dial-controlled electrical synthesizer of simple speech sounds; this type of circuit was demonstrated publicly by Fletcher in February, 1924.

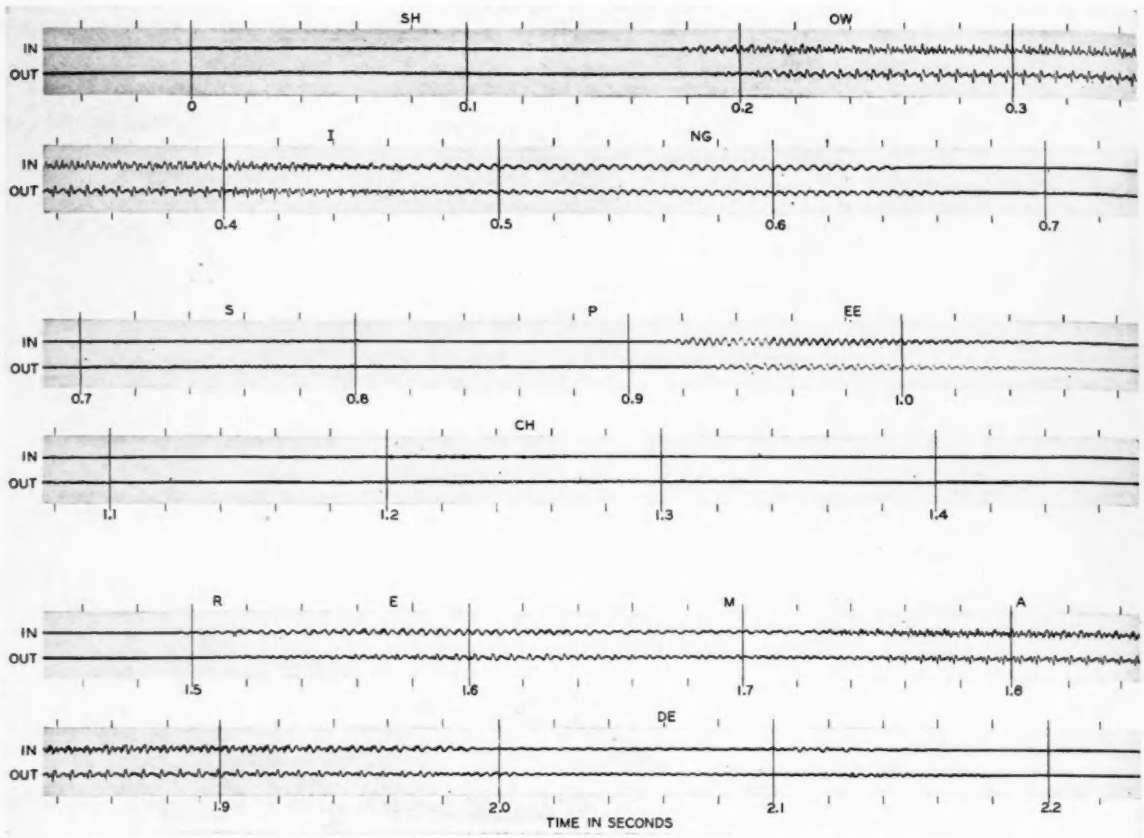

FIG. 1. Oscillogram of original and remade speech.

electrical synthesizing circuit that would be a reasonably good analogue of the vocal system and then providing the necessary controls for operating this synthesizer by currents obtained from the analysis of a talker's speech. This plan is expressed in general circuit terms in Fig. 3 where the synthesizer at the right provides the synthetic vocal system for remaking speech under the control of the analyzer of the original speech shown at the left. Not only can the speech be remade to simulate the original but it can be changed from the original in a variety of ways since there is experimental control of the fundamental parameters between the analyzing and the synthesizing processes.

In the synthesizer two streams of sound are employed as shown in Fig. 3. The properly controlled variations of these two streams of sound produce the intelligible synthetic speech. Such speech when formed from the first sound stream is characterized by three properties: it has a pitch determined by the fundamental frequency of vibration; it has an intensity determined by the total sound power; and it has a spectrum that gives the speech quality and is determined by the relative amount of sound power in various fixed frequency bands. Synthetic speech formed from the second sound stream is characterized by these three properties: it has essentially random frequency components with no true pitch (zero pitch); it has an intensity determined by the total sound power and a spectrum determined by the relative power in fixed frequency bands. Although human speech has sounds corresponding to the presence of both sound streams at the same instant, vocoder tests indicated that a provision for the mixture of sound streams was not necessary for intelligible synthetic speech, so no such provision was made.

The complete formation of synthetic speech then requires control of the three speech properties, pitch, spectrum and intensity, as well as a

FIG. 2. Photograph of the portable circuit for remaking speech with Mr. Vadersen talking into the microphone.

means for switching from one sound stream to the other. Actually as shown in Fig. 3 only the pitch and spectrum controls are provided. The intensity control is obtained by making the spectrum control on an absolute power basis rather than a relative power basis while the selection of sound stream is made by the pitch control. When zero pitch is observed by the analyzer the sound stream connected in circuit in the synthesizer is the second one which will hereafter be referred to briefly as the "hiss" from the nature of its random noise. However, when a voiced sound is analyzed the pitch control sets up a current proportional to the pitch (pitch is used in this paper as synonymous with fundamental frequency for a periodic sound). This pitch-proportional current serves two purposes in the synthesizer as shown in Fig. 3: first, it switches from the hiss sound stream to the first sound stream which will hereafter be referred to simply as a buzz because it sounds like the tone from a buzzer; second, it adjusts the pitch of the buzz to the proper frequency. It is seen then that the pitch and spectrum analysis of the original speech suffices to insure that the remade speech shall have the proper pitch, spectrum and intensity and to a fair approximation the proper sound stream.

The more detailed circuit discussion will proceed by taking up the pitch control branch in both the analyzer and synthesizer before proceeding to the spectrum control branch.

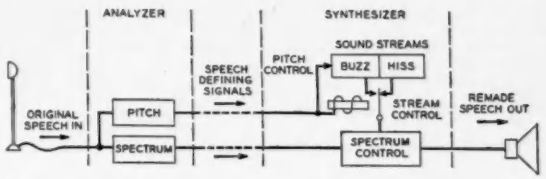

FIG. 3. Plan of the circuit for remaking speech.

PITCH CONTROL

There is shown in detail in Fig. 4 the pitch control branch of the circuit of Fig. 3, starting at the pick-up from the original speech and terminating with the output sound stream as selected

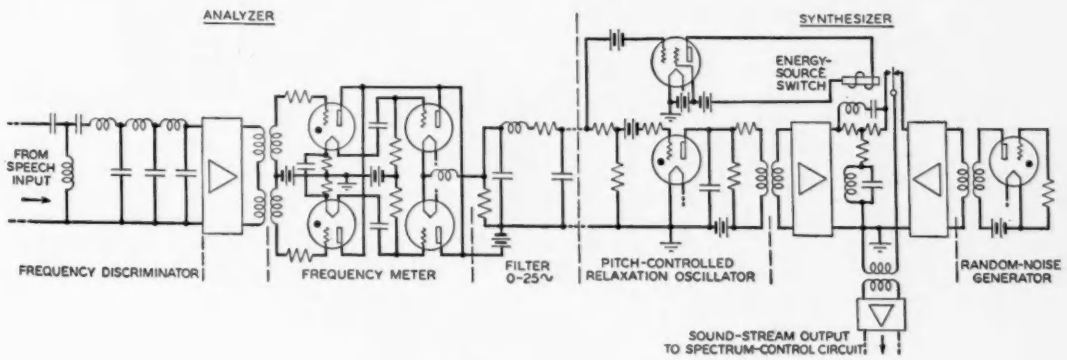

FIG. 4. Pitch control circuit.

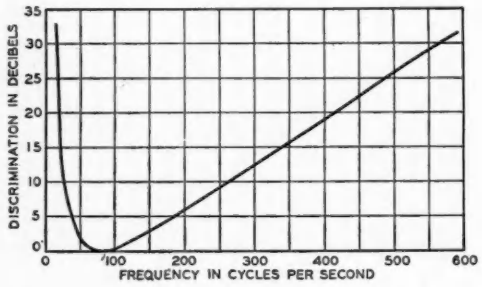

FIG. 5. Transmission characteristic of frequency discriminator.

by the selecting switch of the synthesizer. The pitch analysis consists in obtaining the fundamental frequency of the voice in reasonably pure form and then measuring it with a frequency meter.

The purification of the fundamental frequency results from a frequency discriminator which cuts out both the higher frequencies of the voice and the very low frequencies, particularly as the frequency becomes less than 50 cycles so as to eliminate certain puffs from the voice which are of large enough power to be troublesome in pitch analysis. The loss at the higher frequencies is made sufficiently sharp to insure that the fundamental frequency itself will get through much the strongest of any component and so be in reasonably pure form. The transmission characteristic of the frequency discriminator is shown in Fig. 5.

The reasonably pure fundamental frequency obtained from the frequency discriminator is applied next to a frequency meter circuit, which is essentially a gas-tube pulsing circuit developed by Hull.[3] This circuit sets up a fairly uniform pulse each time the current swings to a sufficiently

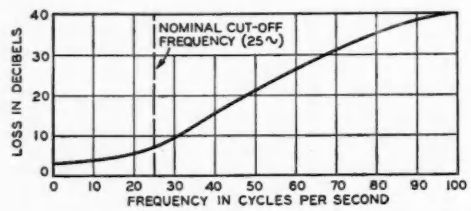

FIG. 6. Loss characteristic of low-pass filter.

[3] Gen. Elec. Rev. **32**, 397 (1929); Physics **4**, 75 (1933). Mr. R. R. Riesz is responsible for the modification of this circuit to fit in well with the speech analysis. He also is responsible in large part for the development of the gas-tube energy sources for the buzz and hiss to be described later.

positive or negative value. Accordingly, if a pure frequency is applied two pulses are set up for each cycle. The circuit itself acts as a full wave rectifier of these pulses. The result is a number of pulses per second proportional to the frequency measured. If the upper harmonics of the voice are not sufficiently eliminated by the discriminator then more than two pulses are received per cycle of fundamental frequency giving the effect of increased pitch. When this happens occasionally, the circuit swings from normal pitch measurement to an apparently higher frequency pitch measurement leading to an unpleasant raucousness in the remade speech.

The output pulses from the frequency meter are next passed through a 25-cycle low-pass filter with the loss characteristic shown in Fig. 6. This low-pass filter serves to eliminate all the

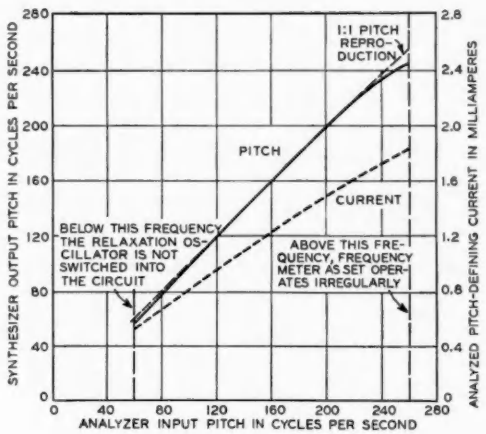

FIG. 7. Pitch relations in circuit for remaking speech.

original frequencies of the voice but to pass a current proportional to the number of pulses received and therefore approximately proportional to the original fundamental frequency. At the output of the low-pass filter, then, there is a pitch-defining current, thus completing the pitch analysis.

The more or less pitch-proportional current from the analyzer is passed to the synthesizer where a division of circuit provides two controls from this single pitch-measuring current. On the one hand, a portion of the pitch-measuring current passes through the biasing resistance of the relaxation oscillator. For a 1 : 1 pitch of the remade speech as compared to the original speech

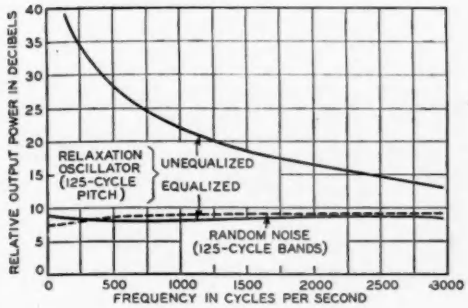

FIG. 8. Energy source output characteristics.

this relaxation oscillator is set so that the frequency of the relaxation pulses is proportional to the biasing current. In this way, the pitch-defining signal controls the pitch of the buzz set up for the voiced sounds. The pitch relations for the entire process of remaking speech of the same pitch are plotted in Fig. 7 which gives the pitch-defining current from the analyzer and the pitch of the remade speech from the synthesizer as a function of the pitch of the original speech signal.

The rest of the pitch control current in the synthesizer goes to a relay to select which sound stream, buzz or hiss, is to be used at the moment. The control here is very simple. When no pitch signal is received the hiss is connected to the output circuit. This condition is important because the hiss is less noticeable than is the buzz noise with its decided pattern. Accordingly, the use of the hiss for the silent intervals means that the amount of sound that does come out of the synthesizer due to slight leaks in the control circuit is not very noticeable. It should be mentioned, in passing, that the synthesizing circuit depends on the spectrum control to obtain zero output for the quiet intervals. The unvoiced sounds of normal speech and all whispered speech are made from the hiss, while the voiced sounds are made from the buzz. The energy output from each source is shown in Fig. 8. The top solid line is for the relaxation oscillator output as generated. The lower solid line shows how this output is equalized to be essentially flat with frequency. The dotted curve shows the hiss output plotted in terms of power in 125-cycle bands, 125 cycles being the frequency used for the pitch when measuring the relaxation oscillator output. The curves are plotted only to 3000 cycles as this frequency is the top limit of this model of the analyzer and the synthesizer, a limit chosen as representative of commercial telephone circuits.

SPECTRUM CONTROL

There is shown in detail in Fig. 9 a typical spectrum control branch of the circuit of Fig. 3 from the input speech to the remade speech with the side connection for the sound stream supplied to the synthesizer. The spectrum is measured electrically in the analyzer and the resulting spectrum-defining currents are then passed to the synthesizer where they control the amount of power at the different frequencies to be used from the energy source for remaking the speech. Since the power of the voice falls off considerably at higher frequencies, particularly in the case of the

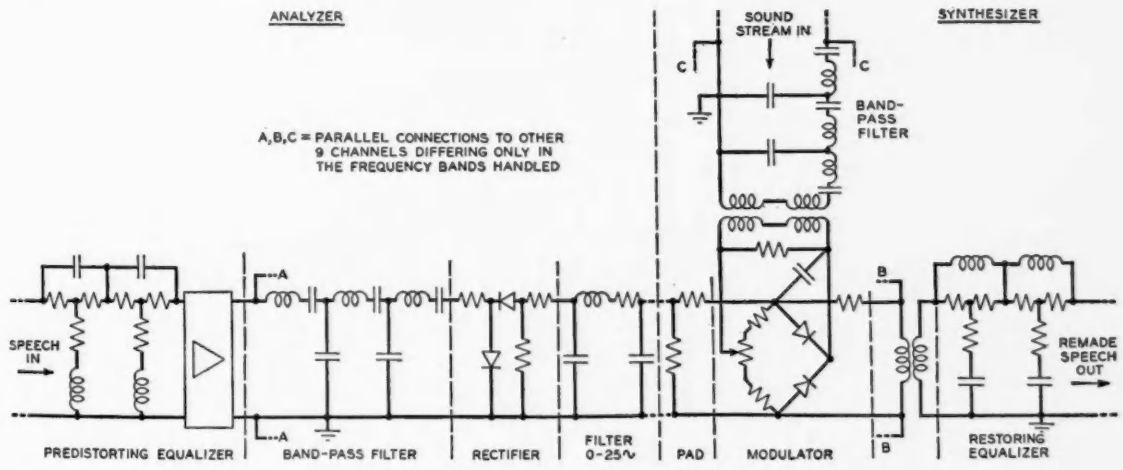

FIG. 9. Spectrum control circuit.

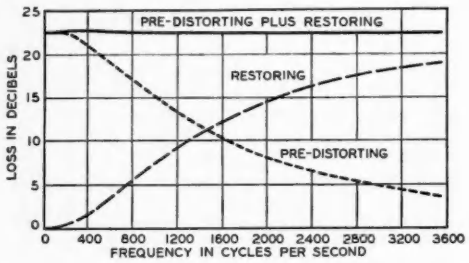

FIG. 10. Transmission characteristics of pre-distorting and restoring equalizers.

voiced sounds which contribute most of the energy to speech, the circuit is made to work more efficiently by inserting, as shown in Fig. 9, a pre-distorting equalizer at the beginning of the analyzer with a corresponding restoring equalizer after the synthesizer. Fig. 10 indicates that the losses of these equalizers are complementary, giving no net distortion in the over-all circuit.

After the pre-distorting equalizer, the spectrum analysis begins with the separation of the original speech power into frequency bands, the lowest choosing frequencies below 250 cycles and the other nine, 300-cycle bands extending to 2950 cycles, a top figure typical of commercial telephone circuits as stated.

A representative spectrum control channel is shown in Fig. 9. The other nine spectrum control channels are paralleled with this channel. The power selected by the transmitting band filter is rectified to obtain a measure thereof and the resulting current passed through a 25-cycle low-pass filter similar to the one provided in the pitch control circuit (see Fig. 4).

The current so obtained is passed on to the synthesizer where it acts upon a balanced modulator at the other input terminals of which a constant level of power in the same frequency range is supplied from the synthesizer energy sources. Such power finds the copper oxide modulator in a condition of balance and so is not passed on to the output circuit, except to the extent the modulator is unbalanced by the currents received from this spectrum control circuit. When, as shown, a receiving band filter is not used, it is necessary to use a modulator of the perfect product type to prevent setting up troublesome distortion frequencies. The input-output relations in the typical spectrum channel are shown in Fig. 11. Against analyzer input there is plotted the output from the analyzer and from the synthesizer as determined by measurements with a single frequency input.

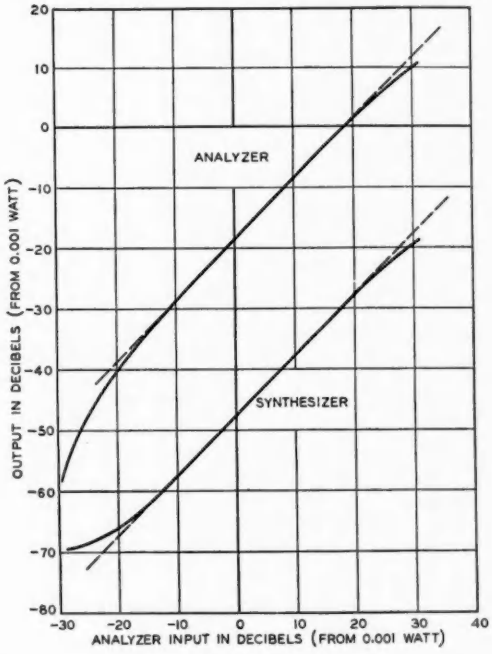

FIG. 11. Operating characteristics of a typical spectrum control circuit.

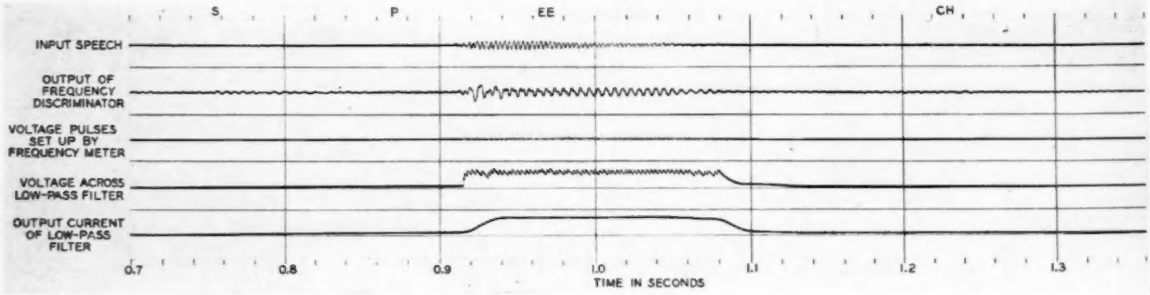
S P EE CH
INPUT SPEECH
OUTPUT OF FREQUENCY DISCRIMINATOR
VOLTAGE PULSES SET UP BY FREQUENCY METER
VOLTAGE ACROSS LOW-PASS FILTER
OUTPUT CURRENT OF LOW-PASS FILTER
0.7 0.8 0.9 1.0 1.1 1.2 1.3
TIME IN SECONDS

FIG. 12. Oscillograms showing the steps in pitch analysis for the word "speech."

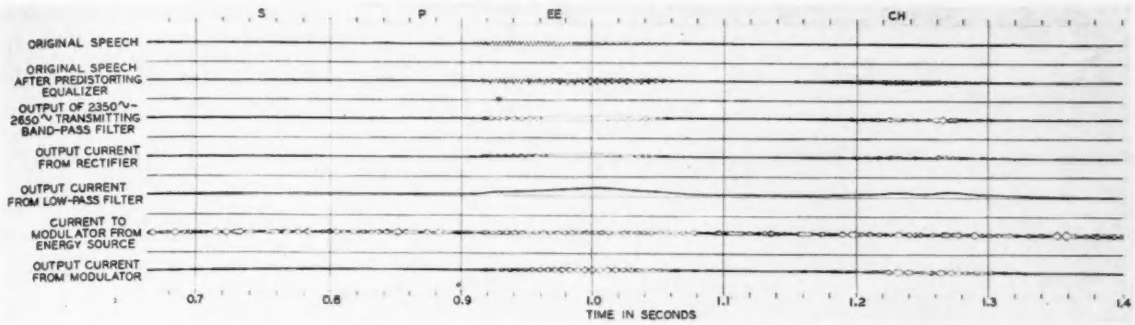

FIG. 13. Oscillograms showing the steps in spectrum control for the word "speech."

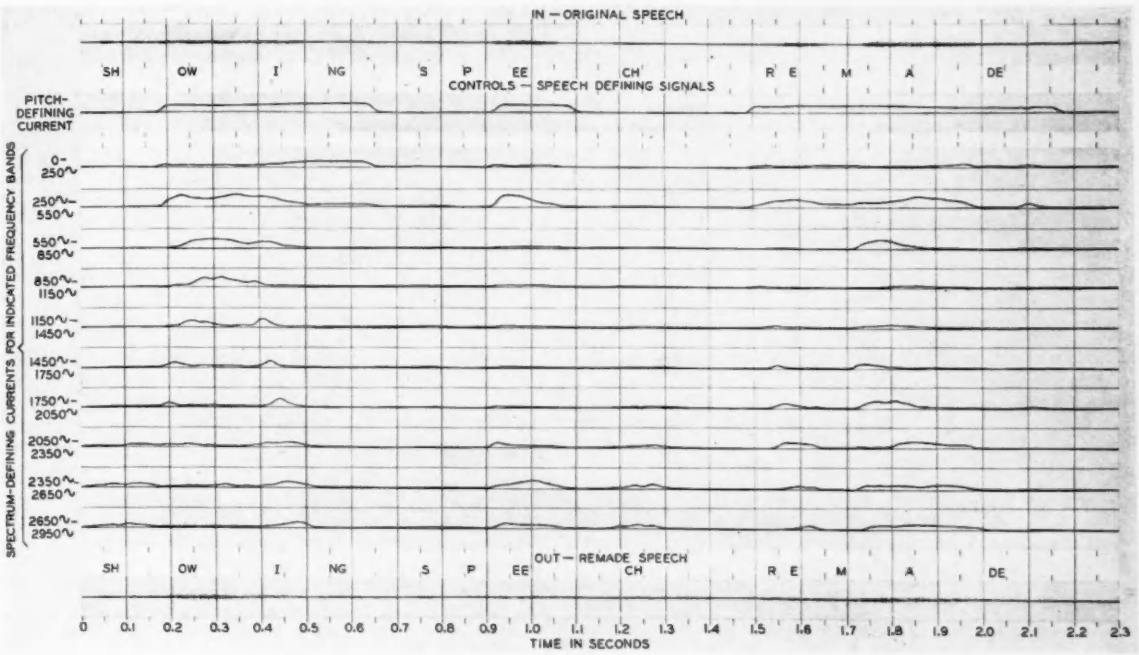
IN — ORIGINAL SPEECH
SH OW I NG S P EE CH R E M A DE
CONTROLS — SPEECH DEFINING SIGNALS
PITCH-DEFINING CURRENT
SPECTRUM-DEFINING CURRENTS FOR INDICATED FREQUENCY BANDS
0-250~
250~-550~
550~-850~
850~-1150~
1150~-1450~
1450~-1750~
1750~-2050~
2050~-2350~
2350~-2650~
2650~-2950~
OUT — REMADE SPEECH
SH OW I NG S P EE CH R E M A DE
0 0.1 0.2 0.3 0.4 0.5 0.6 0.7 0.8 0.9 1.0 1.1 1.2 1.3 1.4 1.5 1.6 1.7 1.8 1.9 2.0 2.1 2.2 2.3
TIME IN SECONDS

FIG. 14. Oscillogram of the speech defining signals for the words "showing speech remade." The original and remade speech are shown in greater detail in Fig. 1.

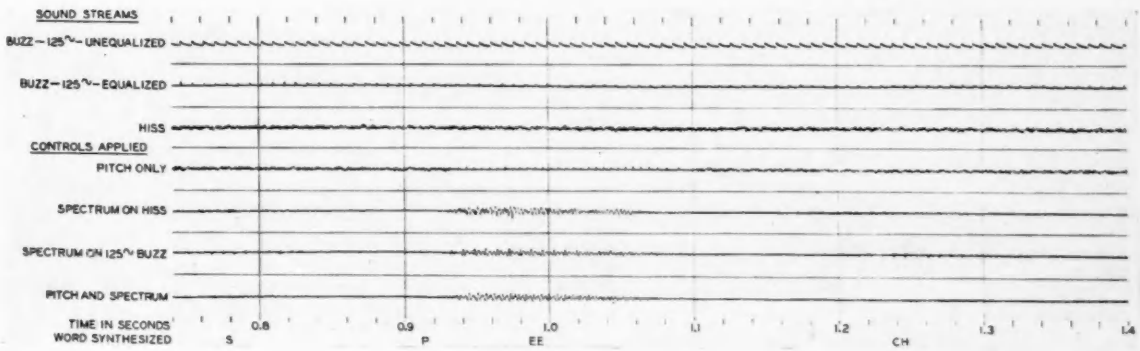

FIG. 15. Oscillograms of the steps in speech synthesizing for the word "speech."

Oscillograms Showing Circuit Operation

It is interesting to look at a number of oscillograms showing how the various parts of the circuit function. These oscillograms must not be interpreted too closely for the ear does not observe phase shift *per se*, while to the eye phase shift appears as an important change in amplitude with time. If this is kept in mind, however, the oscillograms do present an illuminating picture of the operation of the circuit. All these oscillograms as well as that of Fig. 1 were made from a single recording of the words "Showing speech remade" on a high quality magnetic tape recorder. While this recorded speech is not handled as well by the vocoder as is direct microphone pick-up of original speech, it was nevertheless used because in this way the reader can compare the oscillograms of Figs. 1, 12, 13, 14 and 15 point by point. To assist this comparison the same timing scale is used in all the figures. There was some difficulty in making the oscillograph run at a uniform rate. However, by retaking the trace enough times the deviations in the final mounted oscillograms were kept within ± 0.005 second.

The set of oscillograms in Fig. 12 is for the steps in the pitch analysis of the word "speech." The first trace gives the input speech wave. The second trace gives the output of the fundamental frequency discriminator to indicate how pure a wave form is obtained. The third trace shows the voltage pulses from the frequency meter while the fourth trace gives the resulting voltage across the low-pass filter indicating the storage effect of the large condensers in this filter. The last trace shows the syllabic current output from the low-pass filter indicating how the pitch is actually measured as can be seen by comparing with the second trace. The entire absence of original audible speech components from this last trace is readily apparent.

The spectrum control process is similarly shown in Fig. 13 for the same word "speech." The first trace shows the input speech wave and the second trace shows the speech wave after passing through the pre-distorting equalizer. The third trace shows the output of the transmitting band filter for a typical channel (2350–2650 cycles) from which the variations in level from instant to instant can be seen for this word. The fourth trace shows the output current from the rectifier with its uni-directional pulses. The fifth trace shows the current output of the low-pass filter varying at a syllabic rate with none of the original speech frequencies present and yet giving a complete definition of the amount of power in the third trace. It is only this syllabic current that is sent down the line to set up at the receiving end a current approximately like that shown in the third trace. The last two traces show the currents from the synthesizer energy sources before and after the modulator. The current before the modulator shows the effect of the change in pitch which has been controlled by the pitch channel while the last trace shows, in addition to this, the amplitude control obtained from this spectrum channel.

The two sets of oscillograms in Figs. 12 and 13 show the speech remaking from source to loudspeaker. It is also interesting to examine the currents obtained from the analyzer at its output and so the synthesizer input and the currents indicating the synthesizing steps.

In Fig. 14 there is shown the set of speech-defining signals for the whole phrase "Showing speech remade." The timing, as stated before, is such that reference can be made to Fig. 1 as well as to the single word shown in the oscillograms of Figs. 12 and 13. The interesting thing about these speech-defining signals is that they contain all of the speech information although they themselves vary at slow rates. In this way, they are equivalent to lip and other motions, that is, they are the parametric equivalents of such syllabic motions which contain the real speech message that is impressed upon the cord tone and the breath tone as carriers.[4]

The various synthesizing steps are shown by the oscillograms in Fig. 15. The first three traces give energy source characteristics, the first one being a 125-cycle buzz unequalized, the second the 125-cycle buzz equalized and the third, the

[4] In transmission engineering parlance the two streams of sound may be regarded as carriers (complex multi-frequency carriers), and the slow variations as signals. These signals have been impressed on the voiced carrier by both frequency modulation (pitch change) and selective amplitude modulation and on the unvoiced carrier by selective amplitude modulation. The analyzing process demodulates the inaudible signals from the audible carriers in the speech and the synthesizing process uses them in turn to modulate independently generated carriers.

hiss. The other four traces show the effect of applying the pitch and amplitude controls automatically when the word "speech" from the tape record is applied to the analyzer. The first of these later traces shows the pitch control only applied. The next trace, No. 5, shows the effect of applying the amplitude control to the hiss whereas No. 6 shows the effect of applying it to the 125-cycle buzz. Finally, the last trace shows the effect of applying simultaneously the pitch and selective amplitude controls. The entire set of 10 spectrum controls furnish the final selective amplitude control, of course.

With this description of what happens in the circuit, Fig. 1 will be examined in greater detail. It is seen that the remade speech has a delay of about 18 milliseconds as compared to the original speech. It is seen also that the damping factors in the original speech periods of around 0.01 second are not present in the remade speech. This is natural because the remade speech tends to have more nearly random phases of its component frequencies and not such as would show damping. In terms of phasing, damping means that the high amplitudes of the various components occur more or less simultaneously. In the remade speech something of this sort happens when the buzz wave is set up. However, it tends to disappear rapidly thereafter because of the filter and modulating processes, in the same way as normal speech waves, when sent over a distorting circuit such as a telephone line, will soon lose their appearance of damped characteristic within the periods. Other operating features, such as switching from one source to the other, the handling of stop consonants, etc., can be seen in Fig. 1 and so do not require any comment here.

Conclusion

This equipment for remaking speech has value for speech study. This can be shown more easily by demonstrating it to the ear than by writing a description for the eye to read. The information from the analyzer can be presented satisfactorily graphically as in Fig. 14 but the information from the synthesizer loses much of its message if presented graphically rather than aurally. This applies particularly to the changes in the remade speech as compared to the original speech. Since the fundamental parameters of speech are available for control between the analyzer and the synthesizer the speech may be remade to a great variety of specifications. Important variables in speech are thus isolated so that each can be varied independently for scientific investigation.

Striking demonstrations[5] indicate that the essential contribution to intelligibility comes from the spectrum while the emotional content is due chiefly to the pitch, particularly to the inflection of the pitch. Speech formed from either the hiss alone or the buzz is quite intelligible, the former sounding like a coarse whisper, the latter like a monotone chant. Forming unvoiced sounds from the buzz sound stream does not destroy the intelligibility; neither does forming the voiced sounds from the hiss sound stream. The great value of a good-sized inflection range may be shown either by automatically altering the pitch-range of the talker or by using a hand control to adjust the pitch. The contribution of pitch range may likewise be shown by converting the melody of a song into a monotone. Converting a song into a whisper permits the observer to see how well the spectrum is retained. Similarly normal speech when converted by this device to a whisper, can be more easily examined for differentiation of the phonetic elements particularly such as are found in different sections of the country. The relative contributions of voiced and unvoiced sounds are brought out. A new method is available for studying the nature of tremulous and pulsating effects such as the vibrato, trill, warble, tremolo and quaver, the method being of especial value because it inherently differentiates the pitch variation from the spectrum variation.

An effective tool is presented for checking the resonance theory of vowels and for other sounds as well. A new approach is offered to an understanding of the basic nature of hearing. Above all stress is laid on the basic nature of speech as composed of audible sound streams on which the intelligence content is impressed by modulation processes of the true message-bearing waves which, however, by themselves, are inaudible.

[5] A set of such demonstrations was presented May 16, 1939, at the Tenth Anniversary Meeting of the Acoustical Society of America.

Filtration of Oblique Elastic Waves in Stratified Media

R. B. LINDSAY
Brown University, Providence, Rhode Island

(Received July 14, 1939)

Previous work has been done on the problem of the transmission of plane compressional elastic waves normally through a stratified medium consisting of alternate plane parallel layers of two different substances. Such a structure acts as a low-pass elastic wave filter. The present paper extends the analysis to the case of oblique transmission. This proves to be comparatively simple when the layer substances are both fluid. The transmission and attenuation (i.e., reflection) bands are found to depend on the angle of obliquity in a characteristic way. When one of the layer substances is solid, the problem is more difficult. Account must here be taken of the fact that compressional waves in the fluid layers give rise to both dilatational and shear waves in the solid layers. The result is somewhat more complicated than in the previous case but the structure still turns out to be a low-pass elastic wave filter for angles of obliquity less than the critical angle. As before the transmission and reflection bands are a function of the angle. In the special case in which the thickness of the solid layers is small compared with that of the fluid layers one obtains the elastic wave analog of the Bragg reflection law for x-rays, that is, one gets reflection approximately for the wave-lengths $\lambda_n = 2l/n \cdot \sin\theta$, where l is the distance between successive solid layers and n is integral.

FILTRATION OF OBLIQUE ELASTIC WAVES IN STRATIFIED MEDIA

A PREVIOUS paper[1] discusses the passage of compressional waves through a stratified medium consisting of an infinite set of alternating layers of two different media, solid or fluid, the direction of propagation being assumed to be normal to the layers. It was shown that such a structure acts as a low-pass compressional wave filter. It is the purpose of the present paper to investigate the transmission of *oblique* elastic waves through such a stratified medium.

I. BOTH COMPONENTS FLUID

We first discuss the case in which both media composing the layers are fluid. Fig. 1 represents an infinite series of alternating layers of two different fluid media denoted by I and II, respectively. The layers have thicknesses $2l_1$ and $2l_2$, respectively, and are all taken parallel to the xy plane of a set of rectangular axes with the z axis normal to the interfaces. The mean densities of the media are ρ_1 and ρ_2, respectively, and the compressional wave velocities in them c_1 and c_2, respectively. The mid-points of the layers are indicated by the numbers 1, 2, 3$\cdots$ and quantities taken at the interfaces are indicated by the subscripts 12, 21, 23, 32, $\cdots$ to conform with the notation of the previous paper. A plane harmonic compressional wave is incident at 12 from medium I with the angle of incidence θ_1. The angle of refraction into II is θ_2. We wish to find the conditions for the transmission of this type of wave motion through the structure.

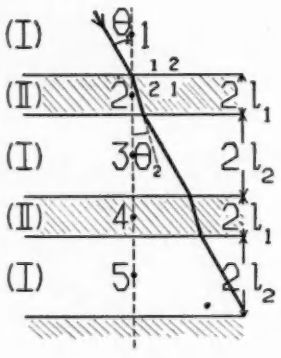

FIG. 1.

Denoting by p the excess pressure and by $\dot{\xi}$ the displacement velocity normal to the interface we can write for any point z in medium I at time t

$$p = \left[p_1 \cos(k_1 z \cos\theta_1) - \frac{i\omega\rho_1}{k_1 \cos\theta_1} \xi_1 \sin(k_1 z \cos\theta_1) \right] e^{i\omega t}, \tag{1}$$

$$\dot{\xi} = \left[\dot{\xi}_1 \cos(k_1 z \cos\theta_1) - \frac{ik_1 \cos\theta_1}{\omega\rho_1} p_1 \sin(k_1 z \cos\theta_1) \right] e^{i\omega t},$$

[1] Lindsay, Lewis and Albright, J. Acous. Soc. Am. 5, 202 (1934).

in which p_1 and $\dot{\xi}_1$ are the excess pressure and velocity, respectively, at point 1 in I. (See Appendix for the derivation of (1).) As usual $k_1=\omega/c_1$.

We introduce the abbreviations

$$k_1 l_1 \cos\theta_1 = Q_1, \quad k_2 l_2 \cos\theta_2 = Q_2, \tag{2}$$

$$\frac{\omega\rho_1}{k_1\cos\theta_1} = Z_1, \quad \frac{\omega\rho_2}{k_2\cos\theta_2} = Z_2. \tag{3}$$

We recall that the law of refraction gives the relation between θ_1 and θ_2, *viz.*, $\sin\theta_1/\sin\theta_2 = c_1/c_2$. Boundary conditions may now be introduced as follows

$$\begin{aligned} p_{12} &= p_1\cos Q_1 - iZ_1\xi_1\sin Q_1 = p_{21}, \\ \dot{\xi}_{12} &= \dot{\xi}_1\cos Q_1 - i/Z_1\cdot p_1\sin Q_1 = \dot{\xi}_{21}, \end{aligned} \tag{4}$$

$$\begin{aligned} p_{23} &= p_{21}\cos 2Q_2 - iZ_2\dot{\xi}_{21}\sin 2Q_2 = p_{32}, \\ \dot{\xi}_{23} &= \dot{\xi}_{21}\cos 2Q_2 - i/Z_2\cdot p_{21}\sin 2Q_2 = \dot{\xi}_{32}, \end{aligned} \tag{5}$$

while

$$\begin{aligned} p_3 &= p_{32}\cos Q_1 - iZ_1\dot{\xi}_{32}\sin Q_1, \\ \dot{\xi}_3 &= \dot{\xi}_{32}\cos Q_1 - i/Z_1\cdot p_{32}\sin Q_1. \end{aligned} \tag{6}$$

By the use of (4), (5) and (6) we can express p_3 and $\dot{\xi}_3$ in terms of p_1 and $\dot{\xi}_1$, the final result being

$$p_3 = Ap_1 - iZ_1B\dot{\xi}_1, \qquad \dot{\xi}_3 = A\dot{\xi}_1 - i/Z_1\cdot Cp_1, \tag{7}$$

where

$$\begin{aligned} A &= \cos 2Q_1\cdot\cos 2Q_2 - \tfrac{1}{2}(Z_2/Z_1 + Z_1/Z_2)\sin 2Q_1\cdot\sin 2Q_2, \\ B &= \sin 2Q_1\cdot\cos 2Q_2 + \sin 2Q_2(Z_2/Z_1\cdot\cos^2 Q_1 - Z_1/Z_2\cdot\sin^2 Q_1), \\ C &= \sin 2Q_1\cdot\cos 2Q_2 + \sin 2Q_2(Z_1/Z_2\cdot\cos^2 Q_1 - Z_2/Z_1\cdot\sin^2 Q_1). \end{aligned} \tag{8}$$

It can now be shown that A, B and C satisfy the relation

$$A^2 + BC = 1. \tag{9}$$

Hence if we set

$$A = \cos W, \tag{10}$$

we shall have $B=(B/C)^{\frac{1}{2}}\cdot\sin W$ and $C=(C/B)^{\frac{1}{2}}\cdot\sin W$.

Equations (7) can now be written in more general form expressing p_{j+2} and $\dot{\xi}_{j+2}$ in terms of p_j and $\dot{\xi}_j$ where j is any integer. Thus

$$\begin{aligned} p_{j+2} &= p_j\cos W - iZ_1(B/C)^{\frac{1}{2}}\cdot\dot{\xi}_j\sin W \\ \dot{\xi}_{j+2} &= \dot{\xi}_j\cos W - i/Z_1\cdot(C/B)^{\frac{1}{2}}p_j\sin W. \end{aligned} \tag{11}$$

Following the method of previous papers,[2] we conclude that the filtration characteristics of the structure under consideration are given by

$$\cos W = \cos 2Q_1\cdot\cos 2Q_2 - \tfrac{1}{2}(Z_2/Z_1 + Z_1/Z_2)\sin 2Q_1\cdot\sin 2Q_2 \tag{12}$$

with transmission for $|\cos W|\leq 1$ and attenuation for $|\cos W|>1$. Examination at once discloses that the stratified medium acts like a low-pass compressional wave filter as in the normal incidence case. However, $\cos W$ now depends on the angle of incidence θ_1 and hence the transmission bands are also a function of θ_1. The situation is depicted graphically in Fig. 2 which shows the plot of $\cos W$ as a function of frequency for the liquids water and ethyl ether for various angles of incidence. In this particular example, $l_1=4$ cm and $l_2=2$ cm. Four curves are plotted, namely for $\theta_1=20°$, 40°, 60° and 75°. The low-pass filtration character of the structure for all angles of obliquity is well brought out. As θ_1 increases the cut-off frequency for the first transmission band increases and the successive transmission and reflection bands are displaced toward higher frequencies. For each angle θ_1 the width of the bands remains approximately constant. Further investigation of (12) indicates that for a particular angle θ_1 increasing the ratio l_1/l_2 decreases the width of both transmission and reflection bands.

II. Fluid—Solid Media

We shall now assume that one of the two materials composing the layers in the stratified medium is solid, while the other is fluid. This considerably complicates the transmission problem for oblique waves, since compressional waves in the fluid will set up both shear and dilatational waves in the solid layers. We here generalize with some modifications a procedure adopted by Reissner[3] in studying the oblique transmission of an elastic wave in a fluid through a single plane parallel solid plate immersed in the fluid.

[2] Cf. reference (1). A general review of acoustic filtration will also be found in J. App. Phys. **9**, 612 (1938). In particular, cf. p. 615.

[3] Reissner, Helv. Phys. Acta, **11**, 140 (1938).

Referring again to Fig. 1, we suppose that the plane compressional wave incident on the interface between fluid and solid gives rise in the solid to: (1) a solid dilatational plane wave with

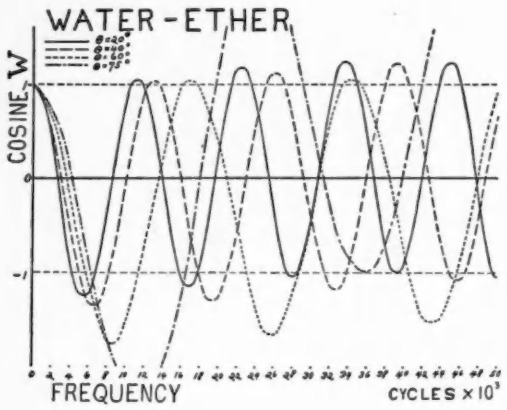

FIG. 2.

velocity c_δ and (2) a shear plane wave with velocity c_s. The angles of refraction for these waves are θ_δ and θ_s, respectively. Snell's law applies to these in the form

$$k_1 \sin\theta_1 = k_\delta \sin\theta_\delta = k_s \sin\theta_s \qquad (13)$$

with, as usual, $k_1=\omega/c_1$, $k_\delta=\omega/c_\delta$, $k_s=\omega/c_s$. If the bulk and shear moduli of the solid are E_s and μ, respectively, and its density is ρ_s we have from ordinary elasticity theory

$$c_\delta=\left(\frac{E_s+4/3\cdot\mu}{\rho_s}\right)^{\frac{1}{2}}, \quad c_s=(\mu/\rho_s)^{\frac{1}{2}}. \qquad (14)$$

Taking the rectangular coordinate axes as indicated in Fig. 1 we denote the component displacements from equilibrium in the solid layer by ξ_s, η_s, ζ_s, respectively. The resultant dilatation is given by

$$\delta_s=\partial\xi_s/\partial x+\partial\eta_s/\partial y+\partial\zeta_s/\partial z. \qquad (15)$$

The shear wave in the solid is characterized by the so-called "rotation" components ω_x, ω_y and ω_z, where

$$\omega_x=\frac{\partial\zeta_s}{\partial y}-\frac{\partial\eta_s}{\partial z}, \quad \omega_y=\frac{\partial\xi_s}{\partial z}-\frac{\partial\zeta_s}{\partial x}, \quad \omega_z=\frac{\partial\eta_s}{\partial x}-\frac{\partial\xi_s}{\partial y}. \qquad (16)$$

These satisfy the wave equation in the form

$$\nabla^2\omega_{x,\,y,\,z}=(\rho_s/\mu)\ddot{\omega}_{x,\,y,\,z}. \qquad (17)$$

Since we are dealing with plane waves, $\eta_s=0$. Moreover, ζ_s and ξ_s are not functions of y. Hence ω_x and ω_z are both zero and only ω_y is nonvanishing. The only nonvanishing shearing stress is

$$X_z=Z_x=\mu(\partial\xi_s/\partial z+\partial\zeta_s/\partial x). \qquad (18)$$

The dilatational or tensile stresses are

$$\begin{aligned} X_x&=(E_s-\tfrac{2}{3}\mu)\delta_s+2\mu\partial\xi_s/\partial x\\ Y_y&=(E_s-\tfrac{2}{3}\mu)\delta_s+2\mu\partial\eta_s/\partial y\\ Z_z&=(E_s-\tfrac{2}{3}\mu)\delta_s+2\mu\partial\zeta_s/\partial z. \end{aligned} \qquad (19)$$

Of these the one of chief interest in the present problem is Z_z.

We shall express the dilatation in the solid by

$$\delta_s=B_1e^{-ik_\delta(x\sin\theta_\delta+z\cos\theta_\delta)}+B_2e^{-ik_\delta(x\sin\theta_\delta-z\cos\theta_\delta)} \qquad (20)$$

while the rotation component ω_y is

$$\omega_y=C_1e^{-ik_s(x\sin\theta_s+z\cos\theta_s)}+C_2e^{-ik_s(x\sin\theta_s-z\cos\theta_s)}. \qquad (21)$$

The trivial time factor $e^{i\omega t}$ is omitted for convenience. From these we must obtain the expressions for ξ_s, ζ_s, Z_x and Z_z from (15), (17), (18) and (19). The combination of (15) and (16) yields

$$\partial^2\zeta_s/\partial x^2+\partial^2\zeta_s/\partial z^2=\partial\delta_s/\partial z-\partial\omega_y/\partial x, \qquad (22)$$

whence by substituting (20) and (21) and solving we get the particular integral suitable for our present purpose

$$\zeta_s=\frac{i\cos\theta_\delta}{k_\delta}(B_1e^{-ik_\delta(\Delta_+)}-B_2e^{-ik_\delta(\Delta_-)})-\frac{i\sin\theta_s}{k_s}(C_1e^{-ik_s(S_+)}+C_2e^{-ik_s(S_-)}), \qquad (23)$$

where Δ_+ and Δ_- are abbreviations for the first and second parentheses in (20), respectively, and S_+ and S_- replace the first and second parentheses in (21). In similar fashion we obtain

$$\xi_s=\frac{i\sin\theta_\delta}{k_\delta}(B_1e^{-ik_\delta(\Delta_+)}+B_2e^{-ik_\delta(\Delta_-)})+\frac{i\cos\theta_s}{k_s}(C_1e^{-ik_s(S_+)}-C_2e^{-ik_s(S_-)}). \qquad (24)$$

From (18) and (19) we get

$$X_z/\mu = \sin 2\theta_\delta (B_1 e^{-ik\delta(\Delta_+)} - B_2 e^{-ik\delta(\Delta_-)}) + \cos 2\theta_s (C_1 e^{-ik_s(S_+)} + C_2 e^{-ik_s(S_-)}) \quad (25)$$

and by the use of a little manipulation

$$Z_z = \rho_s c_\delta^2 \cos 2\theta_s (B_1 e^{-ik\delta(\Delta_+)} + B_2 e^{-ik\delta(\Delta_-)}) - \mu \sin 2\theta_s (C_1 e^{-ik_s(S_+)} - C_2 e^{-ik_s(S_-)}). \quad (26)$$

There are now three boundary conditions to be satisfied at each interface for all values of x namely: (1) Continuity of particle velocity normal to the interface. (2) Continuity of dilatational stress. (3) Vanishing of the shearing stress. As in Part I we shall represent the excess pressure and particle velocity at the point 1, assumed to be in the fluid, by p_1 and $\dot{\xi}_1$, respectively. The top surface of the first solid layer will be taken to correspond with $z=0$. As before we wish to derive the expressions for p_3 and $\dot{\xi}_3$ in terms of p_1 and $\dot{\xi}_1$, since these expressions will be of the same form for any successive mid-fluid points, if the structure is infinite in extent. Keeping this in mind and utilizing Eqs. (13) and following the notation of Part I as far as the fluid is concerned we finally write the boundary conditions in the form: (a) for the top of the solid layer,

$$\begin{aligned} \dot{\xi}_{12} &= -\frac{\omega \cos\theta_\delta}{k_\delta}(B_1 - B_2) + \frac{\omega \sin\theta_s}{k_s}(C_1 + C_2), \\ p_{12} &= -\rho_s C^2 \cos 2\theta_s (B_1 + B_2) + \mu \sin 2\theta_s (C_1 - C_2), \\ (B_1 - B_2) \sin 2\theta_\delta &+ (C_1 + C_2) \cos 2\theta_s = 0, \end{aligned} \quad (27)$$

and (b) for the bottom of the solid layer,

$$\begin{aligned} \dot{\xi}_{32} &= -\frac{\omega \cos\theta_\delta}{k_\delta}(B_1 e^{-iP} - B_2 e^{iP}) + \frac{\omega \sin\theta_s}{k_s}(C_1 e^{-iQ} + C_2 e^{iQ}), \\ p_{32} &= -\rho_s C^2 \cos 2\theta_s (B_1 e^{-iP} + B_2 e^{iP}) + \mu \sin 2\theta_s (C_1 e^{-iQ} - C_2 e^{iQ}), \\ (B_1 e^{-iP} - B_2 e^{iP}) \sin 2\theta_\delta &+ (C_1 e^{-iQ} + C_2 e^{iQ}) \cos 2\theta_s = 0, \end{aligned} \quad (28)$$

where for convenience we have placed

$$P = 2k_\delta l_2 \cos\theta_\delta, \qquad Q = 2k_s l_2 \cos\theta_s. \quad (29)$$

To the six equations in (27) and (28) must be added the fluid equations analogous to those occurring in (4) and (5) in Part I. We write these in somewhat different notation, *viz.*,

$$\begin{aligned} p_{12} &= p_1 \cos R/2 - \frac{i\omega\rho_1}{k_1 \cos\theta_1}\dot{\xi}_1 \sin R/2, \\ \dot{\xi}_{12} &= \dot{\xi}_1 \cos R/2 - \frac{ik_1 \cos\theta_1}{\omega\rho_1} p_1 \sin R/2. \end{aligned} \quad (30)$$

$$\begin{aligned} p_\delta &= p_{32} \cos R/2 - \frac{i\omega\rho_1}{k_1 \cos\theta_1}\dot{\xi}_{32} \sin R/2, \\ \dot{\xi}_3 &= \dot{\xi}_{32} \cos R/2 - \frac{ik_1 \cos\theta_1}{\omega\rho_1} p_{32} \sin R/2, \end{aligned} \quad (31)$$

where now

$$R = 2k_1 l_1 \cos\theta_1. \quad (32)$$

The problem is to eliminate the quantities p_{12}, ξ_{12}, p_{32}, ξ_{32}, B_1, B_2, C_1 and C_2 from the ten equations in (27), (28), (30) and (31) and thus express p_3 in terms of p_1 and ξ_1, etc. The final result is as follows.

$$p_3=\alpha p_1-iZ_1\beta\xi_1, \qquad \xi_3=\alpha\xi_1-i/Z_1\cdot\gamma p_1, \tag{33}$$

with

$$\alpha=\frac{1}{M_1+M_2}\cdot\left\{\cos R\cdot[M_2e^{-iP}+M_1e^{iP}]+\sin R\left[Z\sin P-\frac{i}{2Z}\cdot(M_1^2e^{iP}-M_2^2e^{-iP})\right]\right\},$$

$$\beta=\frac{1}{M_1+M_2}\cdot\left\{\sin R[M_2e^{-iP}+M_1e^{iP}]-i\left[2iZ\sin P\sin^2 R/2-\frac{1}{Z}(M_1^2e^{iP}-M_2^2e^{-iP})\cos^2\frac{R}{2}\right]\right\}, \tag{34}$$

$$\gamma=\frac{1}{M_1+M_2}\cdot\left\{\sin R[M_2e^{-iP}+M_1e^{iP}]-i\left[\frac{1}{Z}\cdot(M_1^2e^{iP}-M_2^2e^{-iP})\sin^2\frac{R}{2}-2Z\sin P\cos^2\frac{R}{2}\right]\right\},$$

wherein moreover

$$M_1=-\rho_s c_\delta^2\cos 2\theta_s-\frac{i\mu\sin 2\theta_\delta\cdot\sin 2\theta_s}{\cos 2\theta_s\cdot\sin Q}e^{-iP}+\frac{i\mu\sin 2\theta\cdot\sin 2\theta_s}{\cos 2\theta_s\cdot\sin Q}\cos Q,$$

$$M_2=-\rho_s c_\delta^2\cos 2\theta_s+\frac{i\mu\sin 2\theta_s\cdot\sin 2\theta_\delta}{\cos 2\theta_s\cdot\sin Q}e^{iP}-\frac{i\mu\sin 2\theta_\delta\cdot\sin 2\theta_s}{\cos 2\theta_s\sin Q}\cos Q, \tag{35}$$

$$Z=Z_1\left(c_\delta\cos\theta_\delta+c_s\cdot\frac{\sin 2\theta_\delta\cdot\sin\theta_s}{\cos 2\theta_s}\right), \quad Z_1=\omega\rho_1/k_1\cos\theta_1.$$

Inspection shows as in Part I, that

$$\alpha^2+\beta\gamma=1. \tag{36}$$

The usual analysis suggests therefore that the transmission characteristics of the structure are given by

$$\cos W=\alpha. \tag{37}$$

This proves to be the case. $\cos W$ turns out to be real and may indeed be written in the somewhat more simple form:

$$\cos W=\cos R\cos Q\cdot X_2/X_1+\frac{\sin R\cdot\cos Q}{2X_1Z\sin P}[Z^2\sin^2 P+X_1^2/\cos^2 Q-X_2^2], \tag{38}$$

where

$$X_1=-\rho_s c_\delta^2\cos 2\theta_s\cos Q-\frac{\mu\sin 2\theta\cdot\sin 2\theta_s}{\cos 2\theta_s}\cot Q\cdot\sin P,$$

$$X_2=-\rho_s c_\delta^2\cos 2\theta_s\cos P-\frac{\mu\sin 2\theta_\delta\cdot\sin 2\theta_s}{\cos 2\theta_s}\cot Q\cdot\sin P. \tag{39}$$

Comparison of (38) with the corresponding expression in Part I, i.e., Eq. (12), indicates that the structure under consideration here also acts, for every angle θ less than the critical angle, as a low-pass filter for compressional waves in the fluid separating the solid layers. Indeed for $\nu=0$, $X_1=X_2$, $\cos Q=\cos R=1$, while $\sin R/\sin P$ remains finite. The result is that for $\nu=0$, $\cos W=1$ and transmission is assured for low frequencies.

Considerable interest attaches to the special case in which the thickness of the solid layers is much less than that of the fluid layers, i.e., $l_2 \ll l_1$. From the form of P, Q and R we see that for a considerable range of frequencies beginning with $\nu=0$, $|\sin P|$ and $|\sin Q|$ will be much less than unity while $\cos Q$ and $\cos P$ will approximate unity. Hence in this range $X_1 \doteq X_2$ and the expression (38) will take on the approximate form

$$\cos W = \cos R + \epsilon(\nu), \tag{40}$$

where $\epsilon(\nu)$ is a periodic function of the frequency with an amplitude considerably less than unity. For the greater part of the frequency range in question $|\cos W| \leq 1$. However, in the neighborhood of the frequencies for which $R=\pi, 2\pi, 3\pi, 4\pi, \cdots$ the effect of $\epsilon(\nu)$ is to increase $|\cos W|$ for a short interval to a value in excess of unity. This leads to attenuation or reflection bands in the vicinity of the frequencies just indicated. These are given by

$$2l_1 \cdot \frac{2\pi\nu}{c_1} \cdot \cos\theta_1 = n\pi,$$

where n is integral. Hence

$$\nu = nc_1/4l_1 \cos\theta_1, \tag{41}$$

with the corresponding wave-lengths

$$\lambda = 4l_1 \cos\theta_1/n. \tag{42}$$

If we replace θ_1 by its complement θ_1', the angle which the wave normal makes with the fluid-solid boundary, $\cos\theta_1 = \sin\theta_1'$. Moreover, since $l_2 \ll l_1$, we may call $2l_1$ effectively the distance between successive solid layers. Denoting it by l, the result is that the wave-lengths

$$\lambda = 2l \sin\theta_1'/n \tag{43}$$

are selectively reflected by the stratified structure. Formula (43) is the elastic wave analog of the Bragg law in the reflection of x-rays. The same situation, of course, is encountered in Part I where both layers are fluid.

Figure 3 shows the plot of $\cos W$ as a function of frequency for the special case in which the layers are 1 cm of water and 0.5 cm of Celluloid, respectively. The angles chosen are 10° and 45°, respectively. The low-pass character of the structure is well brought out. Especially interesting is the attenuation band introduced by the infinite discontinuity in $\cos W$.

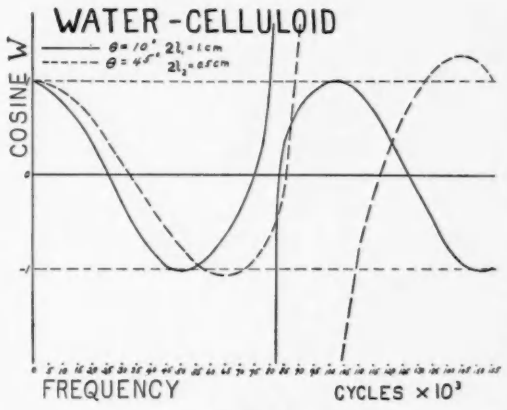

FIG. 3.

The author wishes to make grateful acknowledgment of assistance in connection with arithmetical calculations and curve plotting rendered by Messrs. W. I. Fox, L. W. Labaw and W. J. Yost, graduate students in the Department of Physics in Brown University.

APPENDIX

Derivation of Eq. (1)

The general expression for the resultant velocity potential for incident and reflected plane harmonic waves in medium I with wave fronts parallel to the y axis and making angle θ_1 with the interface is[4]

$$\phi = e^{-ik_1 x \sin\theta_1}(Ae^{-ik_1 z \cos\theta_1} + Be^{ik_1 z \cos\theta_1})e^{i\omega t}, \tag{a}$$

where A and B are arbitrary constants to be evaluated from the assumed boundary conditions. From this the excess pressure p and normal displacement velocity $\dot{\xi}$ can be obtained by the use of the fundamental acoustical relations

$$p = -\rho_1\dot{\phi}; \qquad \dot{\xi} = \partial\phi/\partial z. \tag{b}$$

If we let the *resultant* values of p and $\dot{\xi}$ at point 1 in I (where z is taken to be zero) be denoted by p_1 and $\dot{\xi}_1$, respectively, we can use (b) to express A and B in terms of p_1 and $\dot{\xi}_1$. The result is the two equations given under (1).

[4] Cf. Stewart and Lindsay, *Acoustics*, p. 97f.

Normal Modes of Vibration in Room Acoustics: Experimental Investigations in Nonrectangular Enclosures*

RICHARD H. BOLT**
University of California at Los Angeles, California
(Received August 17, 1939)

Existing theories of room acoustics have long been recognized as incomplete. The inadequacy is particularly disturbing in the lack of agreement between absorption coefficients measured in different laboratories. Also, the acoustic behavior of small rooms cannot always be prescribed with certainty. Several investigators have shown the necessity of analyzing a room as an assemblage of normal modes of vibration in a three-dimensional continuum. The present paper reports preliminary studies of one aspect of the "wave" approach: the influence of boundary shape on normal modes of vibration. An experimental method reported previously, (reference 25) has been improved and further developed for exploring the distribution of sound in small reflective enclosures of various shape. Standing wave patterns have been plotted for the lowest four or five modes of vibration in each of three models: a parallelogram in plan, a trapezoid in plan, and a model with an "alcove" or coupled space. A number of normal frequencies have been measured in each model, and the nature of the frequency distributions has been studied. The results have been summarized with respect to their significance for room acoustics. In particular, it appears that rooms of irregular shape still possess discrete normal modes and standing wave patterns as pronounced as those which occur in simple shapes.

INTRODUCTION

THE present practice of room acoustics is based on approximate theory, evolved from exhaustive experiments and simplified theoretical concepts which lead to the convenient observable quantity, the reverberation time.[1–6] Different forms of a reverberation equation have been derived to fit specified conditions,† and the success of these formulas is evidenced by their widespread application to the improvement of hearing conditions in auditoriums and large rooms.

Numerous discrepancies between calculated and observed reverberation times have shown that these formulas are reliable only under very special conditions, frequently not realized in actual rooms. For one thing, the decay of sound in small reverberant rooms is not smooth and logarithmic, as is required by the definition of reverberation time. Decay curves are often modulated by irregularities, and may have two or more distinct slopes. Also, the decay characteristics may vary markedly with position in the room. The restricted applicability of the simple reverberation formulas has been recognized for many years.[3, 7–12, etc.] Confident prediction of reverberation time has been confined, in general, to fairly large rooms of reasonably simple shape, having absorptive materials distributed over the walls with comparatively uniform coverage.

* This is the last of three papers reporting the research work offered by the author in partial satisfaction of the requirements for the degree of Doctor of Philosophy in Physics, conferred by the University of California. The first paper was: "Frequency Distribution of Eigentones in a Three-Dimensional Continuum," J. Acous. Soc. Am. **10**, 228 (1939). The second paper was: "Normal Modes of Vibration in Room Acoustics: Angular Distribution Theory," J. Acous. Soc. Am. **11**, 74 (1939).

** Now a National Research Fellow in Physics 1939–40, at the Massachusetts Institute of Technology.

[1] W. C. Sabine, *Collected Papers on Acoustics* (Harvard University Press, 1922).

[2] G. Jaeger, Wiener Akad. Ber. Mathem. Nat. Kl. 120 Abt. **IIa**, 613 (1911). Also Am. Arch. **108**, 369 (1915).

[3] K. Schuster and E. Waetzmann, Ann. d. Physik **1**, 671 (1929).

[4] C. F. Eyring, J. Acous. Soc. Am. **1**, 217 (1930).

[5] R. F. Norris, "A derivation of the reverberation formula, Appendix II," *Architectural Acoustics* by V. O. Knudsen (1932).

[6] G. Millington, J. Acous. Soc. Am. **4**, 69 (1932).

† For example, the Sabine-Jaeger form is applicable to *live* rooms only, while the form proposed by Schuster and Waetzmann, Eyring, and Norris applies to *dead* rooms also. Both forms assume uniform, diffuse distribution of sound.

[7] M. J. O. Strutt, Phil. Mag. **8**, 236 (1929); Ann. d. Physik IV, **87**, 145 (1928).

[8] V. O. Knudsen, "Resonance in Small Rooms," J. Acous. Soc. Am. **4**, 20 (1932).

[9] V. O. Knudsen, *Architectural Acoustics* (Wiley, 1932), esp. pages 128–130.

[10] S. J. Parkinson, "Area and Pattern Effects in the Measurement of Sound Absorption," J. Acous. Soc. Am. **2**, 112 (1930).

[11] V. L. Chrisler, "Dependence of Sound Absorption Upon the Area and Distribution of the Absorbent Materials," Nat. Bur. Stand. J. Research **13**, 169 (1934).

[12] R. M. Morris, G. M. Nixon and J. S. Parkinson, "Variations in Sound Absorption Coefficients as Obtained by the Reverberation Chamber Method," J. Acous. Soc. Am. **9**, 234 (1938).

The inadequacy of reverberation theory has been particularly consequential in the use of reverberation chambers, which are employed in the standard methods of absorption coefficient measurement. Numerous artifices have been utilized, with varying success, in an effort to realize experimentally the conditions assumed in reverberation theory. Rotating vanes, nonparallel walls,[13] acoustically rough walls,[14, 15] various obstacles,[16] and warble tones have been tried in an effort to obtain uniform diffuse distribution of sound energy. In some cases a certain degree of success has been attained, as has been evidenced by improved consistency in absorption coefficients. However, these means are only empirical procedures of a tentative nature, and do not constitute a fundamentally satisfactory solution of the problem.

The nature of a valid approach to room acoustics has been recognized for some time.[3, 7–9] The air in a room should be treated as an assemblage of resonators, normal modes of vibration which are selectively excited, maintained, and damped out under the influence of a number of controlling factors. In other words, a "wave theory" approach is required, and this attack has inspired numerous recent studies.[17–28] The present paper reports preliminary experiments on one limited aspect of the wave approach: the influence of boundary shape on normal modes of vibration.

Purpose and Scope of Investigation

The influence of boundary shape is of importance to room acoustics for several reasons. Reverberation chambers of irregular shape have been proposed, and a few have been constructed,[13, *] in an effort to smooth out the standing wave patterns which are very marked in conventional chambers at low frequencies. Reverberation theory assumes a diffuse sound field, but this condition is not fulfilled when pronounced wave patterns are present. Not only does the steady-state intensity vary with position, but the measured reverberation time may depend on the location of the source and the detecting device in the room. Some investigators have hoped that an irregular shape would reduce the standing wave patterns, while others[15, 16] have cast doubt on the probable efficacy of nonrectangular reverberation chambers for this purpose. To provide additional evidence bearing on this question is one of the objectives of the present research.

It is known from empirical evidence and from geometrical analyses that certain shapes are superior to others for small rooms and music studios. A study of the influence of boundary shape on normal modes may lead to a better understanding of the acoustical behavior of small rooms.

A complete evaluation of the effective absorption of a material in a room may have to consider the angular distribution of the normal modes which combine to carry the sound.[20] For rooms of rectangular shape a simple theory of angular distribution can be worked out and applied, with minor modifications, to the case of absorption.[26] But the exact role of angular distribution in nonrectangular rooms probably

[13] G. W. C. Kaye, "The Acoustical Work of the National Physical Laboratory," J. Acous. Soc. Am. **7**, 167 (1936).
[14] E. Meyer, Akustiche Zeits. **2**, 179 (1937).
[15] E. Meyer, "Reverberation and Absorption of Sound," J. Acous. Soc. Am. **8**, 155 (1937).
[16] P. E. Sabine, "Effects of Cylindrical Pillars in a Reverberation Chamber," J. Acous. Soc. Am. **10**, 1 (1938).
[17] E. C. Wente, J. Acous. Soc. Am. **7**, 123 (1935).
[18] P. M. Morse, *Vibration and Sound* (McGraw-Hill, 1936), Chapter VIII.
[19] H. Cremer and L. Cremer, Akustiche Zeits. **2**, 225; 296 (1937).
[20] F. V. Hunt, "Investigation of Room Acoustics by Steady-State Transmission Measurements," J. Acous. Soc. Am. **10**, 216 (1939).
[21] P. M. Morse and P. J. Rubenstein, "Diffraction of Sound by Ribbons and Slits," Phys. Rev. **54**, 895 (1938).
[22] F. J. Willig, "Comparison of Sound Absorption Coefficients by Different Methods," J. Acous. Soc. Am. **10**, 293 (1939).
[23] R. H. Bolt, "Frequency Distribution of Eigentones in a Three-Dimensional Continuum," J. Acous. Soc. Am. **10**, 228 (1939).
[24] D. Y. Maa, "Distribution of Eigentones in a Rectangular Chamber at Low Frequency Range," J. Acous. Soc. Am. **10**, 235 (1939).
[25] R. H. Bolt, "Spatial Resonance and Standing Wave Patterns in Small Models of Various Shape," J. Acous. Soc. Am. **10**, 258(A) (1939).
[26] R. H. Bolt, "Normal Modes of Vibration in Room Acoustics: Angular Distribution Theory," J. Acous. Soc. Am. **11**, 74 (1939).
[27] F. V. Hunt, L. L. Beranek and D. Y. Maa, "Analysis of Sound Decay in Rectangular Rooms," J. Acous. Soc. Am. **11**, 80 (1939).
[28] P. M. Morse, "Some Aspects of the Theory of Room Acoustics," J. Acous. Soc. Am. **11**, 56 (1939).
* There are nonrectangular chambers at the National Physical Laboratory, at the Johns-Manville Laboratory, one in Italy, and perhaps others.

cannot be predicted accurately without recourse to experimental studies, especially at low frequencies. To complicate the situation further, the presence of absorption in a room distorts the shape of the standing waves, and this change in shape, a sort of diffraction, influences the degree of damping which the absorbing material exerts on the wave. An exact theoretical analysis of this condition has been developed by Morse[28] for certain simple configurations of material in a rectangular room. Extensions of this theory to nonrectangular rooms may have to incorporate experimental studies of wave patterns, or generalizations derived therefrom.

In addition to these points which bear directly on room acoustics, the study of wave patterns in an arbitrary shape may prove to be of interest to general wave theory. Wave equation solutions are available for a rectangular enclosure, a sphere, a cylinder, an ellipsoid, and a few other simple shapes.[18, 29] Beyond these, the solution of the wave equation is difficult. In general, the equation must be expressed in coordinates in which the variables are separable, which requires that the bounding surfaces of the enclosure must fit the coordinate lines in some simple manner. For slight variations from a simple shape, the method of perturbations could perhaps be applied. Experimentally obtained plots of wave patterns may suggest at least approximate mathematical methods of extending the theory of vibrations in variously bounded continuua.

The specific objectives of the present investigation are:

(1) To develop a simple and practicable experimental method for exploring wave patterns in enclosures of readily adjustable shape.
(2) To obtain preliminary data in the form of accurate wave patterns for the lowest few normal modes of vibration in each of three simple nonrectangular enclosures.
(3) To provide additional evidence on the probable efficacy of nonrectangular reverberation chambers as a means of attaining a more uniform distribution of sound energy.
(4) Incidentally, to measure a number of normal frequencies in each enclosure, and to correlate the results with the frequency distribution theory previously worked out.[23]

[29] Rayleigh, *Theory of Sound* (Macmillan, Ltd., 1929).

Experimental Method

An experimental method has been developed using small models which are easily assembled in a variety of shapes. Standing waves are maintained by a steady tone which is generated by an oscillator and introduced into the models through an adapted crystal phone. The wave patterns are explored by moving the models about a fixed exploring tube of small diameter, projecting up through a flat-topped table which serves as the floor for all models. The data are plotted directly at full scale in the form of sound pressure contour maps, each plot depicting the spatial wave form at one horizontal section.

Construction of models

Two types of models were used in the course of this research. The earlier experiments[25] and some of the frequency distribution studies reported in the present paper utilized a wood and fiber board construction, while the wave patterns presented in this paper were obtained in models made of brass.

Referring to the former type first, it was found that a large number of models could be assembled from comparatively few standard wall units, bolted together by corner posts. The interior surface of a wall unit is hard tempered Masonite fiber board, backed by a wooden frame which is filled in with plaster of paris to increase the rigidity and mass. All wall units are 8″ high, and the floor and ceiling of all models are parallel to each other so that variations in shape are possible in plan alone. About ten wall units are sufficient to produce a rectangle, a triangle, a trapezoid, a parallelogram, a completely skew plan, a model with coupled spaces, and several others. These models are from 8″ to 16″ in plan dimensions.

The ceiling for these models is a $2\frac{1}{4}$″ thick board, built up solidly with wood and faced with tempered Masonite. A Brush crystal phone, with the ear-cap turned flat, is set flush in the interior surface of the top board, and a hole $\frac{1}{4}$″ in diameter leads the sound from the phone into

the model, at any desired position relative to the plan.

The floor for all models is a flat sheet of $\frac{3}{8}''$ steel flange plate, 3′ by 4′, which just covers the top of a table of sturdy construction. The steel face was polished with a disk grinder. The steel plate, after being shimmed up at the corners, was found to sag less than $\frac{1}{64}''$ at the center, and no center support was found necessary.

The brass models are essentially "two-dimensional," i.e., the vertical dimension is so much less than the horizontal plan dimensions that no normal modes with vertical components of vibration occur in the low frequency range employed here. In this case, a plot at a single section is sufficient to indicate the vibration form of a normal mode. Also, the mechanical details are simplified, and the normal frequencies are more widely spread resulting in well isolated normal modes for study.

These metal models are 2″ high, and from 7″ to 10″ in plan. The top for the models is a sheet of brass $\frac{3}{8}''\times14''\times16''$, and the floor for the models is the steel plate described above. The side walls are formed by four strips of brass which overlap each other successively, as shown in Fig. 1, and are clamped to the top plate at the outer edges. Two of the wall strips are 14″ long, two are 16″ long, and they are made of $\frac{1}{4}''\times2''$ brass with a $\frac{1}{2}''\times\frac{1}{2}''$ brass bar screwed and soldered along the entire length of the back

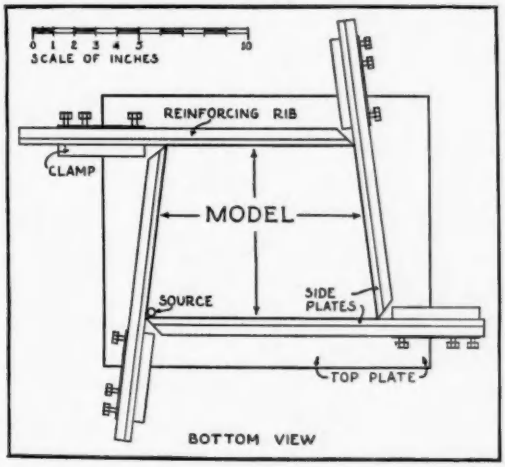

FIG. 1. Inside plan view of brass model assembled in the shape of a trapezoid. The sound source is a crystal receiver sealed in a brass case; a threaded tube conducts the sound into the model through a hole in the top-plate.

to supply additional rigidity and mass. One end of each strip is beveled at 45° resulting in a sharp edge which butts firmly against its neighboring wall, at any angle up to 135°. As the

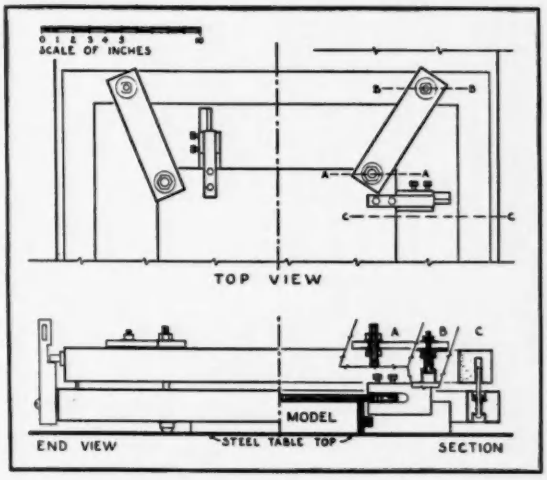

FIG. 2. Details of brass model assembly and moving frame. The model is suspended from the upper frame by four projecting steel bars and vertical threaded rods which engage *U*-brackets slipped over the edges of the model top-plate.

strips were all milled at the same time they are accurately of the same height. Special clamps were fabricated and milled for the purpose of fastening the wall strips to the top plate. The details of the clamps and the wall strips are shown in Figs. 1 and 2.

When the desired shape is formed, as in Fig. 3 for example, the bolts on the clamps are tightened up gradually, in rotation. With proper care, the distance between parallel walls can be made uniform to within $\frac{1}{64}''$, and adjustments to other positions can be made with corresponding accuracy. All joints are coated with shellac just before assembly and are sealed with wax until no light leaks can be seen through the joints of the completed model. Finally, two or three layers of rubber dam gasket are cemented to the edges which will rest on the steel table top. Care must be taken to have the top surface of the rubber gasket smooth and without appreciable gaps, as very slight leaks are sufficient to cause marked irregularities and dissymmetries in the wave patterns.

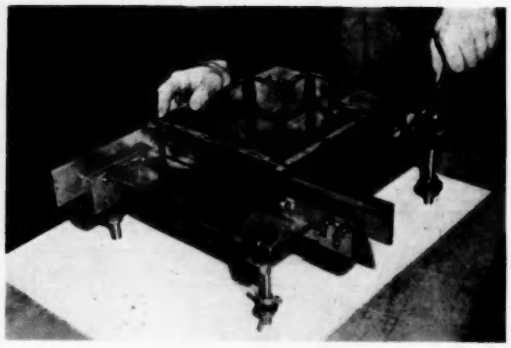

FIG. 3. Brass model assembled with an alcove or coupled space as used for model C in this paper. The alcove is formed by brass-faced hardwood blocks, cemented into two corners. Sealing wax, seen along all inside edges, is necessary to prevent air leaks, and several layers of rubber dam gasket around the open side ensure a good seal on the steel table top.

Exploring mechanism

This experiment required an exploring method which could be adapted readily to variously shaped models. In the method developed, the model is moved around the exploring tube instead of the usual reverse procedure of moving the microphone within the enclosure. At the same time, a full scale plan moves integrally with the model. A pointer, fixed with respect to the table, always indicates on the plan drawing exactly where the pick-up tube is within the model itself. The angular orientation of the model must be maintained constant, with relation to the table. Since the plan is drawn on coordinate paper, the alignment is effected by keeping the coordinate lines parallel to a straight-edge which is fixed to the table, as shown in Fig. 4.

The brass exploring tube of $\frac{1}{4}''$ outside and $\frac{1}{8}''$ inside diameter, projects up through the table to any desired height in the model. The lower end of this tube is joined to a brass cap, specially turned to replace the cap of a W. E. 618-A dynamic microphone. The length of the tube can be varied in order to "tune" the tube to maximum response for any particular frequency, although this adjustment is not usually critical.

One of the technical problems was to devise a means for moving the models. The method chosen uses a large wooden frame supplied with four ball bearing spherical casters which roll easily on the table top. The front part of the frame carries a drawing board for the plan drawings. Above the back of the frame is suspended another frame, guided by four pins on which the upper frame slides up and down. The model is fastened to this upper frame, which can be raised and lowered by the simultaneous action of four cams, actuated by a lever handle which projects to the front of the drawing board. The assembly is pictured in Fig. 4, ready for operation with one of the fiber-board models in place, secured to the upper frame by wood blocks and wedges. The metal models are suspended from the upper frame by projecting steel bars and vertical threaded rods. Fig. 5 shows a simplified drawing of the moving frame.

FIG. 4. Moving-frame exploring mechanism with fiber-board model in place. The exploring tube projects up through the table, into the model. The sound source, a crystal receiver, is set flush in the top board which has been removed for this photograph.

A refinement in the exploring mechanism has proved useful. The observed wave patterns frequently exhibit space variations as great as 10 db in 0.1". In order to plot such sharp troughs with accuracy it is advantageous to provide a slow motion exploring device. The upper end of the exploring tube is fitted with a short section of brass tubing, $\frac{1}{8}''$ outside and $\frac{1}{16}''$ inside diameter, which is offset 1" from the axis of the microphone and primary exploring tube. When the microphone is rotated slightly the open end of the offset tube describes a small arc

which is very nearly a straight path (sagitta of about 0.005″ for a chord of 0.2″) at right angles to the connecting tube. The microphone is rotated by a handle which projects to the front of the table. The operator controls this device from the same position in which he moves the model. The handle is fitted with a pointer and scale. A motion of about 8″ at this scale corresponds to a motion of 0.2 in. of the exploring end. The scale is calibrated to read the motion of the exploring end, and is graduated to 0.01″, which is the limit of graphical accuracy in recording data.

The slow motion device makes possible the direct location of points of equal output. In the earlier part of this research, output readings were recorded at a number of coordinate intersections, these values were projected and joined to form smooth curves of wave cross sections, and points of equal output were found by graphical interpolation. With the slow motion mechanism, the operator, after making a brief over-all survey of a given mode, is able to make settings of equal pressure close enough so that an additional motion of $\pm 0.1''$ is usually sufficient to locate the desired point exactly. Each contour is sketched in as it is plotted, so that the final inking of the plots becomes a very straightforward procedure.

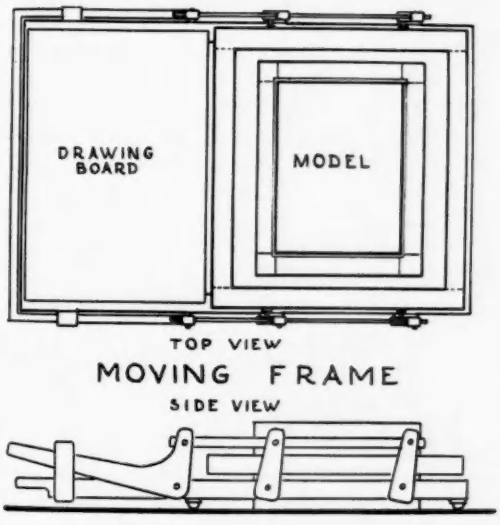

FIG. 5. Simplified drawing of the moving frame. The model is raised and lowered by four cams actuated by the lever handle which projects to the front of the drawing board.

Electrical circuit

The essential features of the electrical circuit are shown in Fig. 6. A pure tone (distortion unobservable oscillographically) is generated by an oscillator* and fed to the ear phone which is flush in a wall of the model. The current entering the receiver is monitored by an input meter. Sound in the model is picked up by the exploring tube and led to the microphone which feeds into an amplifier, through a calibrated attenuator, to another amplifier, and into an output meter. The amplifiers are operated well within their linear range. Readings are taken from the attenuator setting, plus or minus a fraction of a decibel as read on the output meter. The total drift variation in the output of the electrical circuit can be kept to ± 0.2 db, which is sufficient accuracy to yield good wave patterns.

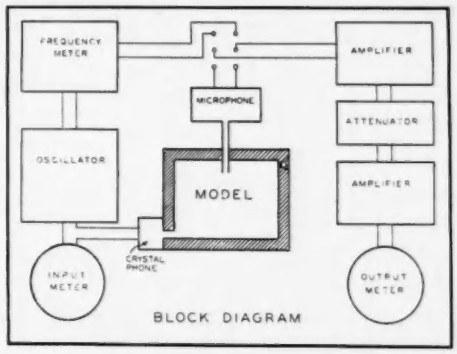

FIG. 6. Simplified block diagram of electrical circuit. The switch at the top makes it possible to select either the microphone output, for observing resonance peaks and wave patterns, or the output from the frequency meter, for measuring the normal frequencies. In the latter use, balance of the bridge-type meter is detected by a pair of phones connected across the output meter; the gain of the amplifying system greatly facilitates the location of the balance point.

The frequency of a normal mode is measured with a Campbell frequency meter, a commercial bridge-type device, rated accurate to 0.1 percent. Balance is detected aurally, using a pair of headphones connected across the output meter. It is found that, with proper precautions, readings can be repeated consistently (with deviations of not more than 0.1 percent) between 1000 and

* Part of the work was done with a G. R. 377-B oscillator, and part with a W. E. 8-A oscillator. Both are of the resistance stabilized feed-back type, and were found to be adequately stable after they were warmed up.

2000 c.p.s., but the meter is somewhat less accurate at lower frequencies, as a complete balance is difficult to obtain. The meter is calibrated against a set of standard Duratone tuning forks at 512, 1024 and 2048 c.p.s. These forks are claimed accurate to ±0.05 percent, with a temperature coefficient which may be considered insignificant in the present experiment. The probable error of frequency measurement is not more than ±0.15 percent, in the frequency range of this experiment.

Presentation and Discussion of Data

Standing wave patterns in nonrectangular enclosures

Figures 7 to 24 present some of the experimental results of the study of wave patterns in small models of various shape. There are three sets of data, a series of six figures for each of three models investigated: model *A*, a parallelogram; model *B*, a trapezoid; and model *C*, a coupled-space or "alcove" model. The exact dimensions (to 0.01″) of each model are given in the first illustration in each series. All models are 2″ in height, and the lateral dimensions are, approximately, from $7\frac{3}{4}$″ to 9″.

The matter of designating modes in irregular shapes is subject to ambiguity. In the method adopted we imagine a particular shape to be fitted approximately into a simple rectangle of about the same average dimensions, and apply the terminology commonly used for rectangles. A normal mode of vibration is uniquely designated by three numbers: (n_x, n_y, n_z), where n_x is associated with L_x, the longest dimension, and n_z is associated with L_z the shortest dimension of the enclosure.

The first three patterns plotted for each model are for the same modes, the (0, 1),* (1, 1) and (2, 0), in order to facilitate direct comparisons between models. It was believed that these simple modes might be particularly useful in subsequent attempts to find mathematical solutions for the observed patterns, and a theoretical study of this sort is proposed for future research. In addition, two more plots are presented for each model, representing a variety of modes.

All the mode-types sought were found to exist, in all three shapes investigated. These modes were equally sharp† and spatially-pronounced in all three shapes, so far as the experimental capabilities of the apparatus could reveal. The lower modes are seen to have an over-all range of about 45 db in the wave patterns. Above 2000 c.p.s. there is a diminution of output due to the reduced response of the exploring tube and source, while the lower threshold of the apparatus is determined by background noise. Allowing for the known sources of limitation, it can be stated with confidence that in the models investigated the modes are characterized by *space variations equally pronounced in the three shapes.*

The low frequency modes are seen to be the least regular in each case. A cursory examination of the (1, 0) modes near 700 c.p.s. showed them to be even more distorted than the (0, 1) modes presented here. A possible explanation is that the side walls resonate rather vigorously at the lower frequencies, in spite of the reinforcing added to the brass plates. Since mass reactance increases with frequency, the walls would be expected to vibrate with appreciably smaller amplitudes at higher frequencies.

The position of the source has but slight influence on the general nature of a wave pattern, but does determine the magnitude of response, as predicted by theory. The sound pressure in a room, excited by a point source, is given by Morse,[18] Eq. (34.10), page 317. The response is proportional to the values of the wave function at the source and at the pick-up positions. Figs. 9 and 12 compare two plots of the (1, 1) mode in the parallelogram model. In Fig. 9 the source is in a corner, and the wave function has a maximum (at least in a true rectangle) at this position. In Fig. 12 the source was moved to a position, near the center of one wall, at which the wave pattern response was about 18 db below the maximum value. The resulting

* These plots are obtained in shallow "two-dimensional" enclosures, and none of the modes studied involve vibration parallel to the shortest dimension. Therefore, two numbers suffice to designate the modes plotted.

† Steady-state transmission curves were taken in each model, and several peak-widths were analyzed by the method used by Hunt (reference 20). As long as the wall material remained the same, the peak-widths were not significantly changed by variations in model shape, and the measured peaks in each case led to a reasonable value of α for brass.

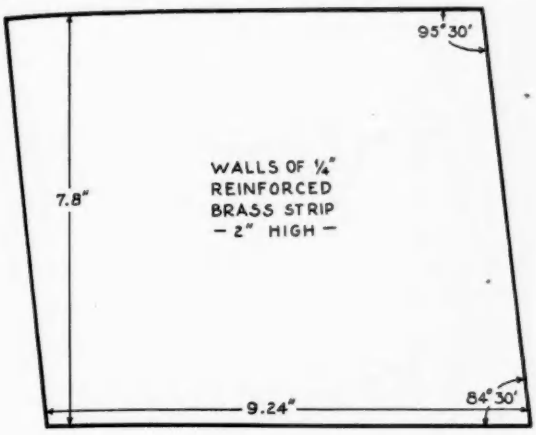

FIG. 7.

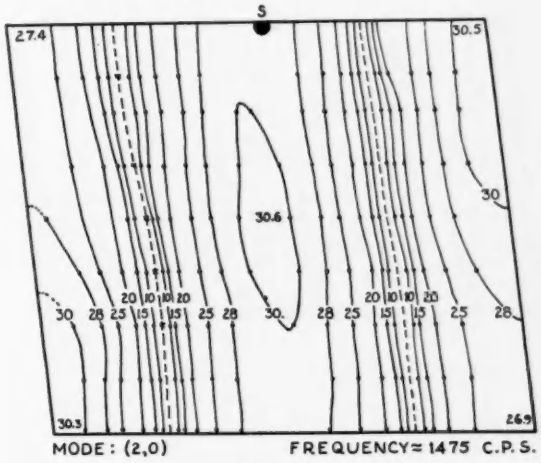

FIG. 10.

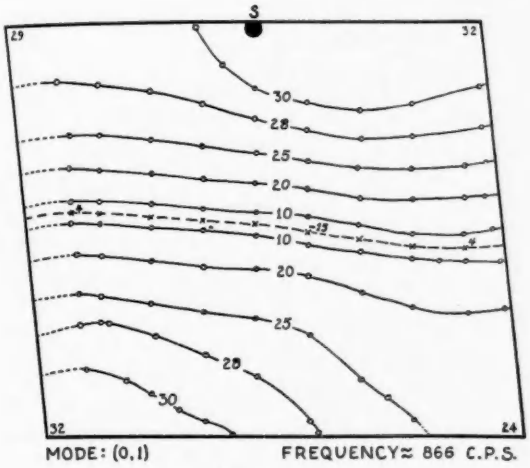

FIG. 8.

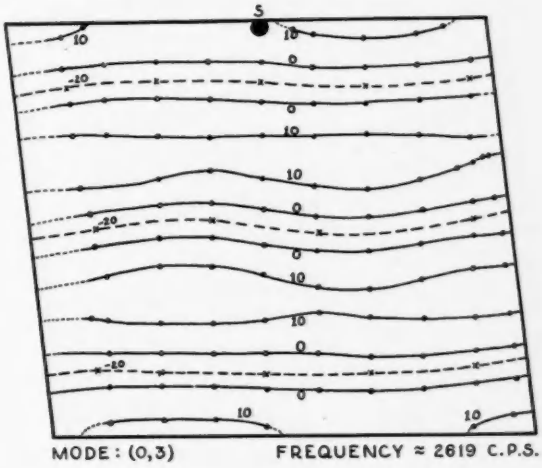

FIG. 11.

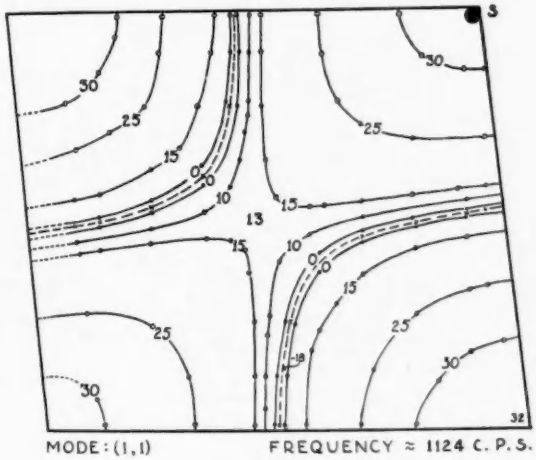

FIG. 9.

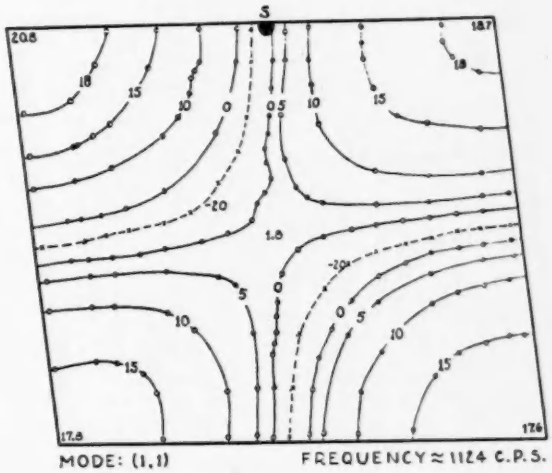

FIG. 12.

MODEL A. Standing wave patterns in parallelogram model.

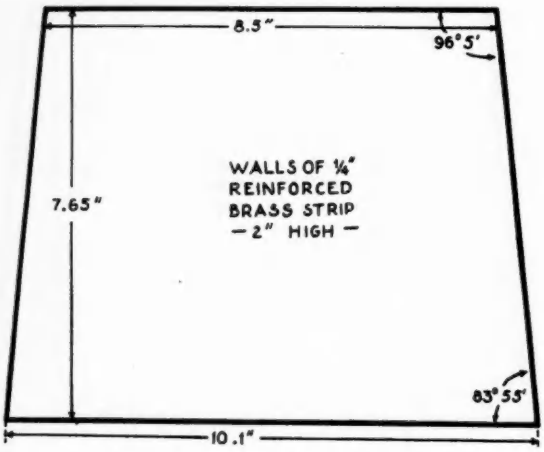

FIG. 13.

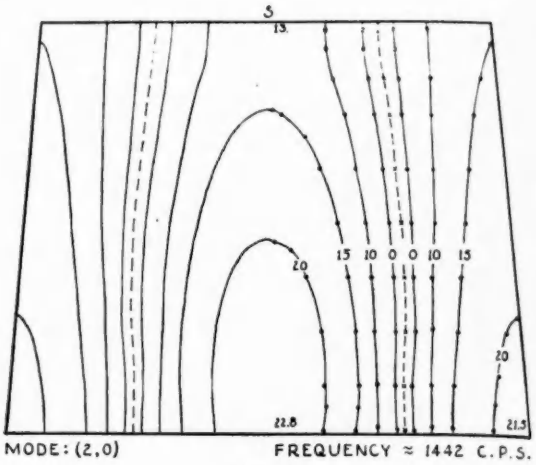

FIG. 16.

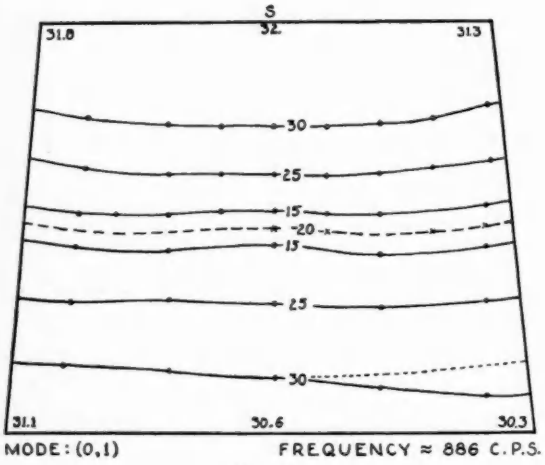

FIG. 14.

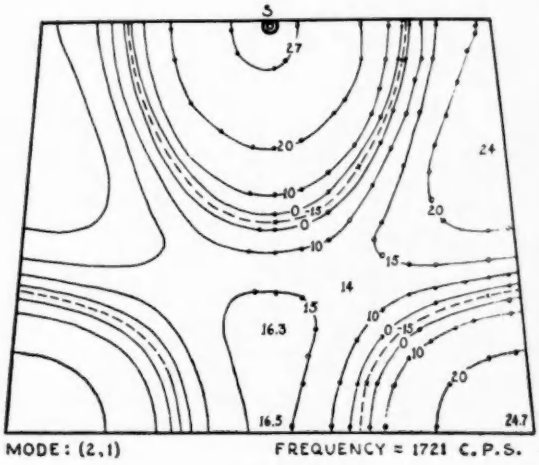

FIG. 17.

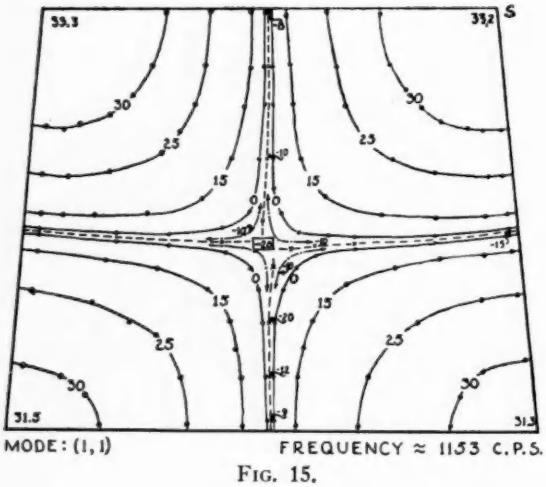

FIG. 15.

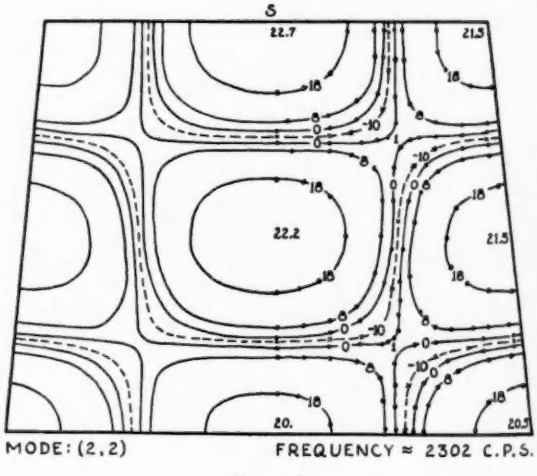

FIG. 18.

MODEL B. Standing wave patterns in trapezoid model.

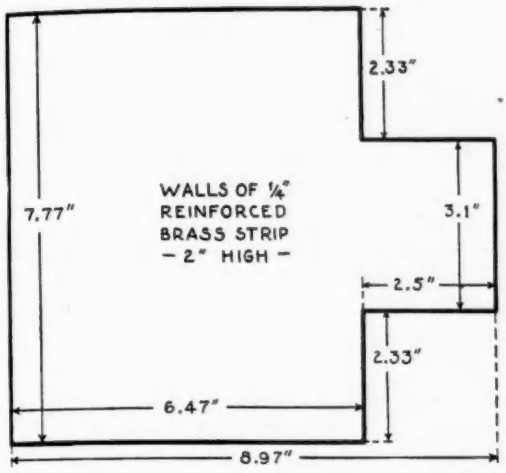

FIG. 19.

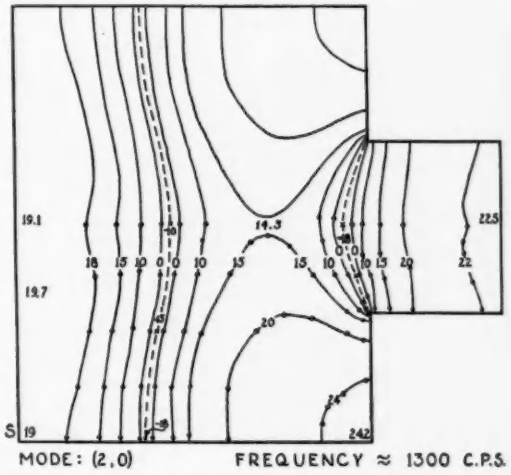

FIG. 22.

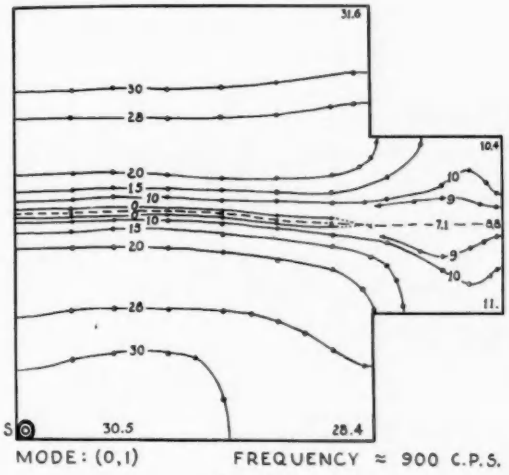

FIG. 20.

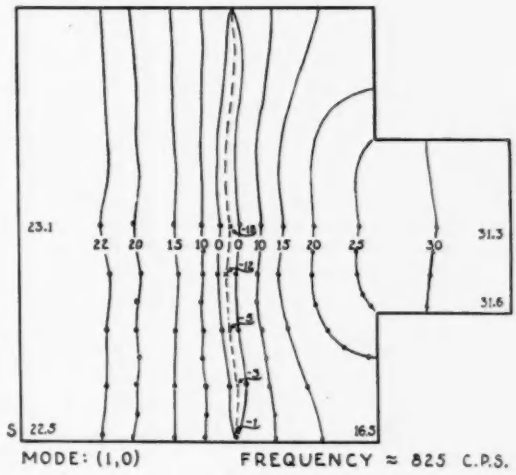

FIG. 23.

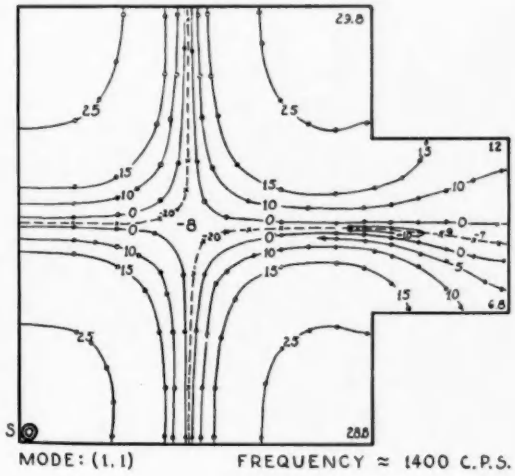

FIG. 21.

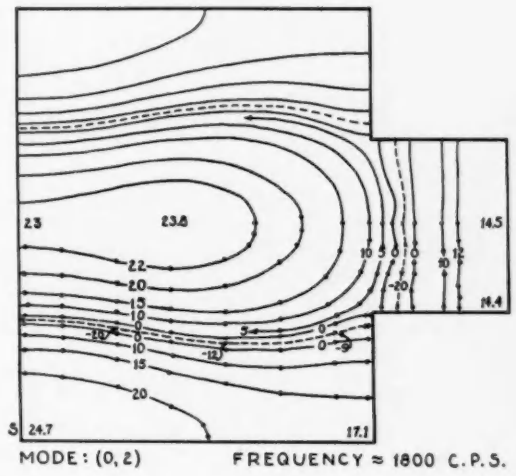

FIG. 24.

MODEL C. Standing wave patterns in coupled-space model.

plot, Fig. 12, was found to be about 18 db lower at all points than the plot in Fig. 9.† The only notable difference, besides this drop in level, is the slight irregularity along the "zero" contours in Fig. 12. This may be due to the increased effectiveness of direct sound from the source in the region of reduced resonance response. Aside from the different choice of contour levels in the two plots, it is apparent that the vibration forms are quite similar and that the patterns are equally pronounced in the plots representing two different source positions.

Examination of the patterns reveals another important aspect of normal modes in reflective enclosures. For perfectly reflecting walls, the boundary conditions require that the normal component of the particle velocity vanish at the walls. Particle velocity is proportional to the pressure gradient in a standing wave system, and is therefore normal to the lines of equal pressure. It is clear that pressure contours must enter a perfectly reflecting wall normally, or else lie parallel with the wall, the latter case occurring, for example, along a pressure maximum in a one-dimensional vibration. All the patterns observed here do, indeed, indicate that the pressure contours tend to enter the walls at normal incidence.

In model *A* the (0, 1) mode, which in a rectangle would have straight contours parallel to the x walls, exhibits contours which are slightly curved, apparently in such a way as to allow them to enter the 7.8″ end walls at normal incidence.* Thus the contours which strike both end walls possess a sort of *S* curvature. The two ends of the trough are displaced towards the acute angles of the model. The (1, 1) mode in model *A* is similar to a (1, 1) mode in a rectangle, but with the troughs pulled away from the center so that they no longer intersect. Here again the curvature of the lines is adjusted so that they meet the walls normally. The (2, 0) and (0, 3) modes repeat the tendencies found in the (0, 1) mode.

In model *B*, the first three modes are again quite similar to those in a true rectangle, but with the distortion necessary to bring the contours around to normal incidence with the slanting walls. The (2, 1) mode appears to bear least resemblance to its rectangular counterpart, for the troughs are pulled far apart at their "intersection" regions. It is clear, however, that there are two minima along each of the *X* walls and one minimum along the slanting *Y* walls, as would be expected in a (2, 1) mode. The contours of the (0, 1) mode, and the troughs of the (0, 1), (1, 1), and (2, 2) modes appear to approximate arcs of circles with centers near the intersection of the extensions of the two slanting walls. The *Y* direction troughs of the (1, 1), (2, 0), and (2, 2) modes appear to lie approximately along sections of radii which converge at the extended intersection of the slant walls. These observations suggest that, at least to a first approximation, the wave patterns in the trapezoidal model *B* might be analyzed by fitting the model into a segment of a cylindrical coordinate system and by using the familiar wave equation solutions for that system. Since the *X* walls are not truly arcs, however, additional considerations, perhaps in the form of perturbation terms, must be included to satisfy the condition of zero normal velocity component at the boundaries.

In model *C* there appears to be a small amount of vibration in the alcove, at right angles to the primary direction of the (0, 1) mode, as indicated by the peculiar curvature of the contours in the alcove in Fig. 20. In the (0, 2) mode, Fig. 24, this alcove vibration becomes very pronounced, a sharp trough appearing just inside the opening to the smaller space. In this connection it should be pointed out that the first resonance of the alcove itself, with a trough parallel to the opening and a crest along the extreme right wall, would have a frequency of about 1350 c.p.s. If the L_y dimension of the primary space were so chosen as to have a natural frequency of about this value, the alcove might be expected to possess a vibration with a trough parallel to its opening. The (0, 2) mode at 1800 c.p.s. is too high to show this effect, and the trough is inside the alcove opening, while the (2, 0) mode at 1300 is too low, with the resulting "bulge" of the trough at the alcove opening.

† For convenience in observation, an additional gain of about 5 db was used in Fig. 12 over the level in Fig. 9, so that the levels as marked are only about 13 db lower in Fig. 12.

* The dissymmetry of the pattern may be attributed to experimental difficulties, mentioned previously. The writer is inclined to believe that the upper half of the pattern is more nearly correct than the lower half, due to a suspected leak near the lower right-hand corner.

Normal frequencies in nonrectangular enclosures

It is of interest to point out some relations concerning the observed normal frequencies in the three models. The observed frequencies for the (0, 1) mode are listed in Table I, together

TABLE I.

	MODEL A	MODEL B	MODEL C
Calculated frequency	865	883	869
Observed frequency	866	886	900

with the theoretical values as computed from the Y dimensions of each model. The agreement between the calculated and observed values in the first two shapes indicates that the fundamental mode in the Y direction is not appreciably influenced (with regard to frequency) by minor alterations in the X direction. In model C the observed (0, 1) frequency corresponds to a length of 7.5″ instead of the actual dimension $L_y = 7.77''$. The addition of the alcove has the influence of slightly shortening the effective "wave-length" of the mode which grazes the alcove opening. The same influence is observed in the (2, 0) mode of model C, at 1800 c.p.s.

An apparent inconsistency exists in the relation between the (1, 0) mode and the (2, 0) mode at 825 and 1300 c.p.s., respectively, in model C. In a simple rectangle there is a frequency ratio of two to one between these modes. The nonharmonic relationship observed here is dependent on the behavior of the coupled spaces, but an exact analysis has not yet been pursued.

It appears that the normal frequencies of the one-dimensional modes which strike the slanting walls in a trapezoidal enclosure may be calculated approximately by using the average distance between these walls, substituted in the simple formula: $\nu = nc/2L$. In model B, for example, the average x dimension is 9.3″ and the observed frequency of the (2, 0) mode is 1442 c.p.s., which corresponds to an effective length (from the above formula) of 9.36″. For further evidence, a model was assembled with fiber board walls. The parallel sides of this model were 13″ and 16″ long, the connecting sides were 12″ long, the angles in plan were about 83° and 97°, and the height of the model was about 8″. The lowest four x modes were measured and found to correspond, with a maximum deviation of ±0.3 percent, to an effective length of 14.7″, while the average x dimension of this model was 14.5″. In each case the average length between the slanting walls agrees approximately with the effective length computed from the observed frequencies. More accurately, the frequencies calculated in this way are from 0.7 to 1.4 percent too high in the cases observed, but this simple rule may be used for approximations.

In the parallelogram model, all of the one-dimensional normal modes occur at frequencies which correspond approximately to the perpendicular distance between the walls in question. This was discussed previously for the (0, 1) mode in model A, and has been observed for the (2, 0) and (0, 3) modes in this model, and for several modes in a fiber board parallelogram model. This generalization is restricted to cases in which the angles between walls are not greatly different from 90°, and the experimental observations have included only the lowest four or five modes of vibration in each case.

Frequency distribution of normal modes in nonrectangular enclosures

Frequency distribution theory for acoustics has been studied recently[23, 24] with the result that the asymptotic equations have been replaced by more accurate forms to be used in the low frequency acoustical range. General vibration theory predicts that the frequency distribution at very high frequencies is independent of the shape of the enclosure.[7] However, the modified low frequency equations[23, 24] were derived for the special case of a rectangular room, and the corrections are shape-dependent. While a general theoretical solution of this problem is fraught with great mathematical difficulty, an approximate understanding of the low frequency distribution in irregular enclosures may be gained empirically from experimental evidence.

About twenty normal frequencies were measured in a fiber board rectangular model, by the method described earlier in this paper. The probable error of frequency measurement was about ±0.15 percent. The average deviation of the observed frequencies from their calculated values (using dimensions measured to 0.1 per-

cent) was found to be +0.26 percent,* and the greatest deviation in this series was +0.7 percent.

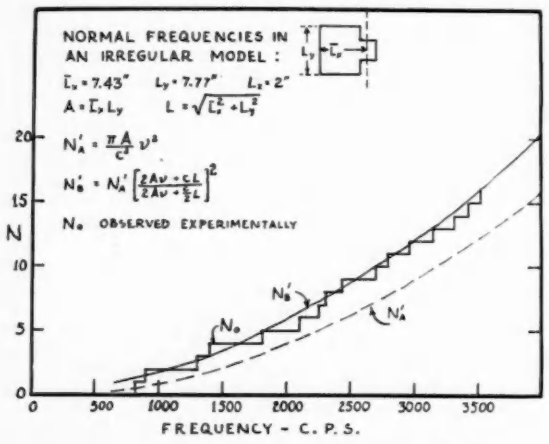

FIG. 25. Frequency distribution of normal modes observed in the coupled-space model C. N_a' plots the asymptotic distribution equation for a two-dimensional continuum. N_b' plots the low frequency modified distribution equation.

The plan of the rectangular model was then shifted to form a parallelogram with angles 83° and 97°, the wall lengths remaining 12″ and 16″ in plan. A number of normal frequencies were again measured, and each of these was found to lie fairly close to one of the frequencies in the rectangular model. In fact, if the frequencies observed in the parallelogram model are compared with those calculated for the rectangular model, the deviations of 19 normal frequencies were found to range from −1.52 to +3.5 percent, and if the perpendicular distance between walls is used for calculation as suggested in the previous section, the deviations are even less. Since each mode of vibration in the parallelogram has its counterpart in the rectangular model, the frequency distribution of normal modes is essentially the same in the two cases. A plot of the distribution in the 8″×12″×16″ model has been given previously,[23] and this same plot may now be taken to represent approximately the distribution in the slightly altered model.

The frequency distribution in the coupled-space model *C* has been studied, and is plotted up through the first 16 observed normal frequencies in Fig. 25. In attempting to fit this distribution to a smooth function, it must be remembered that model *C* is "two-dimensional" and that only (n_x, n_y) modes occur in the range studied. Equations for the frequency distribution in a two-dimensional continuum may be derived by any of the familiar methods.[18, 23, 24] Using the approach followed by the writer,[23] the two-dimensional low frequency forms are found to be

$$N_b' = \frac{\pi\nu^2 A}{c^2}\left[\frac{2A\nu + cL}{2A\nu + (c/2)L}\right]^2$$

and

$$dN_b' = \frac{\pi A}{c^2}\left[\nu^2 + \frac{cL}{2A}\nu\right]d\nu,$$

where $A = L_x L_y$, $L = (L_x^2 + L_y^2)^{\frac{1}{2}}$, and the primed notation is used to distinguish these from the three-dimensional equations for N_b and dN_b derived previously.[23]

In Fig. 25 is plotted N_b' for model *C*, using the true length L_y as marked, and an average dimension $\bar{L}_x$ such that the actual plan area of the model is given by $A = \bar{L}_x L_y$. This $\bar{L}_x$ is used in the value for L also. This empirically adjusted theoretical curve for the distribution, N_b', is seen to agree well with the observed distribution given by the stepped curve. Another curve marked N_a' plots the asymptotic form, obtained by dropping the correction factor from N_b', and is seen to be too low.

Substantially similar deductions may be made regarding the frequency distribution in models *A* and *B* and in other nonrectangular models not discussed here. These observations indicate rather convincingly that frequency distribution in irregular rooms is similar, at least in general trend, to the distribution in simple rectangular rooms. The equations derived previously[23] may be applied, with appropriate empirical modifications, to predict, even at low frequencies, the distribution of normal modes in nonrectangular enclosures.

CONCLUSIONS WITH REGARD TO ROOM ACOUSTICS

This investigation of normal modes of vibration in nonrectangular enclosures has resulted in certain findings which have a bearing on the

* A small positive error in observed frequencies in reflective enclosures was noted by Knudsen also (reference 8). With damping in the room these frequencies drop to about one percent below the calculated values.

practice of room acoustics. The selection of data presented in this paper may be considered typical of the results of the research. Conclusive generalizations are not claimed, in view of the limited scope of the study, but the following deductions appear to be justified.

(1) Small models offer a practicable and convenient means of investigating certain properties of normal modes of vibration as related to room acoustics.

(2) Rooms of irregular shape possess discrete normal frequencies as sharp as those in simple rectangular rooms.

(3) The frequency distribution in slightly modified shapes is similar in general trend to that in simple rectangular shapes. The distribution function for irregular shapes can be approximated by using average dimensions in the simple formulas.

(4) Rooms of irregular shape possess well-defined standing wave patterns.

(5) To a first approximation, the general nature of the wave patterns of the lower modes in a slightly irregular shape can be predicted qualitatively by analogy to a rectangular shape of similar size and proportion.

(6) The over-all spatial variation in a standing wave is as great in a room of irregular shape as in a simple one, provided the damping of the walls and other conditions are similar in the two cases. In the three shapes investigated, the lower modes exhibited a variation of about 45 db irrespective of shape.

These deductions are not conclusive evidence, however, that reverberation chambers remain unimproved by slanting the walls. Practical measurements frequently involve a warble tone or band of frequencies which excite a number of normal modes simultaneously. In rectangular enclosures, various series of modes are related harmonically, and have coincident regions of maximum and minimum pressure. For example, the (1, 0, 0), (3, 0, 0), (5, 0, 0) etc. modes all have pressure minima in the plane $x=L_x/2$. When several such modes in a series are excited simultaneously, there result very pronounced fluctuations in the standing wave pattern. In nonrectangular enclosures, on the other hand, the harmonic relations of such a series are upset, and these modes do not necessarily have clearly defined regions of coincident reinforcement. In this case the average spatial response may be more uniform in a nonrectangular than in a rectangular reverberation chamber, provided an appropriate number and selection of modes are excited. It is questionable, however, if this effect leads to marked improvement in standard reverberation chambers at the lower frequency ranges used in absorption tests.*

It appears reasonable to make the tentative generalization that difficulties arising from standing wave patterns in small rooms cannot be alleviated to any great extent by minor alterations in the shape of the room.

Acknowledgment

The author is indebted to Professor Vern O. Knudsen for suggesting this problem and for his interest and guidance during the course of the research. Acknowledgment is made to Mr. Cyril M. Harris for his assistance in building some of the experimental apparatus, and to the University of California at Los Angeles for its grant of a University Fellowship in Physics.

* The phenomenon of flutter echo is sometimes a cause of disturbance, particularly in rooms in which one pair of walls is much less absorptive than the rest. If these walls are made nonparallel, the flutter echo will be reduced or eliminated; this effect is not included in the above discussion.

The Effect of Rotatory and Lateral Inertia on Flexural Vibration of Prismatic Bars

WILLIAM T. THOMSON
Department of Applied Mechanics, Kansas State College, Manhattan, Kansas

(Received May 1, 1939)

The problem of the flexural vibration of prismatic bars neglecting the rotatory and lateral inertia is treated in various texts on sound and vibrations. The effect of neglecting these two terms introduces no appreciable error when the cross section of the bar is small in comparison to its length. For bars of large cross section the error introduced in neglecting these terms is sufficient to warrant attention. In his text on sound Rayleigh offers an approximate solution introducing a correction term for the rotatory inertia, under certain boundary conditions. In a more recent paper Mason gives an exact solution for the frequency of vibration, where the rotatory and lateral inertia are taken into account. The disadvantage of this solution lies in the fact that his Eq. (14) for the eigenvalues of the frequency is extremely complicated, thereby throwing up a barrier to further analysis. Also no mention is made by previous investigators of the effect of the rotatory and lateral inertia on the node positions or the shape of the deflection curve. It is the purpose of this paper to present a simplified exact solution and to determine the effect of the two terms mentioned on the position of the nodes and the relative amplitude of vibration. Curves applicable to the solution of any type of constant cross section are included.

THE differential equation for the flexural vibration of a prismatic bar including the rotatory inertia[1] is known to be

$$a^2k^2\partial^4y/\partial x^4+\partial^2y/\partial t^2-k^2\partial^4y/\partial x^2\partial t^2=0, \quad (1)$$

where the last term represents the effect of the rotatory inertia. When the lateral inertia is also taken into account, the equation becomes[2]

$$a^2k^2\partial^4y/\partial x^4+\partial^2y/\partial t^2-k^2(1+\sigma)\partial^4y/\partial x^2\partial t^2=0, \quad (2)^*$$

where:

y = displacement,
x = distance along bar when $y=0$,
t = time,
$a=(E/\rho)^{\frac{1}{2}}$ = transmission velocity of longitudinal waves,
E = modulus of elasticity,
ρ = mass density,
k = radius of gyration of cross section about the neutral axis,
σ = Poisson's ratio.

The two equations are alike except for the factor $(1+\sigma)$ appearing in the last term and for the sake of simplicity Eq. (1) will be used. Conversion of results to fit Eq. (2) can be taken care of by a simple manipulation.

If we assume the solution of (1) to be of the form

$$y=YT, \quad (3)$$

where Y = function of x only and T = function of t only, substitution into the differential equation results in the following expression:

$$\frac{a^2k^2d^4Y/dx^4}{k^2d^2Y/dx^2-Y}=\frac{1}{T}\frac{d^2T}{dt^2}=\text{a constant}. \quad (4)$$

The equation for T is that of simple harmonic motion reducing (3) to the form,

$$y=Y\sin\omega t.$$

The constant of Eq. (4) is therefore ω^2, and the differential equation for the maximum amplitude reduces to

$$\frac{d^4Y}{dx^4}+k^2\left(\frac{\omega}{ak}\right)^2\frac{d^2Y}{dx^2}-\left(\frac{\omega}{ak}\right)^2Y=0. \quad (5)$$

The usual method of substituting an exponential into the linear differential equation indicates that the roots of the characteristic equation result in two real and two imaginary numbers $\pm\alpha$ and $\pm j\beta$; therefore the general equation can be represented as

$$Y=A_1\cosh\alpha(x/L)+A_2\cos\beta(x/L)+A_3\sinh\alpha(x/L)+A_4\sin\beta(x/L). \quad (6)$$

[1] (a) Rayleigh, *Theory of Sound*, Vol. I, page 258. (b) Love, *Mathematical Theory of Elasticity*, Ed. 4, p. 430.
[2] (a) Love, reference 1b, p. 431. (b) Timoshenko, Phil. Mag. [6], **41**, 744 (1921); **43**, 125 (1922). (c) Timoshenko, *Vibration Problems in Engineering*. Ed. 1, page 228 and page 231.
* See Appendix.

If the axes are so chosen that $x=0$ at the center of the bar, the even function will represent the solution for the fundamental, third tone, fifth tone, etc. while the odd function will represent the second tone, forth tones, etc. This is equivalent to substituting the boundary condition at $x=0$.

Even Function

Taking first the even functions,

$$Y=A_1\cosh\alpha(x/L)+A_2\cos\beta(x/L) \qquad (7)$$

and substituting into (5)

$$\left\{\left(\frac{\alpha}{L}\right)^4+\left(\frac{\omega}{ak}\right)^2\left[\alpha^2\left(\frac{k}{L}\right)^2-1\right]\right\}A_1\cosh\alpha\left(\frac{x}{L}\right)$$
$$+\left\{\left(\frac{\beta}{L}\right)^4-\left(\frac{\omega}{ak}\right)^2\left[\beta^2\left(\frac{k}{L}\right)^2+1\right]\right\}$$
$$\times A_2\cos\beta\left(\frac{x}{L}\right)=0.$$

Since the coefficients of this equation must necessarily be zero,

$$\left(\frac{\omega}{ak}\right)^2=\left\{\frac{\alpha^4}{1-\alpha^2(k/L)^2}\right\}\frac{1}{L^4}$$
$$=\left\{\frac{\beta^4}{1+\beta^2(k/L)^2}\right\}\frac{1}{L^4}=\frac{m^4}{L^4} \qquad (8)$$

and the frequency equation becomes

$$\omega=2\pi f=m^2ka/L^2, \qquad (9)$$

where

$$m^2=\frac{\beta^2}{[1+\beta^2(k/L)^2]^{\frac{1}{2}}}=\frac{\alpha^2}{[1-\alpha^2(k/L)^2]^{\frac{1}{2}}}.$$

The values of α and β must be found from the boundary conditions which regardless of the mode of vibration requires that the bending moment and shear at the ends be zero for the "free-free bar." Expressing these boundary conditions mathematically; At $x=\pm L/2$

$$\text{Moment}=EI\partial^2y/\partial x^2=0$$

resulting in $$d^2Y/dx^2=0. \qquad (10)$$

$$\text{Shear}=EI\partial^3y/\partial x^3-\rho Ak^2\partial^3y/\partial x\partial t^2=0$$

therefore

$$a^2\partial^3y/\partial x^3-\partial^3y/\partial x\partial t^2=0$$

and $$a^2d^3Y/dx^3+\omega^2dY/dx=0. \qquad (11)$$

Substituting (7) into (10) and (11) and dividing (11) by (10)

$$\left\{\frac{(\alpha/L)^2 1/k^2+(\omega/ak)^2}{(\alpha/L)}\right\}\tanh\frac{\alpha}{2}$$
$$=\left\{\frac{(\beta/L)^2 1/k^2-(\omega/ak)^2}{(\beta/L)}\right\}\tan\frac{\beta}{2}.$$

Replacing (ω/ak) from (8), the above equation reduces to

$$-\frac{1}{\alpha^3}\tanh\frac{\alpha}{2}=\frac{1}{\beta^3}\tan\frac{\beta}{2}.$$

In order to obtain α in terms of β Eq. (8) can be rewritten as follows:

$$\alpha^4+\{(k/L)^2m^4\}\alpha^2-m^4=0$$
$$\beta^4-\{(k/L)^2m^4\}\beta^2-m^4=0.$$

Subtracting we obtain

$$(\alpha^4-\beta^4)=(\alpha^2+\beta^2)(\alpha^2-\beta^2)=-(k/L)^2m^4(\alpha^2+\beta^2),$$
$$\alpha^2=\frac{\beta^2}{1+\beta^2(k/L)^2}. \qquad (12)$$

The equation for the eigenvalues therefore reduces to

$$-\left\{1+\beta^2\left(\frac{k}{L}\right)^2\right\}^{\frac{1}{2}}\tanh\frac{\beta}{2}\left\{1+\beta^2\left(\frac{k}{L}\right)^2\right\}^{-\frac{1}{2}}$$
$$=\tan\frac{\beta}{2}. \qquad (13)$$

The solution of this equation is seen to be a function of (k/L), k being expressable as some linear dimension of cross section depending on the shape under consideration.

Equation (13) is plotted on the negative part of Fig. 1 for various values of (k/L) these curves being applicable for the fundamental, third tone, etc., and for any cross section.

It should be noticed that when $k/L=0$, m is equal to β which is found to be 4.73 for the

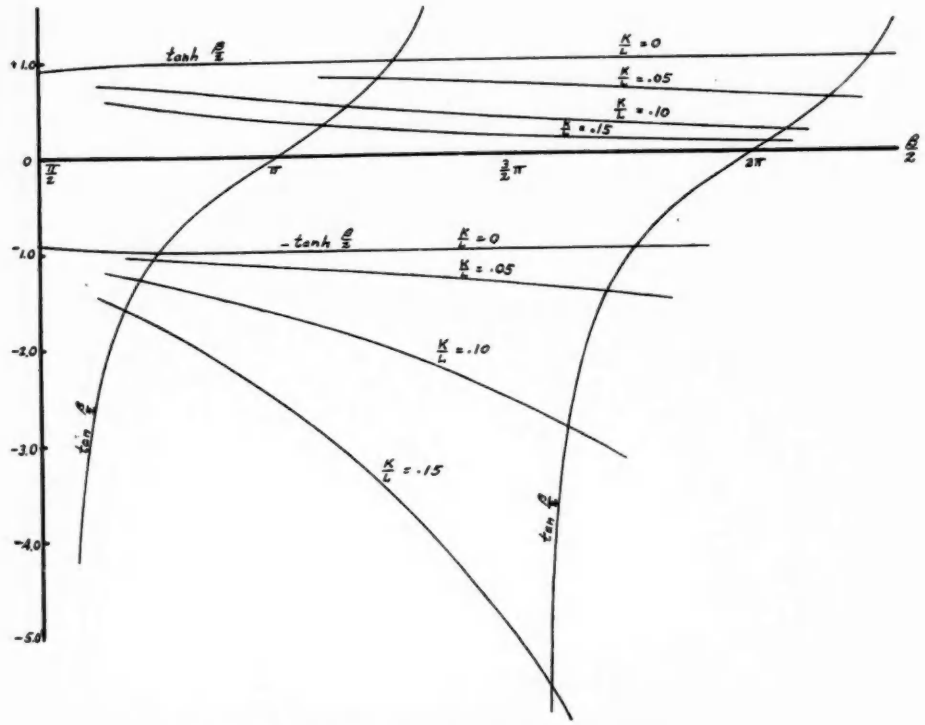

FIG. 1. Curves for the eigenvalues of Eqs. (13) and (16).

fundamental and 10.99 for the third tone. This is in agreement with the case where the rotatory inertia is neglected.

EFFECT OF LATERAL INERTIA

When Eq. (2) is used, Eq. (8) reduces to

$$\left(\frac{\omega}{ak}\right)^2=\left\{\frac{\alpha^4}{1-\alpha^2(k/L)^2(1+\sigma)}\right\}\frac{1}{L^4}$$

$$=\left\{\frac{\beta^4}{1+\beta^2(k/L)^2(1+\sigma)}\right\}\frac{1}{L^4}=\frac{m^4}{L^4}$$

and in place of Eq. (13) the following expression must be used:

$$-\left\{1+\beta^2\left(\frac{k}{L}\right)^2(1+\sigma)\right\}^{\frac{1}{2}}$$

$$\times\tanh\frac{\beta}{2}\left\{1+\beta^2\left(\frac{k}{L}\right)^2(1+\sigma)\right\}^{-\frac{1}{2}}=\tan\frac{\beta}{2}. \quad (14)$$

It is readily seen then that Fig. 1 can be used by looking up the value of $(k/L)(1+\sigma)^{\frac{1}{2}}$ instead of (k/L).

ODD FUNCTION

For the second tone, fourth tone, etc., the odd function must be used, e.g.;

$$Y=A_3\sinh\alpha(x/L)+A_4\sin\beta(x/L). \quad (15)$$

It is readily seen that Eq. (8) remains unchanged but the substitution of the boundary conditions results in a different equation for the eigenvalues. In place of (13), the equation applicable for the odd function becomes

$$\frac{1}{\{1+\beta^2(k/L)^2\}^{\frac{1}{2}}}\tanh\frac{\beta}{2}\left\{1+\beta^2\left(\frac{k}{L}\right)^2\right\}^{-\frac{1}{2}}$$

$$=\tan\frac{\beta}{2}. \quad (16)$$

the only change being the reciprocal relation and sign of the factor on the left side of the equation.

The curves representing Eq. (16) are plotted on the positive side of Fig. 1, and, as in the case for the even function, the lateral inertia can be taken into account by using $(k/L)(1+\sigma)^{\frac{1}{2}}$ in place of (k/L).

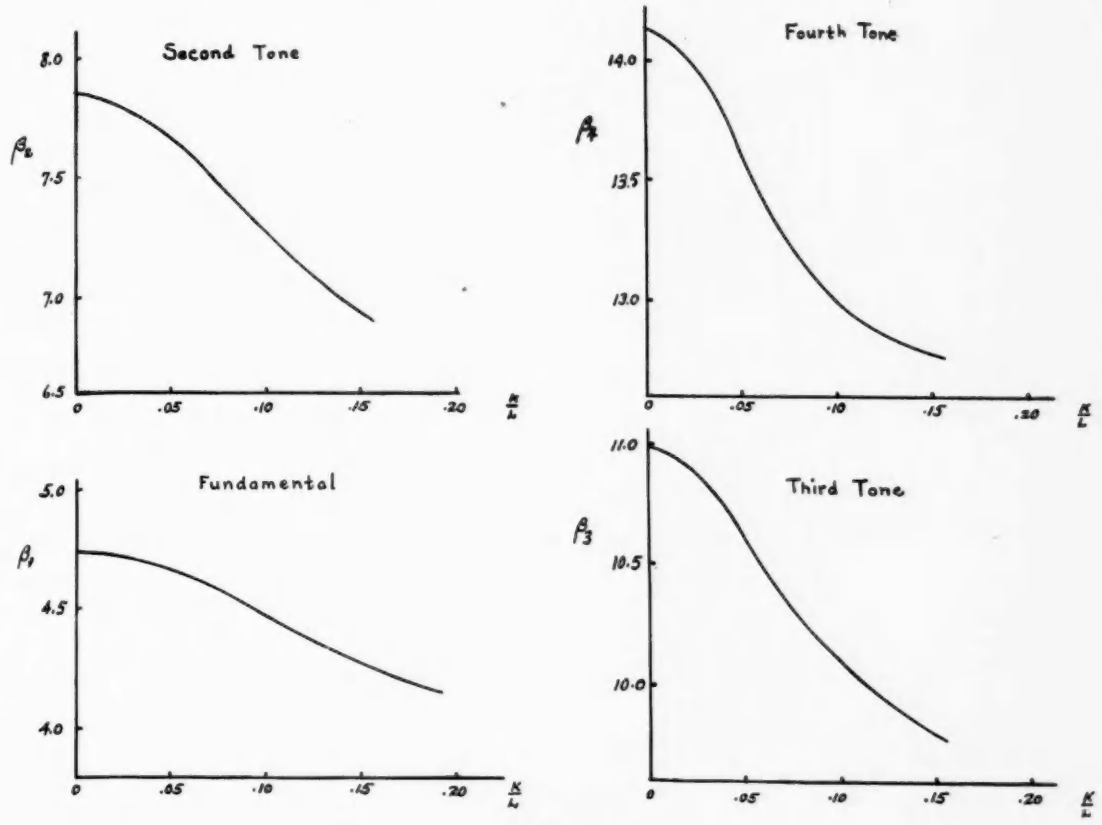

FIG. 2.

As in the previous case, when $k/L=0$ the values for $m=\beta$ are in conformity with the simple case. It is also apparent from Fig. 1 that the rotatory and lateral inertia terms become of greater significance for the higher frequencies. The values of β for the various modes of vibration are plotted in Fig. 2 and the values of m in Fig. 3. It is readily seen from Fig. 1 that for the case where $k/L=0$, m for any mode of vibration can be expressed approximately as

$$m=(n+\tfrac{1}{2})\pi,$$

where $n=1, 2, 3, 4$. For the fundamental, m can be expressed with sufficient accuracy by the following equation when k/L is less than 0.13

$$m=4.73/[1+4.73^2(k/L)^2]^{\frac{1}{2}}.$$

DEFLECTION CURVE AND THE LOCATION OF NODES

For the shape of the deflection curve and the location of the nodes (excluding rotatory and lateral inertia) the reader is referred to pages 282–284 of reference 3a. For the fundamental, the value given for the node position is $0.2242L$ from the ends, while the ratio of the amplitude at ends to that at the center is 1.645.

When the rotatory and lateral inertia terms are included these values are no longer correct; the shape of the curve and the node positions being a function of $(k/L)(1+\sigma)^{\frac{1}{2}}$

A. Even function

Starting from Eq. (7) and using the boundary condition (10), one of the constants can be eliminated such that Y can be expressed as

$$Y=A_1\left\{\cosh\alpha\left(\frac{x}{L}\right)+\left(\frac{\alpha}{\beta}\right)^2\frac{\cosh\alpha/2}{\cos\beta/2}\cos\beta\left(\frac{x}{L}\right)\right\}.$$

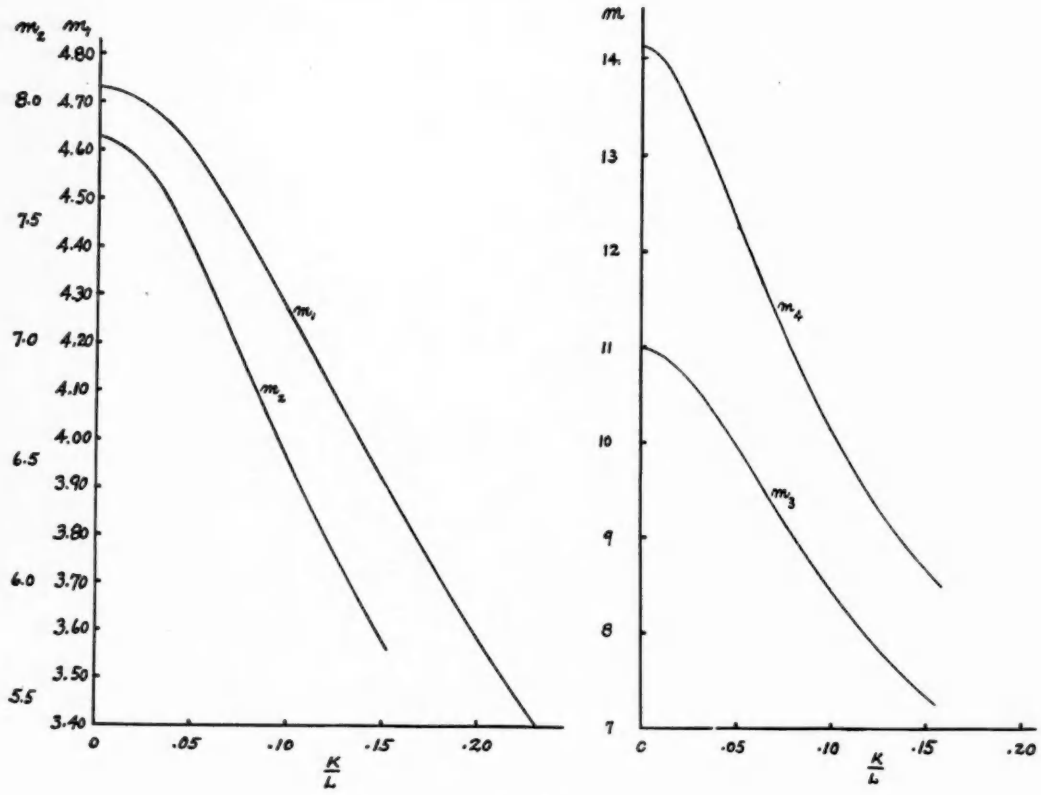

FIG. 3.

Replacing α in terms of β from (12)

$$Y=A_1\left\{\cosh\frac{\beta}{[1+\beta^2(k/L)^2]^{\frac{1}{2}}}\left(\frac{x}{L}\right)+\frac{1}{1+\beta^2(k/L)^2}\left(\frac{\cosh\beta/2[1+\beta^2(k/L)^2]^{\frac{1}{2}}}{\cos\beta/2}\right)\times\cos\beta\left(\frac{x}{L}\right)\right\}. \quad (17)$$

For the nodes $Y=0$ and

$$\cosh\frac{\beta}{[1+\beta^2(k/L)^2]^{\frac{1}{2}}}\left(\frac{x}{L}\right)=-\frac{1}{1+\beta^2(k/L)^2}\times\left(\frac{\cosh\beta/2[1+\beta^2(k/L)^2]^{\frac{1}{2}}}{\cos\beta/2}\right)\cos\beta\left(\frac{x}{L}\right). \quad (18)$$

When k/L is zero the above equation gives the value of x/L for the fundamental as 0.2758, placing the nodes at a distance of $0.2242L$ from the ends as shown by Rayleigh. When $k/L=0.15$, the value of x/L for the nodes is found to be 0.2783 placing the nodes at points 0.2217 from the ends. It is seen then that the rotatory and lateral inertia tend to shift the nodes toward the ends of the bar. This shift is quite small for the fundamental but will be shown to be of more importance in the case of the second mode of vibration.

From (17) the deflections at the ends and center of the beam are

$$Y_{x=\pm L/2}=A_1\left\{1+\frac{1}{1+\beta^2(k/L)^2}\right\}\times\cosh\frac{\beta}{2[1+\beta^2(k/L)^2]^{\frac{1}{2}}},$$

$$Y_{x=0}=A_1\left\{1+\frac{1}{1+\beta^2(k/L)^2}\cdot\frac{\cosh\beta/2[1+\beta^2(k/L)^2]^{\frac{1}{2}}}{\cos\beta/2}\right\}.$$

Therefore, the ratio of the deflection at the ends to that at the center is

$$\frac{Y_{x=\pm L/2}}{Y_{x=0}}=\frac{\left\{1+\dfrac{1}{1+\beta^2(k/L)^2}\right\}\cosh\dfrac{\beta}{2[1+\beta^2(k/L)^2]^{\frac{1}{2}}}}{\left\{1+\dfrac{1}{1+\beta^2(k/L)^2}\cdot\dfrac{\cosh\beta/2[1+\beta^2(k/L)^2]^{\frac{1}{2}}}{\cos\beta/2}\right\}}. \tag{19}$$

To obtain the entire deflection curve, Eq. (17) can be solved for Y/A_1. Here also the ratio as formed from (19) agrees with the simple case when $k/L=0$. The deflection curve for the fundamental showing the node position and relative amplitude is plotted in Fig. 4 for the case $k/L=0.15$. It should be noted from Table I that the maximum amplitude is reduced approximately to $\frac{1}{2}$ when $k/L=0.15$.

B. Odd function

Observation of Eq. (15) indicates that the node position for the odd function can be obtained from Eq. (18) when the cosine and cosh terms are replaced by sin and sinh, respectively. The node equation then becomes

$$\sinh\frac{\beta}{[1+\beta^2(k/L)^2]^{\frac{1}{2}}}\left(\frac{x}{L}\right)=\frac{-1}{\{1+\beta^2(k/L)^2\}}\times\frac{\sinh\beta/2[1+\beta^2(k/L)^2]^{\frac{1}{2}}}{\sin\beta/2}\cdot\sin\beta\left(\frac{x}{L}\right). \tag{20}$$

Since the deflection at the center will be zero for odd functions, the elastic curve must be obtained in terms of the deflection at the ends. This ratio is expressed by the following equation:

$$\frac{Y}{Y_{x=\pm L/2}}=\frac{\left\{\sinh\dfrac{\beta}{[1+\beta^2(k/L)^2]^{\frac{1}{2}}}\left(\dfrac{x}{L}\right)+\dfrac{1}{1+\beta^2(k/L)^2}\left(\dfrac{\sinh\beta/2[1+\beta^2(k/L)^2]^{\frac{1}{2}}}{\sin\beta/2}\right)\sin\beta\left(\dfrac{x}{L}\right)\right\}}{\{1+1/(1+\beta^2(k/L)^2)\}\sinh\beta/2[1+\beta^2(k/L)^2]^{\frac{1}{2}}}. \tag{21}$$

For comparative purposes the elastic curve for $k/L=0.15$ is plotted in Fig. 5 against the curve for $k/L=$ zero. It is seen here that the effect of the rotatory and lateral inertia is more pronounced than in the fundamental mode of vibration. The node is displaced towards the ends as in the previous case and has been shifted from 0.1321 to 0.1050 from the ends. The ratio of amplitude at the loop to that at the ends has also been changed from 0.664 to 0.859.

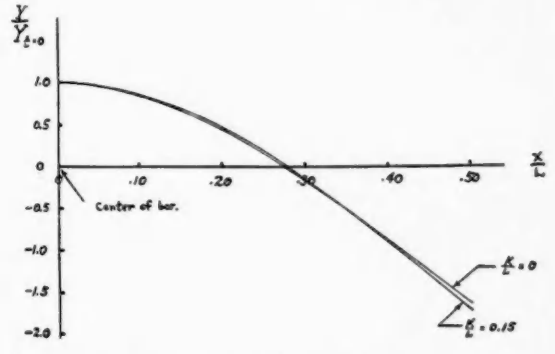

FIG. 4. Deflection curve of "free-free" bar including rotatory and lateral inertia. Vibration with two nodes.

APPENDIX

The effect of shear

Timoshenko[2b, c] has shown that the effect of shear introduces two additional terms:

$$-k^2\frac{E}{k'G}\frac{\partial^4 y}{\partial x^2\partial t^2}+k^2\frac{\rho}{k'G}\frac{\partial^4 y}{\partial t^4},$$

where $G=$ modulus of elasticity in shear $=E/2(1+\sigma)$

$k'=$ average shear/maximum shear, a factor depending on the shape of the cross section ($k'=\frac{2}{3}$ for a rectangular beam).

It is seen that the second term is negligible compared to the first term and the remaining

TABLE I.

$\frac{x}{L}$	$(Y/A_1)_{k/L=0.15}$	$(Y/Y_0)_{k/L=0.15}$	$(Y/A_1)_{k/L=0}$
Fundamental mode			
0	3.112	1.00	6.53
0.10	2.67	0.8575	
.20	1.43	.459	
.278	0.008	.00257	Amplit. ratio $=\frac{3.112}{6.53}=0.476$
.280	−0.045	− .0144	
.40	−2.787	− .8957	
.50	−5.299	−1.703	−10.73
Second mode			
0	0	0	0
0.05	2.572	0.317	
.10	4.795	.591	
.19	6.975	.859	
.25	6.667	.822	
.30	5.224	.646	Amplit. ratio $=\frac{8.11}{50.72}=0.160$
.370	1.651	.203	
.380	1.008	.124	
.390	0.343	.0422	
.395	−0.0011	− .00013	
.45	−4.096	− .505	
.50	−8.11	−1.00	−50.72

term may be written as:

$$-k^2\frac{2(1+\sigma)}{k'}\frac{\partial^4 y}{\partial x^2\partial t^2}.$$

When substituted in Eq. (2), the differential equation becomes

$$a^2k^2\frac{\partial^4 y}{\partial x^4}+\frac{\partial^2 y}{\partial t^2}-k^2\left\{1+\sigma+\frac{2(1+\sigma)}{k'}\right\}\frac{\partial^4 y}{\partial x^2\partial t^2}=0.$$

As shown by Timoshenko,[2b] the shear term is of greater importance than the rotatory inertia term and the ratio of shear to inertia terms is $2/k'$.

This change due to shear will not affect the general solution presented in this paper and the curves presented are applicable to this case as well. The effect of shear can be taken account

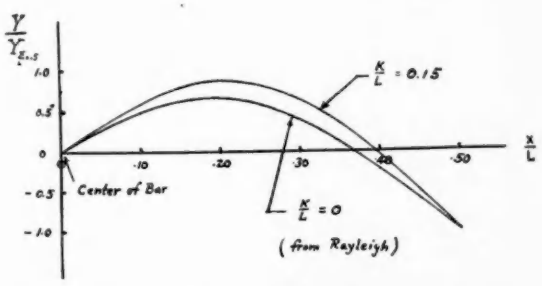

FIG. 5. Deflection curve of "free-free" bar including rotatory and lateral inertia. Vibration with three nodes.

of by exactly the same procedure used in taking account of the lateral inertia and it is only necessary to use the value of

$$k(1+\sigma+2(1+\sigma)/k')^{\frac{1}{2}}$$

in place of k or $k(1+\sigma)^{\frac{1}{2}}$.

In closing, the writer wishes to express thanks to Professor E. E. Weibel of the University of California for suggestions to include the shear term.

[3] (a) Rayleigh, Chap. VIII of reference 1a. (b) A. B. Wood, *A Text Book on Sound*.

[4] Mason, "Motion of a Bar Vibrating in Flexure, including the Effect of Rotatory and Lateral Inertia," J. Acous. Soc. Am. **6**, 246–249 (1935).

The Transmission of Sound Inside Pipes

PHILIP M. MORSE
Eastman Laboratory, Massachusetts Institute of Technology, Cambridge, Massachusetts

(Received August 7, 1939)

Methods developed in a previous paper are used to obtain an exact solution for the transmission of sound inside a rectangular pipe with absorbing material on its inner walls. Plots are given whereby it is possible to determine the phase velocity and attenuation of the simpler type waves in terms of the specific acoustic impedance of the walls and the frequency of the wave. Several examples are given of the effect of the absorbing surfaces on the distribution of the sound pressure amplitude over a plane perpendicular to the axis of the pipe. The effect of the reactive part of the material's acoustic impedance on the attenuation of the sound is also discussed. Formulas are developed for the transmission of sound in tubes of circular cross section. The plots for rectangular pipes can also be used in calculations of the acoustical properties of rectangular rooms.

THE attenuation of sound waves inside capillary tubes is due largely to the viscosity of the air. This phenomenon has been studied by Helmholtz and others. For larger diameter tubes, however, the effect of viscosity is negligible; and the attenuation is due to the absorption of energy by the pipe walls. This phenomenon is similar to the absorption, by the walls, of sound energy in a room; and the theoretical analysis of the problem is very similar to the analysis of room acoustics.[1]

Recent experimental studies[2] have indicated that the absorbing qualities of a surface are measured in terms of its *normal acoustic impedance*, and theoretical techniques[1] have been developed to compute the acoustic properties of some rooms in terms of the impedances of their walls. In the present paper these techniques will be applied to the transmission and attenuation of sound in pipes which are large enough so that the effect of viscosity is negligible. Most of the calculations will be made for rectangular pipes, although circular pipes will be discussed. It will be assumed that one or more of the inner surfaces are uniformly covered with absorbing material, and that the remaining surfaces are perfectly rigid.

[1] P. M. Morse, J. Acous. Soc. Am. **11**, 56 (1939). Hereinafter called I. Note also the comments by L. Brillouin, J. Acous. Soc. Am. **11**, 10 (1939).

[2] F. J. Willig, J. Acous. Soc. Am. **10**, 257(A) (1938); F. V. Hunt, J. Acous. Soc. Am. **10**, 216 (1938); F. V. Hunt, L. L. Beranek and D. Y. Maa, J. Acous. Soc. Am. **11**, 80 (1939); N. B. Bhatt, J. Acous. Soc. Am. **11**, 67 (1939).

One Wall Absorbing

Let us first study the simplest case, that of a rectangular pipe of cross section (ll'), having one inner surface absorbing and the other three surfaces perfectly rigid. We set the axis of the tube parallel to the x axis, and set the absorbing wall in the $y=l$ plane. There are many types of waves which can travel down the tube, some having pressure nodes parallel to the (x, y) plane. The simplest wave, however, has no such nodes, and its pressure is expressed by the formula

$$p=P_0\cosh\left[(\pi y/l)(\kappa-j\mu)\right]\cdot\exp\left[j\omega t-(\omega/c)(\sigma+j\tau)x\right]. \quad (1)$$

The constants κ and μ are fixed by the boundary conditions[1] in a manner discussed in I and treated further later in this paper. For the simplest wave μ is usually smaller than $(\frac{1}{2})$ and p is nearly uniform in magnitude across the tube (i.e., it does not depend very markedly on y). The physical reasons for the fact that p does depend to some extent on y are given in I.

The frequency constant ω is of course determined by the driving mechanism which introduces the wave at one end of the tube. The constants σ and τ are fixed by the values of κ and μ, and therefore by the boundary conditions. The quantity $(2\pi c/\tau\omega)$ is the wave-length of the wave in the tube, and (c/τ) is the phase velocity of the wave, where c is the velocity in free space. The constant σ determines the attenuation of the wave as it travels down the pipe: $e^{-2\pi\sigma}$ being the

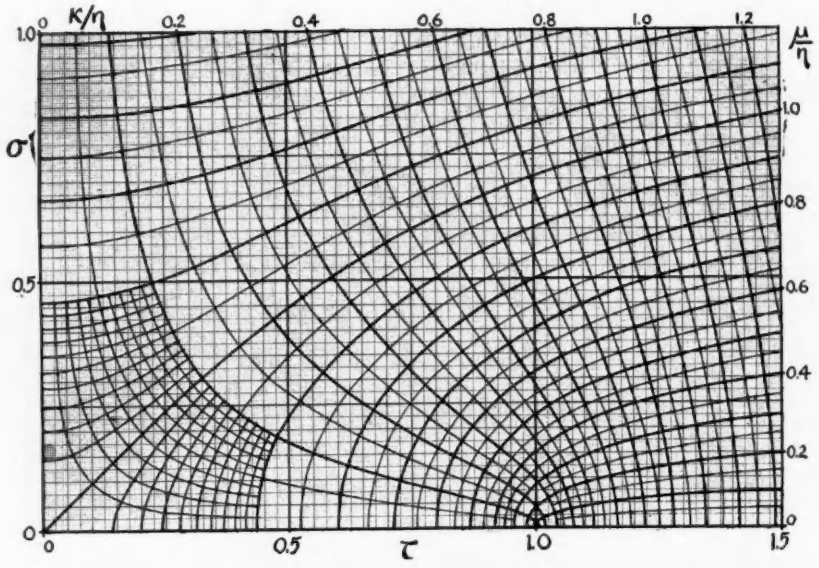

FIG. 1. Conformal transformation between the distribution parameters μ and κ and the transmission parameters τ and σ.

decrease in amplitude per wave-length, 54.6σ the attenuation in db per wave-length, and

$$54.6(\sigma\nu/c)=8.686(\omega\sigma/c)$$
$$=\text{attenuation in db per cm (or foot)}, \quad (2)$$

where c is the velocity of sound in free space in cm (or feet) per sec., and where ν is the frequency of the wave.

To obtain the dependence of σ and τ on κ and μ we set Eq. (1) in the wave equation for the pressure, obtaining

$$(\sigma+j\tau)^2=[(\mu/\eta)+j(\kappa/\eta)]^2-1,$$
$$\eta=(2l\nu/c)=(2l/\lambda). \quad (3)$$

The quantity η may be called the *frequency parameter* for the y walls; it relates the distance between the walls perpendicular to the y axis to the wave-length of the sound in free space. In Fig. 1 is drawn the conformal transformation relating the complex quantity $(1/\eta)(\mu+j\kappa)$ to the complex *transmission parameter* $(\sigma+j\tau)$. By means of this plot the phase velocity and attenuation can be found once μ and κ are known. Since the complex quantity $(\mu+j\kappa)$ determines the distribution of the pressure amplitude across the tube, it will be called the *distribution parameter*.

When κ is small compared to η, the approximate formulas for the transformation are

$$\tau\backsimeq[1+(\kappa/\eta)^2-(\mu/\eta)^2]^{\frac{1}{2}}, \quad \sigma\backsimeq(\mu\kappa/\tau\eta^2). \quad (4)$$

CALCULATION OF THE DISTRIBUTION PARAMETER

Returning to Eq. (1) for the pressure, we note that the boundary conditions[1] at the four walls are

$$\begin{aligned}(\partial p/\partial z)&=0, \quad z=0, \quad z=l',\\ (\partial p/\partial y)&=0, \quad y=0,\\ -(Z/j\omega\rho)(\partial p/\partial x)&=p, \quad y=l,\end{aligned} \quad (5)$$

where ρ is the air density and Z is the specific acoustic impedance of the absorbing surface, the ratio of the pressure at the surface to the normal velocity of the surface. The impedance Z is often complex, having a resistive part X and a reactive part Y; a magnitude $|Z|$ and phase angle φ. Substitution of Eq. (1) in the boundary conditions results in an equation for the distribution parameter $(\mu+j\kappa)$ in terms of the impedance Z of the absorbing surface and of the frequency parameter $\eta=(\omega l/\pi c)$,

$$\frac{\coth[-j\pi(\mu+j\kappa)]}{\mu+j\kappa}=(Z/\rho c\eta)$$
$$=\exp[\ln(|Z|/\rho\eta c)+j\varphi]. \quad (6)$$

This equation corresponds to a conformal transformation between the quantities (μ, κ)

and the quantities $(X/\rho c\eta,\ Y/\rho c\eta)$ or the quantities $\ln(|Z|/\rho c\eta)$ and φ. It is not a single valued transformation, for the hyperbolic cotangent is periodic with μ. Because of the presence of $(\mu+j\kappa)$ in the denominator, however, the quantity $(Z/\rho c\eta)$ is not a periodic function of μ, so that each sheet of the Riemann surface must be plotted separately. The equations for the transformation to the $\ln(|Z|/\rho c\eta)$, φ plane are

$$|Z|/\rho\eta c=\left[\frac{\cosh 2\pi\kappa+\cos 2\pi\mu}{(\cosh 2\pi\kappa-\cos 2\pi\mu)(\mu^2+\kappa^2)}\right]^{\frac{1}{2}}$$
$$\varphi=\tan^{-1}[\sin 2\pi\mu/\sinh 2\pi\kappa]-\tan^{-1}(\kappa/\mu). \tag{7}$$

If $(|Z|/\rho c\eta)$ is plotted on a logarithmic scale, and the scale of φ is adjusted properly, the transformation will be conformal.

Figures 2 and 3 show the first two sheets of this transformation.[3] The vertical scale gives the magnitude of $(Z/\rho c\eta)$ and the horizontal scale the phase angle φ in degrees, divided by the proper scale factor, 13.2. The curved lines represent the orthogonal coordinate system for μ and κ. The blank spaces in each plot represent the transition from one Riemann surface to the next; the κ contours approaching the break from the right on the first sheet joining the κ contours approaching the blank from the left on the second sheet; the junction for the μ contours being in the opposite direction. Series expansions for this transformation were developed in I. An approximation valid for values of $(|Z|/\rho c\eta)$ larger than those given in the plots is

$$\begin{aligned}\mu &\backsimeq \cos[(\pi/4)-(\varphi/2)]\cdot[\rho c\eta/4\pi|Z|]^{\frac{1}{2}}\\ \kappa &\backsimeq \sin[(\pi/4)-(\varphi/2)]\cdot[\rho c\eta/4\pi|Z|]^{\frac{1}{2}}\\ &\qquad\text{for the first cycle}\\ \mu &\backsimeq n+(\rho c\eta/\pi n|Z|)\sin\varphi\\ \kappa &\backsimeq(\rho c\eta/\pi n|Z|)\cos\varphi\\ &\qquad\text{for the } (n+1)\text{th cycle.}\end{aligned} \tag{8}$$

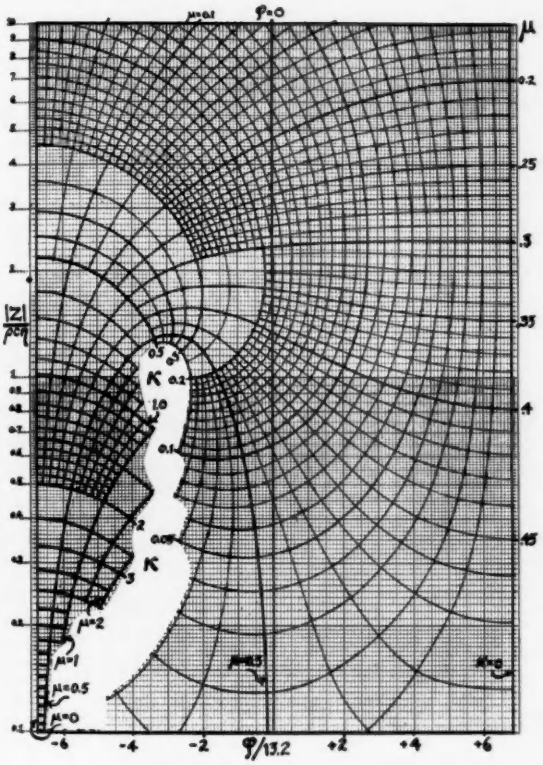

FIG. 2. Transformation between the impedance and frequency parameters and the distribution parameters, for the first cycle. Abscissa is impedance phase angle in degrees, divided by 13.2, to make the transformation conformal. Blank space is at the junction between the first and second cycles of the transformation.

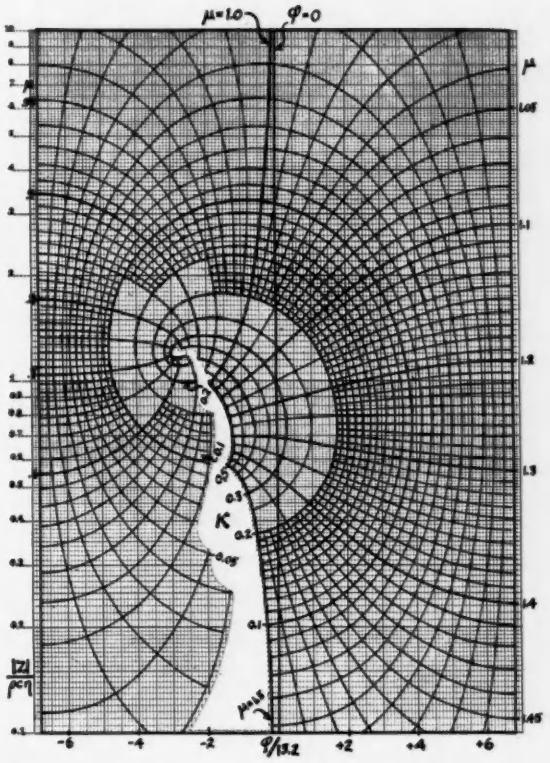

FIG. 3. Transformation between the impedance and frequency parameters and the distribution parameters, for the second cycle.

[3] Hunt, Beranek and Maa, reference 2, Fig. 6, have plotted curves of constant $(\mu\kappa)$ on the log Z, φ plane, but have not included the orthogonal family $(\mu^2-\kappa^2)$. Only the first sheet of the transformation is given.

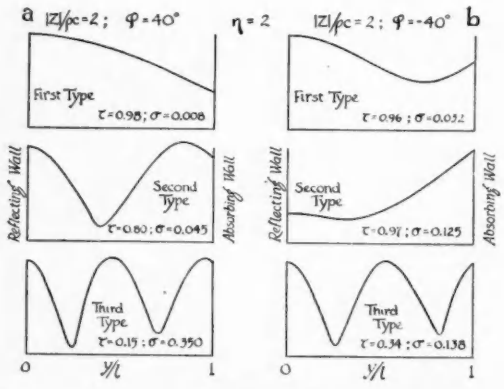

FIG. 4. Distribution of pressure amplitude across a pipe, plotted as function of the distance away from the absorbing wall. Distributions for the first three types of wave are shown, for two different impedance phase angles. Values of the transmission parameters are given for each type wave.

For positive values of φ or large values of $(|Z|/\rho c\eta)$ the relation between the impedance and the distribution parameter is fairly simple. For such values of Z, the different types of waves, corresponding to the different cycles of the transformation, have pressure distributions, across the tube, which are easily distinguishable one from the other. As an example, Fig. 4*a* shows the dependence of the pressure amplitude on y for the first three types of waves, for $(|Z|/\rho c\eta)=1$ and $\varphi=+40°$. The first wave, corresponding to the first cycle (Fig. 2), has no nodal surfaces parallel to the y walls; the second, corresponding to the second cycle, has one "node" (not completely zero because κ is not zero); and the third wave, corresponding to the third cycle, has two "nodes."

On the other hand, there are several regions for negative φ and small values of $(|Z|/\rho c\eta)$ where some of the contours have small loops or even cusps and the distinction between one Riemann surface and the next becomes rather vague. There is no singularity in these regions, however, the transformation being conformal throughout. The region where the first and second sheets are "mixed up" is near $(|Z|/\rho c\eta)=1.2$ and $\varphi=-40°$; the one "mixing up" the second and third sheets is near $(|Z|/\rho c\eta)=0.55$ and $\varphi=-25°$; and so on. For such values of Z it is hard to distinguish between the two types of waves which correspond to the two Riemann surfaces which are "mixed up." For example, Fig. 4*b* shows the distribution of the pressure amplitude across the tube for $(|Z|/\rho c\eta)=1$ and $\varphi=-40°$. It is difficult to decide which of the first and second type waves has no "node," and which has one "node." In this case it has seemed best to call the wave having the smaller value of μ the first type, and that having the larger μ the second type.[4]

In the majority of cases κ is small enough compared to η so that the approximate formulas (4) apply. In this case it is easier to use the conformal transformation from $(Z/\rho c\eta)$ to $(U+jV)=(\mu+j\kappa)^2=\mu^2-\kappa^2+2j\mu\kappa$. In terms of the new parameters, U and V, the approximate formulas for the transmission parameters become

$$\tau \backsimeq [1-(U/\eta^2)]^{\frac{1}{2}}, \quad \sigma \backsimeq (V/2\eta^2\tau), \quad V \ll \eta^2.$$

To this approximation U determines the ratio between the phase velocity of the wave and the

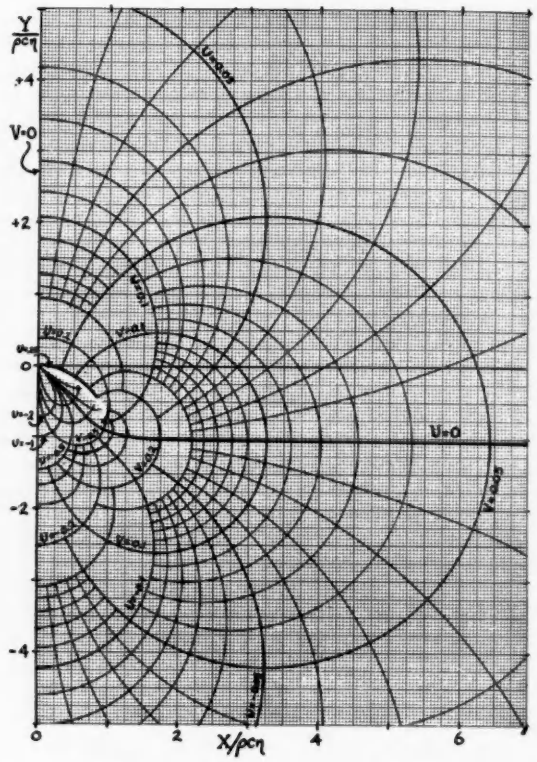

FIG. 5. First cycle of the transformation between acoustic resistance and reactance of the absorbing wall, and the parameters $U=\mu^2-\kappa^2$ and $V=2\mu\kappa$. When V is small compared to η^2, it is proportional to the attenuation of waves in a tube, or to the damping coefficient for waves in a rectangular room.

[4] This is the reason for the difference noted by Hunt, Beranek and Maa, reference 2, page 93, between their curves and those of reference 1. Presumably they consider the wave with the larger value of $(\mu\kappa)$ to be the first type wave.

velocity in free space, and V is proportional to its attenuation along the tube. Figs. 5 and 6 give the first two cycles of the transformation from $(X/\rho c\eta)$, $(Y/\rho c\eta)$ to U and V. We note the resemblance to the bipolar transformation which is useful in electric transmission line calculations, and in calculations determining acoustic impedances looking into a pipe.[5]

For those values of $(|Z|/\rho c\eta)$ larger than shown on the plots, the series formulas given in I show that the approximate formulas

$$\begin{aligned} U &\backsimeq (\rho c\eta/\pi|Z|)\sin\varphi, \\ V &\backsimeq (\rho c\eta/\pi|Z|)\cos\varphi, \end{aligned} \qquad \text{first cycle} \quad (9)$$

$$\begin{aligned} U &\backsimeq n^2+(2\rho c\eta/\pi|Z|)\sin\varphi, \\ V &\backsimeq (2\rho c\eta/\pi|Z|)\cos\varphi, \end{aligned}$$

all other cycles, are valid.

Two or More Walls Absorbing

When both walls perpendicular to the y axis are covered with absorbing material of acoustic impedance Z, the equation for the distribution parameters is, according to I,

$$\frac{\coth\left[-\frac{1}{2}\pi j(\mu+j\kappa)\right]}{\frac{1}{2}(\mu+j\kappa)}=(2Z/\rho c\eta). \qquad (10)$$

A comparison with Eq. (6) shows that Eqs. (7) and (8), and Figs. 2, 3, 5 and 6 can still be used for a pipe with two parallel walls coated with similar absorbing material, provided that $(2Z)$, $(2X)$, $(2Y)$ be substituted for Z, X, Y in the equations and in the plots; and that $(\mu/2)$, $(\kappa/2)$, $(U/4)$, $(V/4)$ be substituted for μ, κ, U, V. Thus for a single absorbing wall with $(|Z|/\rho c\eta)=3$, $\varphi=-40°$, Fig. 2 shows that $\mu=0.2$, $\kappa=0.3$ for the first type wave; whereas for two parallel absorbing walls with $(|Z|/\rho c\eta)=1.5$, $\varphi=-40°$, the corresponding parameters are $\mu=0.4$ and $\kappa=0.6$.

When three or four walls are absorbing, there will be two sets of parameters η, μ, κ; a set for each wall pair. In this case Eq. (3) for the transmission parameter is changed to

$$(\sigma+j\tau)^2=[(\mu_y/\eta_y)+j(\kappa_y/\eta_y)]^2+[(\mu_z/\eta_z)+j(\kappa_z/\eta_z)]^2-1.$$

[5] P. M. Morse, *Vibration and Sound* (McGraw-Hill), p. 192. See also W. M. Hall, J. Acous. Soc. Am., **11**, 142 (1939).

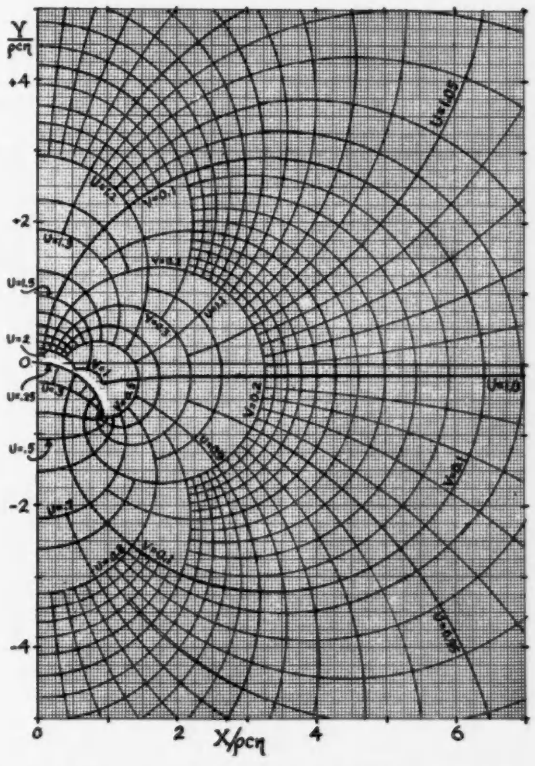

FIG. 6. Transformation between acoustic resistance and reactance of the absorbing wall, and the parameters U and V, for the second cycle of the transformation.

In this case Eq. (4) cannot be used; nor can Fig. 1, except for one special case. When the pipe has a square cross section, all four walls being covered with similar material, and when only the simplest type wave is considered, so that $\mu_y=\mu_z$ and $\kappa_y=\kappa_z$; then Fig. 1 can be used, provided $(2^{\frac{1}{2}}\mu/\eta)$, $(2^{\frac{1}{2}}\kappa/\eta)$ are substituted for (μ/η) and (κ/η) in the labels on the plot.

Cylindrical Pipes

When the pipe has a circular cross section, of radius a, the distribution of pressure for the simplest type wave is

$$p=P_0J_0[(\pi r/a)(\mu+j\kappa)]\cdot\exp\left[j\omega t-(\omega/c)(\sigma+j\tau)x\right], \qquad (11)$$

where the transmission parameter $(\sigma+j\tau)$ is related to $(\mu+j\kappa)$ by Eq. (3) or Fig. 1, if we let $\eta=(4\nu a/c)=(2\omega a/\pi c)$. The radial velocity of the air is

$$u=-(j/\rho c\eta)(\mu+j\kappa)P_0J_1[(\pi r/a)(\mu+j\kappa)]\cdot\exp\left[j\omega t-(\omega/c)(\sigma+j\tau)x\right].$$

The boundary condition at $r=a$ can be put into a form suitable for computation by using the addition rule for Bessel functions:

$$J_m(x+y)=\sum_{n=-\infty}^{\infty} J_{m-n}(x)J_n(y).$$

Using also the definition $J_n(jz)=j^nI_n(z)$, where the function I_n is real, the boundary condition $p=Zu$ at $r=a$ becomes the equation

$$(A-jB)=-j(Z/\rho c\eta)(\mu+j\kappa)(C+jD),$$

where

$$A=J_0(\pi\mu)I_0(\pi\kappa)+2\sum_{n=1}^{\infty}(-1)^nJ_{2n}(\pi\mu)I_{2n}(\pi\kappa),$$

$$B=2\sum_{n=0}^{\infty}(-1)^nJ_{2n+1}(\pi\mu)I_{2n+1}(\pi\kappa), \tag{12}$$

$$C=\sum_{n=0}^{\infty}(-1)^nJ_{2n+1}(\pi\mu)[I_{2n}(\pi\kappa)+I_{2n+2}(\pi\kappa)],$$

$$D=\sum_{n=0}^{\infty}(-1)^nI_{2n+1}(\pi\kappa)[J_{2n}(\pi\mu)-J_{2n+2}(\pi\mu)].$$

The series expressions converge fairly rapidly; as long as κ is less than unity, the first four or five terms will suffice for three-place accuracy.

Conclusions

Several results of interest in the study of sound transmission inside of pipes can be obtained from the preceding calculations and curves. In the first place we notice that, other things being equal, a material with negative acoustic reactance produces more attenuation than one with a positive reactance. In other words a wall which has stiffness plus resistance is, in general, more absorbing than one with mass plus resistance; although there are exceptions to this rule for a narrow range of small values of impedance.

We also notice that for given values of η, X and Y, the attenuation for the simplest wave (with no "nodes," given on the first cycle of the plots) is usually less than that for the more complicated waves. The exception to this rule occurs for impedances near the point $(|Z|/\rho c\eta)\backsimeq 1.18$, $\varphi\backsimeq -40°$, where waves of the first and second type become identical, both having parameters $\mu\leqq 0.7$ and $\kappa\leqq 0.4$. Very near this point both waves are nearly alike, and their attenuations are nearly equal; but the "region of confusion" is quite small, having a spread in the direction of the $(|Z|/\rho c\eta)$ axis of only about 0.05. For large values of $(Z/\rho c\eta)$ Eqs. (9) show that the waves of higher type have twice the attenuation of those of the simplest type. For smaller values of impedance (or larger values of frequency) the ratio is larger than two to one, with the exception of the small region noted above. Therefore if the wave sent in at one end of the tube is a complex one, made up of waves of several different types, by the time the average amplitude has attenuated ten db, the components higher than the first type will have attenuated 20 db or more, and the wave will be hardly distinguishable from a pure first type wave. In general, any acoustic treatment which absorbs to a satisfactory degree the simplest type of wave will absorb all the higher type waves still better.

Thus we see that the distribution parameters μ and κ, determining the departure of the wave from a uniform plane wave, are related to the impedance of the walls on the one hand, and to the transmission parameters on the other. By means of the transformations given in this paper, one can start from a knowledge of the wall impedance, and by obtaining μ and κ as an intermediate step, can predict the attenuation and phase velocity for the simpler waves inside any given rectangular tube. Similarly, from measurements of attenuation and phase velocity in a given tube, one can obtain first the parameters μ and κ, and then the impedance of the tube walls. Finally, if one can obtain the parameters μ and κ directly by measuring the amplitude and phase relations of the wave across a cross section of the tube, then one can compute both the transmission parameters and the wall impedance.

One can also use the plots given in this paper to compute the acoustic properties of a rectangular room, instead of using the curves and series expansions given in I. The discussion in I shows how this can be done.

Sound Insulation Characteristics for Ideal Partitions

KERON C. MORRICAL
RCA Manufacturing Company, Camden, New Jersey
(Received May 23, 1939)

VARIOUS methods of specifying the practical performance of partitions and other building units have been proposed and used from time to time, all tending, for reason of simplicity, to the use of a single number expression.

Let us consider these methods in the order of their appearance. Early measurements on the effectiveness of a partition consisted in observing the sound intensity on the two sides of the partition and expressing the sound reduction as the ratio of these two intensities. This ratio was later expressed in decibels. Because the measurement was made at a single frequency, usually 500 c.p.s., a single number expression existed *per se*. When, later, measurements were extended to include a number of frequencies, the old criterion of specifying the reduction at 500 c.p.s. was still adhered to by some observers, while others used the average value of the results at all the several frequencies used. A yet different method of determining an average figure grew from an attempt to procure uniformity among the different observers by drawing the average value over the arbitrarily selected range 250 c.p.s. to 2000 c.p.s.

Early observers did not always differentiate between transmission loss and reduction factor, which fact led to some uncertainty in the interpretation of the data. The transmittivity, τ, is defined as the ratio of the intensity in the beam transmitted by the partition to the intensity in the beam incident upon the partition. Transmission loss expresses this ratio in decibels as

$$\text{T.L.} = 10 \log_{10} \frac{I_i}{I_t} = 10 \log_{10} \frac{1}{\tau}.$$

The reduction factor, k, is the ratio of the sound energy density in the transmitting room to that in the receiving room, and is related to the transmission loss by the expression

$$\text{R.F. (decibels)} = \text{T.L.} + 10 \log_{10} a/A,$$

where A is the area of the test partition and a is the total absorption in the receiving room. The receiving room conditions therefore appear as a correction to be applied to the reduction factor in order to obtain the transmission loss. In the laboratory this factor may vary over a considerable range either side of zero depending upon whether a dead room or a reverberant room is used as the receiving room. Knudsen[1] performed an invaluable piece of work in analyzing all these various data and expressing the results uniformly in reduction factors.

The writer has long objected to the use of an arbitrary average value of transmission loss on the grounds that any average, no matter how determined, does not present a true picture of the action of a partition. Considering now only the physical side of the problem, the establishment of an average value from the transmission characteristic does not reveal important features such as a pronounced weakness at some particular point within the usable range, or a characteristic in which too much attenuation is provided in regions where it is not required and too little where it is important, with the result that a good average is obtained upon an unsatisfactory structure. The situation is analogous to the attempt to specify the attenuation of an electrical network as an average of the losses introduced at certain frequencies. A true specification for performance should consider the use to which the unit is to be put, the type of conditions under which it must function, and a statement of the minimum rather than of the average performance to be expected. In addition to the physical considerations, the mechanism of hearing must be brought into the picture so that some idea of the effect on the loudness of the sound may be obtained.

Ross[2] has proposed what he termed a "Minimum Loudness Reduction" factor obtained by

[1] V. O. Knudsen, *Architectural Acoustics* (John Wiley & Sons, 1932), Chapter 12.
[2] I. G. Ross, "The Weighting of Sound Insulation Data Against Frequency," J. Acous. Soc. Am. **3**, 313 (1932).

plotting the transmission loss-frequency characteristic of the partition on a background of uniform loudness reduction contours. Fig. 1

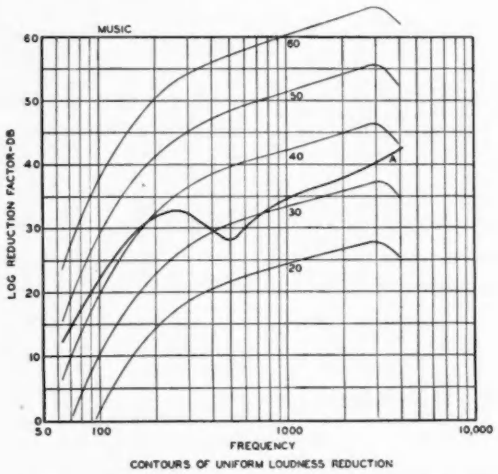

FIG. 1. Contours of uniform loudness reduction for music.

shows such a set of uniform loudness reduction contours with the reduction factor of a partition, (A), drawn on it. These contours show the reduction in intensity required to give the reduction in loudness indicated, and were established after a consideration of the frequency distribution of speech and music, the characteristic of the human ear, and normally encountered noise levels. It is seen that at 65 c.p.s. the partition has a maximum loudness reduction factor of 46 db, and that the factor rapidly drops off to a minimum value of 27 db at 500 c.p.s. Observing the performance of the partition in this manner has the advantage that the magnitude of the weakness and its location in the frequency spectrum are readily apparent. A glance at the figure conveys the information that sounds in the region of 500 c.p.s. will generally be first heard as the intensity of the sound on the other side is increased. This effect is actually experienced in the hearing of a very limited, and therefore very annoying, portion of a neighbor's radio program transmitted through the partition. The minimum loudness reduction figure of 27 db at 500 c.p.s. might be used as a statement of merit of the partition.

Recently Morreau[3] has very carefully analyzed the problem after considering the response of the human ear, the loudness of complex tones and receiving room conditions and comes to the conclusion that "a figure which may be derived by taking the arithmetic mean of a representative number of sound reduction factors over the frequency range 200–2000 c.p.s. does, however, give an approximation to the minimum reduction in equivalent loudness afforded, under practical conditions, by many walls to many sounds." The validity of this conclusion is restricted by the assumption of a mass controlled structure having an attenuation that increases at the rate of 5 db per octave, and by the adoption of 1000 c.p.s. as the highest frequency considered, although, in effect, the value at 700 c.p.s. is taken as the mean.

In general, partitions do not always exhibit a mass reaction, which produces an attenuation that rises monotonically with frequency, but sometimes show an irregularity as in the case of partition A. Irregularities are especially likely to occur in the characteristics of special partitions of high insulating value which consist of one light face resiliently mounted to a heavier structure. In this connection, it might well be said here that measurements of transmission loss should be made on partitions of a size encountered in practice, say $8' \times 16'$, rather than on small specimens, in order that the test partition possess the same mechanical constants as its counterpart in the field. In addition, so that any irregularities in the characteristic are not passed

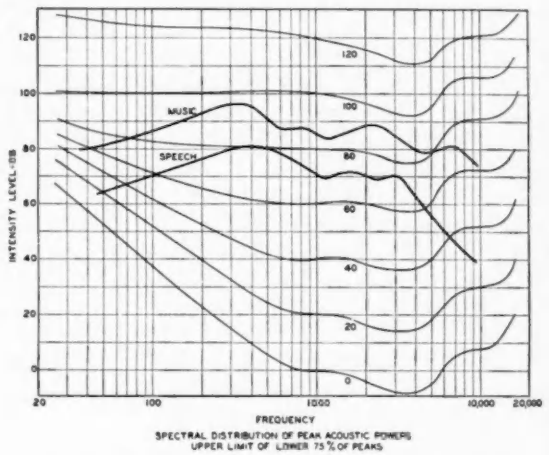

FIG. 2. Spectral distribution of peak acoustic powers in speech and symphony music, showing upper limit of lower 75 percent of peaks.

[3] C. J. Morreau, "The Insulation of Air Borne Sound," J. Acous. Soc. Am. **10**, 45 (1938).

over, the frequency interval between determinations should not be less than $(2)^{1/3}$ (three points per octave) or, what is substantially the same, $(10)^{1/10}$ (ten points per logarithmic cycle).

Morreau's analysis also shows that substantially the same conclusions can be drawn whether the loudness of pure tones is used in the analysis or whether the loudness of complex tones is taken into consideration.

A different approach to the problem of accurately specifying the effectiveness of a sound insulating structure is to consider the loudness level to which the partition will reduce normally encountered sounds. Fig. 2 shows the spectral distribution of energy in representative speech and symphony music, as determined by Sivian[4] and by Sivian, Dunn and White,[5] drawn on a background of Fletcher-Munson equal loudness contours. The data are presented as the upper limit of the lower 75 percent of the peak powers measured. Several characteristics are readily apparent. Peak powers of music have intensity maxima at 350 c.p.s. and 2300 c.p.s., while maxima for speech occur at 400 c.p.s. and 1600–3000 c.p.s. Speech, naturally, has a much lower level than music and contains less high frequency components.

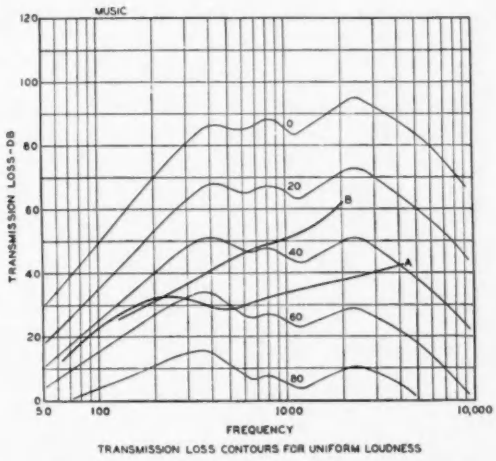

FIG. 3. Contours of transmission loss necessary to reduce symphony music to loudness level indicated. Partition A—3″ Pyrobar plastered both sides. Partition *B*—Double 2″ solid gypsum tile with 2″ air space, unplastered.

[4] L. J. Sivan, "Speech Power and Its Measurement," Bell Sys. Tech. J. **8**, 646 (1929).

[5] L. J. Sivian, H. K. Dunn and S. D. White, "Absolute Amplitudes and Spectra of Certain Musical Instruments and Orchestras," J. Acous. Soc. Am. **2**, 330 (1931).

Figure 3 shows a family of transmission loss contours for music, each curve specifying the attenuation characteristic necessary in a partition if it is to reduce symphony music to the loudness level indicated on the curve. Fig. 4 shows the same contours for speech. The shape of these curves can be considered to be the shape of the transmission characteristic of an ideal partition, which is a partition that has no "un-used" insulation, or one which reduces all components of the incident sound to the same loudness level. Less attenuation is required at low frequencies both because of convergence of the equal loudness contours in that region and because of the lower original energy content in that region. By the same token, insulation in this region is very critical and small differences in T.L. will result in large variations in loudness reduction. This is another condition that the use of average values does not bring out. The same is true to a less degree for the high frequencies. The important point to observe, however, is that the secondary maximum for music peak powers occurs at very nearly the frequency at which the acuity of hearing is greatest, and therefore maximum sound insulation is required for the region of 2000–3000 c.p.s.

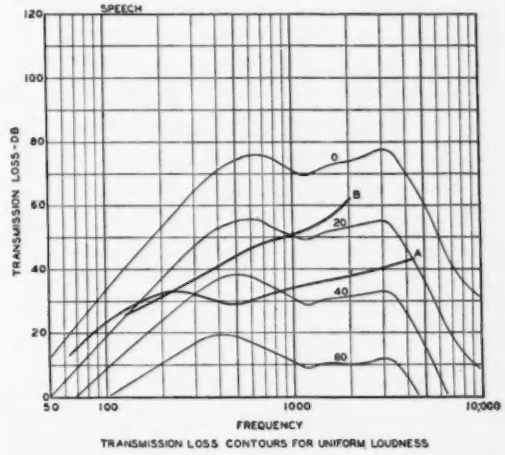

FIG. 4. Contours of transmission loss necessary to reduce declamatory speech to loudness level indicated. Partition *A*—3″ Pyrobar plastered both sides. Partition *B*—double 2″ solid gypsum tile with 2″ air space, unplastered.

The attenuation characteristics of two partitions, *A* and *B*, are drawn on these contours and it is seen that they do not conform to the ideal shape. Partition *A* is 3″ Pyrobar plastered on

both sides. Partition *B* is double 2″ solid gypsum tile, separated 2″, unbridged and structurally isolated and unplastered. On the basis of over-all average, *A* has a T.L. of 31 db and *B* of 44 db. On the basis of the average from 250–2000 c.p.s., *A* has T.L. of 33 db and *B* of 48 db. On a minimum loudness reduction basis (music), *A* possesses a MLR of 27 db at 500 c.p.s. and *B* a MLR of 39 db at 220 c.p.s. Under the proposed plan of specification, *A* is said to be able to reduce symphony music produced on one side to a maximum loudness level of 63 db on the other side, the weakest point occurring at 500 c.p.s. Likewise *B* results in a maximum loudness level of 54 db at 270 c.p.s. For speech, the final maximum levels are 48 db at 500 c.p.s. for *A* and 35 db at 360 c.p.s. for *B*. These values are tabulated in Table I.

TABLE I. *Summary of results of various methods of specifying performance of sound insulating structures.*

	Average	Average 250–2000 c.p.s.	Minimum Loudness Reduction		Maximum Loudness Level	
			Music	Speech	Music	Speech
Partition *A* 3″ Pyrobar plastered both sides	31 db	33 db	27 db at 500 c.p.s.	31 db at 500 c.p.s.	63 db at 500 c.p.s.	48 db at 500 c.p.s
Partition *B* double 2″ solid gypsum tile with 2″ air space unplastered	44 db	48 db	39 db at 220 c.p.s.	49 db at 800 c.p.s.	54 db at 270 c.p.s.	35 db at 360 c.p.s.

If the two partitions are merely to be compared, *A* can be said to be from 9 to 18 db better than *A* since the results from all methods yield differences within this range. If, however, a statement of absolute performance is required, the first two methods state only that certain mean values exist and give no further information. On the other hand, the minimum loudness reduction method specifies the minimum reduction in loudness to be expected, as well as the frequency at which failure of the partition begins. The last method shows the maximum loudness to be expected on the one side of the partition, and the frequency where it occurs, if certain sounds originate on the other. In other words, the last two methods have something definite to say concerning a partition, what can be expected of it, and where its weak point is.

The attenuation characteristics of the partitions have been drawn directly in T.L. since, in contrast to laboratory conditions, conditions in the field are usually such that the area of the partition is numerically of the same order of magnitude as the total sound absorption within the room and the correction between T.L. and reduction factor becomes negligibly small.

It is necessary to compare the maximum loudness of the transmitted sound with the existing noise level in order to determine whether or not the transmitted sound is audible, and therefore the frequency distribution of the ambient noise should be considered. In general, especially in instances of quiet apartments, studios, etc., applications in which sound insulation is really seriously considered, the noise energy is distributed fairly evenly throughout the frequency spectrum, being slightly higher in the mid-range than at either end. The noise level in offices tends to contain more high frequency components. For an approximation, for this purpose, the noise levels encountered can be considered to be uniformly distributed throughout the spectrum and a direct comparison can therefore be made.

The method of reduction to uniform loudness is most readily applied in evaluating sound insulation requirements for studios, etc., because in this instance the original sound is dealt with directly. This application is also one in which maximum sound insulation is required. In apartments, a 90-db level is not likely to be experienced, any original music arising probably having a level 15–30 db below this and insulation must be provided then only against incident sound whose level is much lower than shown by Fig. 2. Moreover, the sound may have a slightly different distribution because of the characteristic of the reproducing system. It seems that the best method of attacking this aspect of the problem is to prepare similar contours based on the reproduction of the same sound at mean levels of say 20 db and 40 db lower, and judging the partition's performance on the set of contours appropriate to the conditions under which the partition will be used in the field. Three different levels could be agreed upon and standardized similar to the procedure used in adopting the *A*, *B* and *C* levels and characteristics in sound level meters. Also performance

values could be agreed upon for several different grades of insulation.

It is frequently necessary to insulate against sounds other than speech and music, such as, for example, noise from rotating and vibrating machinery, traffic noise, etc. Since complete data on the average distribution of energy in these sounds are not available, contours similar to those developed for speech and music have not been prepared. However, in instances in which insulation from certain particular sounds is required, an accurate survey should be made to determine the energy-frequency distribution of the sound and a set of such contours prepared on this basis. Then, with receiving room conditions known, the reduction factors of the partitions can be drawn on the contours and the merit of the structure ascertained under true field conditions. In general, it can be said that more insulation in the low frequency region will be required if noises of types other than speech and music are dealt with.

With the growing consciousness of the desirability of sound insulation and its increasing use in new buildings, the economic factor involved in the selection of the type of structure becomes of increasing importance. Formerly, it was decided that insulation was or was not required, and if it was, nothing was overlooked in the way of massive and elaborate construction, etc., to accomplish this end without too much regard to the cost. Nowadays the insulation of a partition must be accurately known before it can be decided whether or not its cost is justified for the application at hand. Some method similar to the one described must be used to estimate this performance.

Conclusions

The present method of evaluating the effectiveness of sound insulative structures on the basis of mean values of T.L. is inaccurate and unscientific in that it does not predict the performance of the unit in practice. In actual practice, we are interested primarily in what loudness level will result in the insulated room rather than in any physical characteristics of the partition. The transmission characteristic of "ideal" partitions, or partitions which reduce the incident sound to a uniform loudness level, has been derived from a consideration of the intensity and frequency distribution of typically encountered speech and music and of the mechanism of hearing, and it has been shown that a family of these characteristics can be used as a means of predicting the insulation furnished by a particular structure and its manner of failure. The manner of extension of this method to ascertain the merit of a partition for different types of sounds is given. It is suggested that a further study of the subject be undertaken toward the end of specifying certain procedure to follow and methods to use in evaluating the performance of partitions.

A Design for a Keyboard Instrument in Just Intonation

CHAS. WILLIAMSON
Department of Physics, Carnegie Institute of Technology, Pittsburgh, Pennsylvania
(Received April 28, 1939)

In a keyboard instrument, the just scale may be closely approximated by setting up two equally tempered scales, one on the basis of $A440.0$, the other on the basis of $A436.3$, and mechanically selecting from them those frequencies which most nearly satisfy the appropriate ratios. Within one octave above middle C, no scale-step is in error by more than 0.6 vibration per second. The keyboard is exactly the same as that now used, and the instrument is playable in equal temperament when the performer so desires.

FOR three centuries attempts have been made to provide a pipe organ or other keyboard instrument with some approximation to the justly intoned scale. Among these, perhaps the best known are the meantone scale used in many eighteenth century organs,[1] the 19-note cycle of Woolhouse,[2] and the 53-note cycle of Mercator[2] and Bosanquet.[3] Some of them used unconventional keyboards. Recently Fisher[4] has suggested that a contemporary electronic instrument, the Hammond organ, could be furnished with a set of justly intoned generators and a twelve-speed gearset enabling the performer to play in any key. This paper presents a design applicable to most keyboard instruments, allowing the musician to choose between the equally tempered scale and a close approximation to just intonation in any key, while still using the conventional keyboard.

At first sight it might seem that an electronic keyboard instrument might possess mathematically exact just intonation in all keys without being of unmanageable complexity. This is true if only the diatonic or "white-note" scale is considered. But every musician knows that scarcely any music is wholly diatonic; "accidentals" may occur with or without modulation to a new key in the simplest musical selections. Here the complexities begin to appear. Suppose that the instrument is set for the key of C major. What frequencies shall be provided for the black keys? This question is not easily answered. For instance, in just intonation not only are $F\sharp$ and $G\flat$ different, but there are several kinds of each,[5] depending on their harmonic origin! All the pitches thus arising could conceivably be furnished by separate sources, but hardly by a range-changing gearset.

We may make a more promising approach to the problem by seeking a compromise. Let us examine the discrepancies between just intonation and equal temperament.[6] These are set forth in Tables Ia, Ib, the first based on $A440$, the second expressed in logarithmic cents.[7] Table Ib is more convenient for design purposes, inasmuch as it expresses the relative magnitudes of the errors more precisely. It is seen that there are six errors within the octave interval, three small and three large. Fortunately the large errors are all negative and nearly equal. Suppose, therefore, that we set up *two* tempered scales, one minimizing the small errors, the other

TABLE Ia. *Scale of C major. Frequencies given in vibrations per second.*

Just	261.6	294.3	327.0	348.8	392.4	436.0	490.5
Tempered	261.6	293.7	329.6	349.2	392.0	440.0	493.9
Differences	0.0	+0.6	−2.6	−0.4	+0.4	−4.0	−3.4

TABLE Ib. *Major scale. Ratios given in logarithmic cents.*

Just	0	203.9	386.3	498.0	701.9	884.4	1088.3
Tempered	0	200.0	400.0	500.0	700.0	900.0	1100.0
Differences	0	+3.9	−13.7	−2.0	+1.9	−15.6	−11.7

[1] H. v. Helmholtz, *Sensations of Tone*, tr. by Ellis. (Longmans, Green and Co., 1912), p. 433. E. H. Barton, *A Textbook on Sound* (Macmillan, 1926), p. 495.
[2] A. T. Jones, *Sound* (Van Nostrand, 1937), p. 70.
[3] Helmholtz, reference 1, pp. 328, 429, 438, 479. Barton, reference 1, p. 503.
[4] Fisher, Proc. Inst. Radio Eng. **27**, 77 (January, 1939).
[5] C. F. Hagenow, Am. Phys. Teacher **2**, 81 (1934).
[6] F. R. Watson, *Sound* (Wiley, 1935), p. 112.
[7] The number of logarithmic cents in an interval expressed by the ratio n_1/n_2 is given by the equation $L=1200 \log (n_1/n_2)/\log 2$. Their calculation and uses are discussed in references 1, 2, 6.

minimizing the large ones.[8] These are shown in Tables IIa, IIb. By selecting from them only the terms printed in boldface, we obtain the approximations given in Tables IIIa, IIIb. It is seen that no error in Table IIIa is greater than 0.6 vibration per second. The errors in some common musical intervals are given in Table IV. Here also the improvement will be noted.

The construction of an instrument on this basis would offer no great difficulty to the manufacturer, since he could set his temperament as usual on the basis of $A440$, tuning the second rank of pipes or other sound sources by beats,[9] or, in the case of an electronic instrument, by coupling the two sets of rotary generators with gears having the ratio 119 : 118. He would provide twelve stop-knobs, tilting tablets, or combination pistons, each labeled with a key-signature; or alternatively, one selector control having twelve labeled positions. This mechanism would bring into use only those frequencies pertaining to the key in which the instrument was being played. Each keynote would be selected from the upper row of terms in Tables IIa, IIb. All other scale-steps would occupy the same relative positions as in the scale of *C* major. Thus every scale would be treated alike; none would be favored at the expense of others. Moreover, the main advantage of the tempered scale, that of permitting unlimited modulation, would in a sense be retained, since by selecting all keynotes from a single tempered scale—the upper row of Table IIa—we insure that the "cycle of fifths"[5] will return to its starting-point after passing once through each key.

The problem of "accidentals" must now be faced. It is suggested that the terms in italics in Table IIa be furnished in the key of *C* major. These correspond to $F\sharp$, $C\sharp$, $B\flat$, $E\flat$, $A\flat$, which are the accidentals most likely to arise harmonically in simple music. A corresponding choice of accidentals would be made in each new key. The complete scheme is given in Table V.

Two more stop-knobs—or two more positions on the selector control—would permit the choice of either of the tempered scales which the instrument contains. This would facilitate tuning and would allow the performer to play in the tempered scale when he wished. Without this provision the instrument could not be used in concert with the piano or with wind instruments, most of which must perforce use the tempered scale. The just scale would be used if the instrument was played alone or as an accompaniment for strings or voices. In this connection it may as

TABLE IIa. *Two proposed tempered scales. Frequencies in vibrations per second.*

261.6	277.2	**293.7**	*311.1*	329.6	**349.2**	370.0	**392.0**	*415.3*	440.0	*466.2*	493.8
259.4	*274.8*	291.2	308.5	**326.9**	346.3	*366.9*	388.7	411.8	**436.3**	462.2	**489.7**

TABLE IIb. *Two proposed tempered scales. Ratios in logarithmic cents.*

0.0	100.0	**200.0**	*300.0*	400.0	**500.0**	600.0	**700.0**	*800.0*	900.0	*1000.0*	1100.0
−14.6	*85.4*	185.4	285.4	**385.4**	485.4	*585.4*	685.4	785.4	**885.4**	985.4	**1085.4**

TABLE IIIa. *Proposed approximation to just scale. Frequencies in second row are those shown in boldface in Table IIa.*

Just Scale	261.5	294.2	326.9	348.6	392.2	435.8	490.3
Approximation	261.6	293.7	326.9	349.2	392.0	436.3	489.7
Differences	−0.1	+0.5	0.0	−0.6	+0.2	−0.5	+0.6

TABLE IIIb. *Proposed approximation to just scale. Ratios in second row are those shown in boldface in Table IIb.*

Just Scale	−1.0	202.9	385.3	497.0	700.9	883.4	1087.3
Approximation	0.0	200.0	385.4	500.0	700.0	885.4	1085.4
Differences	−1.0	+2.9	−0.1	−3.0	+0.9	−2.0	+1.9

TABLE IV. *Musical intervals with errors in logarithmic cents.*

INTERVAL	JUST INTONATION	EQUAL TEMPERAMENT	ERRORS	PROPOSED APPROXIMATION	ERRORS
Semitone	111.7	100.0	+11.7	114.6	−2.9
Minor whole tone	182.4	200.0	−17.6	185.4	−3.0
Major whole tone	203.9	200.0	+3.9	200.0	+3.9
Minor third	315.6	300.0	+15.6	314.6	+1.0
Major third	386.3	400.0	−13.7	385.4	+0.9
Fourth	498.0	500.0	−2.0	500.0	−2.0
Augmented fourth	590.2	600.0	−9.8	585.4	+4.8
Diminished fifth	609.8	600.0	+9.8	614.6	−4.8
Fifth	702.0	700.0	+2.0	700.0	+2.0
Minor sixth	813.7	800.0	+13.7	814.6	−0.9
Major sixth	884.4	900.0	−15.6	885.4	−1.0
Minor seventh	996.1	1000.0	−3.9	1000.0	−3.9
Major seventh	1088.3	1100.0	−11.7	1085.4	+2.9

[8] The data of Table Ib are selected for this purpose. Since they express only ratios, after ascertaining that the first of our new scales must be 1.0 cent higher, the second 13.6 lower, we may simplify our procedure by leaving one unchanged and setting the other 14.6 lower. Of course, this simplification moves the nearest just scale down a little, as will be seen in Tables IIIa, IIIb.

[9] Beginning with *C* 130.8 in the upper rank, tune the lower rank flat as follows:

Note	*C*	*C*♯	*D*	*D*♯	*E*	*F*	*F*♯	*G*	*G*♯	*A*	*A*♯	*B*
Beats	33	55	36	38	32	50	39	33	35	37	51	52
Seconds	30	47	29	29	23	34	25	20	20	20	26	25

TABLE V. *This table indicates how the terms are to be selected from Table IIa for use in any major key; U from the upper row, L from the lower.*

KEY	NOTE	G♭	D♭	A♭	E♭	B♭	F	C	G	D	A	E	B
G♭		U	U	U	L	L	L	L	L	U	U	U	U
D♭		U	U	U	U	L	L	L	L	L	U	U	U
A♭		U	U	U	U	U	L	L	L	L	L	U	U
E♭		U	U	U	U	U	U	L	L	L	L	L	U
B♭		U	U	U	U	U	U	U	L	L	L	L	L
F		L	U	U	U	U	U	U	U	L	L	L	L
C		L	L	U	U	U	U	U	U	U	L	L	L
G		L	L	L	U	U	U	U	U	U	U	L	L
D		L	L	L	L	U	U	U	U	U	U	U	L
A		L	L	L	L	L	U	U	U	U	U	U	U
E		U	L	L	L	L	L	U	U	U	U	U	U
B		U	U	L	L	L	L	L	U	U	U	U	U

well be admitted that much music is too chromatic to be suited to any instrument built in just intonation. However, it has long been agreed that the discrepancies of the tempered scale are most likely to be noticed when the music is essentially diatonic and sustained in character. An interesting set of conflicting opinions regarding the merits of just intonation has been collected by Jones.[2] With the tuning scheme proposed herein, it should be possible for modern ears to make an immediate comparison between just intonation and equal temperament without such extraneous distractions as a change of tone-quality.

Pipe organs depending upon "unification" for mixtures and mutation effects,[10] as well as electronic instruments which borrow upper notes for harmonic synthesis[11] of tone-quality, would be benefited by the close approach to just intonation furnished by this design. As organ-builders well know, the tempered major third is a poor substitute for the exactly tuned fifth partial which they provide separately as Tierce or in combination with others as a mixture of several ranks. The seventh, eleventh, thirteenth, and fourteenth partials would be lacking, inasmuch as they are not found in the just scale. This is unfortunate, for, assertions to the contrary notwithstanding,[4] they are *not* dissonant[11] if of proper intensity, but extremely valuable in the ensemble and in the synthesis of certain solo effects. However, most organ mixture stops are limited to octaves, fifths, and thirds, all of which are provided closely enough for practical purposes by this design.

In conclusion, it may be helpful to point out that the two scales given in Table IIa are not the only ones that will satisfy the requirements. Any pair of tempered scales having frequencies in the ratio 119 : 118 will serve.

[10] W. H. Barnes, *The Contemporary American Organ* (J. Fischer & Bro., 1930), p. 87.

[11] D. C. Miller, *The Science of Musical Sounds* (Macmillan, 1937), Lecture VI.

A Sound Source for Investigating Microphone Distortion*

WILLIAM D. PHELPS
RCA Manufacturing Company, Camden, New Jersey
(Received May 23, 1939)

INTRODUCTION

IN order to measure the harmonic distortion produced by a microphone, a sound source free of harmonics over a wide pressure range is desired. A speaker in a baffle or a horn loudspeaker is limited in its pressure range. In addition, the room pattern affects the harmonic content of the sound field at the microphone. It is the purpose of this paper to describe a standing wave resonance system[1] which produces a high pressure sound field free of a prescribed harmonic with low power input to the loudspeaker. In Fig. 1 is shown a photograph of the resonance system. It consists of an eight-foot iron pipe ten inches in diameter, and a five-sixteenths-inch wall with an eight-inch dynamic speaker at one end and a movable iron piston at the other. The microphone is supported from the piston.

THEORY

In order to determine the harmonic attenuation by the resonance system, expressions for the pressure and particle velocity will be derived. Undamped plane wave propagation will be assumed. This assumption is sufficiently accurate except at points in the immediate region of the nodal points. Let the particle velocity and pressure in the wave traveling to the right be represented by

$$\dot{\xi}_1 = A_1 \epsilon^{-jkx} \epsilon^{j\omega t}, \tag{1}$$

$$p_1 = \rho c A_1 \epsilon^{-jkx} \epsilon^{j\omega t} \tag{2}$$

and the corresponding quantities in the wave to the left be represented by

$$\dot{\xi}_2 = A_2 \epsilon^{jkx} \epsilon^{j\omega t}, \tag{3}$$

$$p_2 = \rho c A_2 \epsilon^{jkx} \epsilon^{j\omega t}. \tag{4}$$

From the boundary conditions imposed on the volume currents at the two ends of the pipe, one finds at

$$x = 0$$

$$S_2(A_1 - A_2)\epsilon^{j\omega t} = S_1 \dot{\xi}_s. \tag{5}$$

At $x = l$

$$(A_1 \epsilon^{-jkl} - A_2 \epsilon^{jkl}) = 0$$

or

$$A_2 = A_1 \epsilon^{-j2kl}. \tag{6}$$

From the equation of motion for the speaker, one obtains the relation

$$F = S_1^2 (Z_{A_f} + Z_{A_1} - jZ_A \cot kl)\dot{\xi}_s, \tag{7}$$

where Z_{A_f} is the air load at the back of the

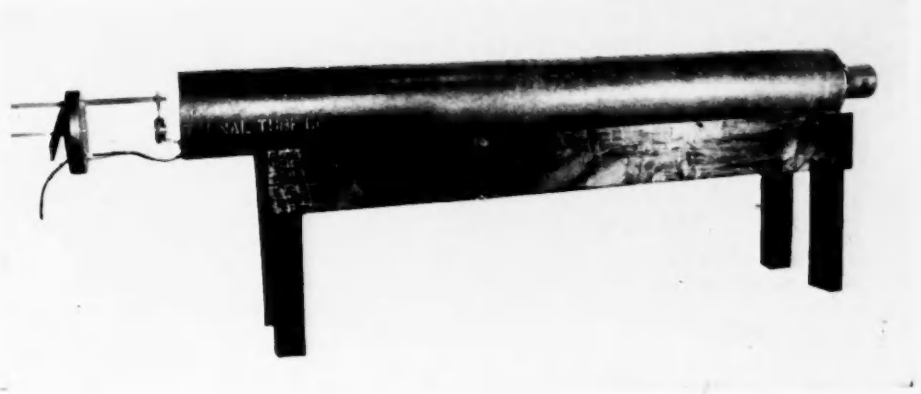

FIG. 1. The standing wave resonance system.

*Presented at the Tenth Anniversary Meeting of the Acoustical Society of America held in New York, May 15, 1939.

[1] W. D. Phelps, "The Rôle of the Speaker Impedance in Resonance in a Closed Pipe," J. Acous. Soc. Am. 9, 308 (1938).

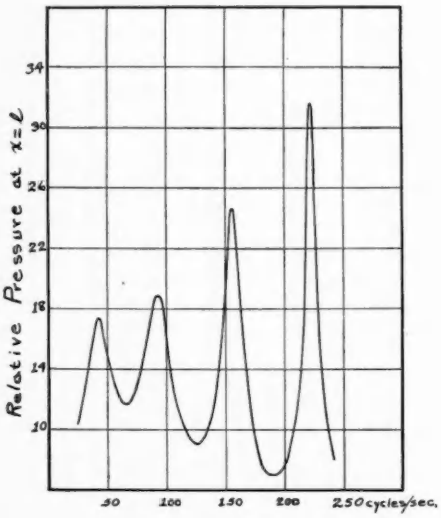

FIG. 2. Computed pressure-frequency characteristic at $x=l$ for the first four resonance frequencies. While the amplitude of the peaks increase with frequency in this region, the harmonics are attenuated since the resonance frequencies are anharmonic.

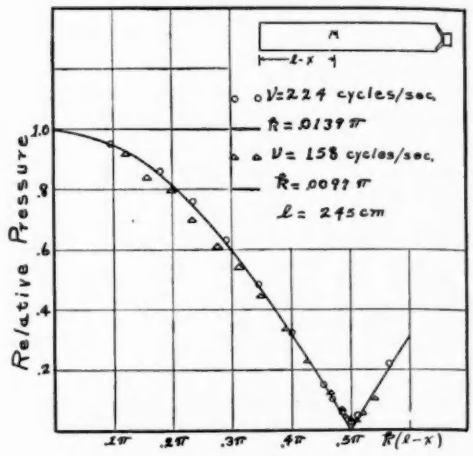

FIG. 3. Attenuation of harmonics along the length of the pipe for two frequencies.

speaker, Z_{A_1} is the speaker impedance including damping due to the electrical circuit, and $-jZ_A \cot kl$ is the input impedance of the closed pipe. From Eqs. (5), (6), and (7) one obtains

$$A_1=\frac{\epsilon^{jkl}F_0}{2S_1S_2[j(Z_{Af}+Z_{A_1})\sin kl+Z_A\cos kl]}. \quad (8)$$

Hence the pressure and velocity distributions in the pipe are given by the relations

$$p=\frac{F_0\rho c\cos k(l-x)\epsilon^{j\omega t}}{S_1S_2[Z_A\cos kl+j(Z_{A_1}+Z_{Af})\sin kl]} \quad (9)$$

and

$$\dot{\xi}=\frac{jF_0\sin k(l-x)\epsilon^{j\omega t}}{S_1S_2[Z_A\cos kl+j(Z_{A_1}+Z_A)\sin kl]}, \quad (10)$$

whence it is seen that by placing a pressure microphone at a quarter-wave or a velocity microphone at a half-wave from the close end, theoretically infinite attenuation of a given harmonic in the sound wave may be attained. In the actual case some damping is present in the air, and the attenuation due to the position of the microphone is, of course, not infinite but it is still great.

In addition to the attenuation due to the position of the microphone, there is a further harmonic attenuation due to the pressure-frequency characteristic at the closed end, shown in Fig. 2 for the first four resonance frequencies. The attenuation factors thus obtained are shown

TABLE I. *Computed harmonic attenuation factors due to the pressure-frequency characteristic at $x=l$.*

Frequency	Attenuation Factor	
	Second Harmonic	Third Harmonic
93	0.40	0.42
155	.26	.14
222	.20	.07

TABLE II. *Maximum harmonic attenuation factor and microphone position.*

Frequency	Second Harmonic		Third Harmonic	
	$l-x$	Attenuation Factor	$l-x$	Attenuation Factor
100	41.5 cm	0.027	27.5 cm	0.016
158	25.5	.018	15.8	.010

TABLE III. *Total harmonic attenuation factor relative to the fundamental given by the resonance system.*

Frequency	Attenuation Factor	
	Second Harmonic	Third Harmonic
100	0.015	0.0078
158	.0067	.0016

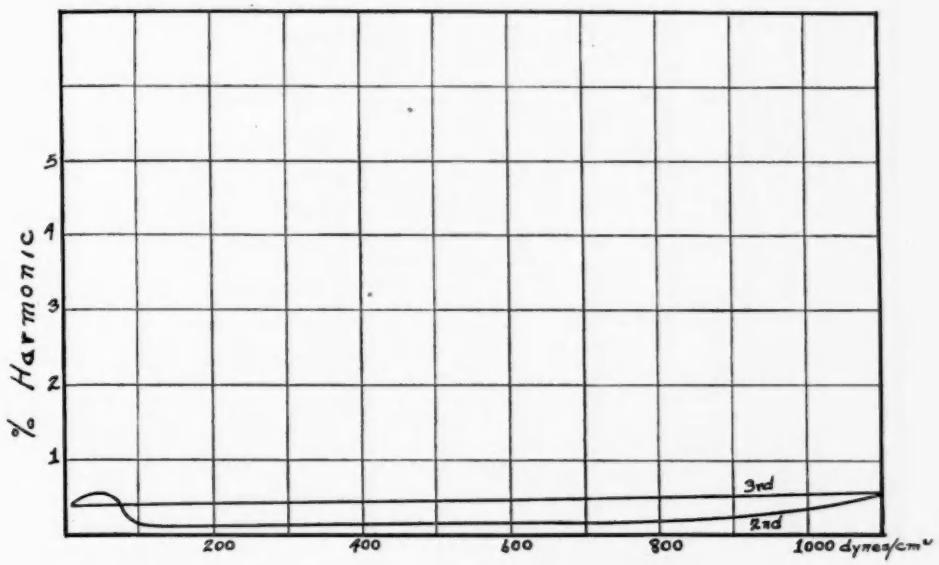

FIG. 4. Harmonic distortion in an RCA-44A microphone and amplifier taken with the standing wave resonance system over a wide pressure range.

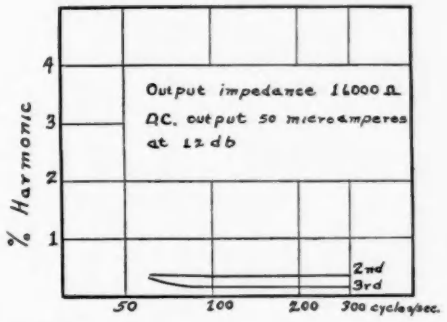

FIG. 5. Harmonic distortion due to the microphone amplifier.

in Table I. The total attenuation then is the product of the two factors due to position in the pipe and frequency characteristic.

RESULTS

Data on harmonic attenuation along the length of the pipe taken on a pressure microphone are shown in Fig. 3 for two frequencies. The heavy curve is computed neglecting damping while the points are experimental. The maximum attenuation factor and the position of the microphone from the closed end are given in Table II. In Table III are shown the total harmonic attenuation factors relative to the fundamental given by the resonance system.

Hence it is seen that with a loudspeaker input voltage containing as much as two to three percent harmonic, the sound field is free of the given harmonic to within a few hundredths of one percent. Using the standing wave resonance system, distortion curves were taken on an RCA-44A microphone at 100 cycles per second over a pressure range of 1100 dynes per cm². These are shown in Fig. 4. The distortion in the microphone amplifier is shown in Fig. 5.

DISCUSSION

It is noted from the pressure-frequency characteristic curve in Fig. 2 that the pressures obtainable at resonance increase with frequency. While high pressures are obtained up to 1000 cycles per second, the placing of the microphone begins to be critical above 300 or 400 cycles per second. At 100 cycles per second a pressure of 1100 dynes per cm² is obtained with less than 0.5 watt input to the loudspeaker.

Microphone Efficiency: A Discussion and Proposed Definition*

FRANK MASSA
RCA Manufacturing Company, Camden, New Jersey
(Received July 14, 1939)

This paper proposes a definition for microphone efficiency, together with a discussion for justifying the points of view presented. Up to the present time, the question of microphone efficiency has been generally ignored and in its place has grown the use of microphone sensitivity, which is the voltage output for a particular value of sound pressure actuating the unit. Although this latter quantity may be quite satisfactory for commercial use, the author feels that from a scientific point of view, we should be interested in the absolute ability of a microphone to absorb acoustic energy from a sound field and convert it into electrical energy: this ability he defines as efficiency. A relation for microphone efficiency is derived and a family of curves are computed which show the efficiency of a microphone as a function of its size, impedance, and sensitivity. One obvious conclusion that can be deduced from the paper is that only a tiny fraction of the acoustic energy intercepted by an average microphone is actually converted into electrical energy. This means that we are yet very far from the theoretical limit and, consequently, great possibilities still exist for fundamental research in the improvement of microphone efficiency.

INTRODUCTION

FOR some reason, the question of microphone efficiency has not been very generally discussed. When comparing the relative outputs of various microphones, it is common practice to use the quantity known as microphone sensitivity, which is a measure of the voltage generated in the unit for a particular value of actuating sound pressure. From a commercial standpoint, this method of rating may be quite satisfactory, but, from a scientific point of view, we should be more concerned with the effectiveness with which a microphone is capable of extracting acoustic energy from a sound wave and converting it into electrical energy. The completeness with which this conversion is made will determine the efficiency of the microphone. In other words, the efficiency of a microphone should include both its ability to draw acoustic energy from its environment as well as the effectiveness with which this energy is converted to electrical energy.

DEFINITION OF MICROPHONE EFFICIENCY

Apparently none of the published acoustical standards attempts to define microphone efficiency, and, in order to establish a basis on which the quantitative expression for efficiency will be derived, the following definition is proposed: *The efficiency of a microphone is the ratio of the maximum electrical power that can be delivered by a microphone into a pure resistance load to the acoustic power which is intercepted by the diaphragm** when immersed in a plane wave with the normal axis of the diaphragm perpendicular to the wave front.*

In the above definition, it will be observed that the energy *intercepted* by the diaphragm is used as the acoustic power rather than the actual energy *absorbed* by the microphone. Thus, if a microphone is of such mechanical impedance that it cannot easily absorb sound energy from its environment, it is charged up as a loss in efficiency just as would be the case were the microphone capable of absorbing a large amount of the acoustic energy and yet not be able to convert it efficiently into electrical energy.

* Presented at the Tenth Anniversary Meeting of the Acoustical Society of America, New York, May 15, 1939.

** For microphones which do not have diaphragms, the unit should be placed with the sound arriving along the axis of maximum sensitivity and the acoustic energy intercepted by the effective area of the structure should be used as the acoustic input to the system. In the case of a microphone which employs some form of horn or concentrator the mouth area of the horn should be considered as the effective diaphragm area. For microphones which consist of multiple cells or wire grids, some question may arise as to whether the sum of the projected areas of each individual cell or wire should be used as the effective area or whether the total area enclosing the group of cells or wires should be employed. This question is a matter of opinion and should be settled by an acoustic standards committee as suggested later in the paper.

Derivation of the Efficiency Equation

Based on the above definition, an expression for microphone efficiency will be derived showing its numerical magnitude as a function of the physical constants of the medium and the microphone. Fig. 1 schematically shows a microphone placed in a plane wave. The acoustic power intercepted by the diaphragm is given by

$$P_A = p^2 A / 10\rho c \text{ microwatts}, \quad (1)$$

where p = free wave sound pressure in dynes/cm^2, A = area of diaphragm in sq. cm, ρ = density of the medium in g/cc, and, c = velocity of sound in cm/sec.

If the microphone has an electrical impedance of magnitude, Z, maximum electrical power output will be delivered to a resistance, R, having the same numerical magnitude. Under optimum load conditions, therefore, the electrical power output from the microphone is given by

$$P_E = V^2/R \text{ microwatts}, \quad (2)$$

where V = millivolts delivered across the load resistor, R = load resistance in ohms ($R = Z$ in magnitude), and Z = microphone impedance in ohms. The efficiency of the microphone is given by the ratio of (2) to (1) which results in

$$\text{Efficiency} = \frac{10\rho c}{RA}\left(\frac{V}{p}\right)^2 \times 100 \text{ percent}. \quad (3)$$

For air under average conditions, Eq. (3) becomes equal to

$$\text{Efficiency} = \frac{41500 S^2}{RA} \text{ percent}, \quad (4)$$

where S = terminal potential generated across the load resistor in millivolts per dyne per sq. cm of sound pressure, R = load resistor in ohms (equal in magnitude to the microphone impedance), and A = diaphragm area in sq. cm.

Discussion and Conclusion

If a microphone has a diaphragm of a definite area and an impedance which is constant at all frequencies, the efficiency is very simply obtained from Eq. (4). For a microphone in which the actuating surface may be a large number of closely spaced cells, some question may arise in the choice of the effective diaphragm area. This difficulty could be easily settled by a Standards Committee which might propose any one of a number of solutions. For example, when the spacing between the assembled elements is less than some arbitrary fixed value, the entire enclosing surface might be used as the diaphragm area. When the spacing is larger, however, the sum of the projected areas of the individual elements could be used.

Another question may arise regarding the value of impedance to use for a microphone, such as the condenser type, which is of variable magnitude. In this case, the impedance is fixed at any particular frequency and the efficiency may be definitely obtained at each frequency by using a load resistance, R, whose magnitude is equal to the impedance value of the microphone at the frequency of interest. For the condenser microphone, therefore, assuming a constant induced voltage per unit sound pressure at all frequencies, the efficiency is directly proportional to the frequency. This simply means that this microphone is 100 times more efficient at 8000 cycles than it is at 80 cycles.

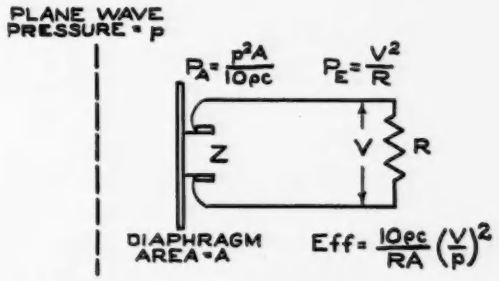

FIG. 1. Schematic arrangement of a microphone diaphragm immersed in a plane wave.

It is true that, in general, we load a condenser microphone with a resistance which is comparable in magnitude to its low frequency impedance, thus not actually profiting by the inherently higher microphone efficiency at the higher frequencies. This fact, however, only shows that the impedance characteristic of the microphone does not permit the realization of its higher efficiency for the particular application. For such cases in which a fixed value of load resistance must be used in order that constant voltage output may be realized at all frequencies, an

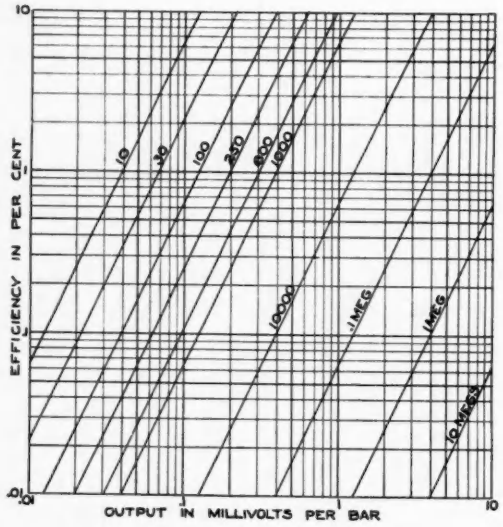

FIG. 2. Microphone efficiency *versus* output voltage across the various resistances shown by the family of curves. *Note*: Efficiency is based on a microphone whose effective diaphragm area is one square inch. For any other area, divide efficiency by area in square inches.

auxiliary definition may be desirable which might be called "effective efficiency" and would be defined by Eq. (4) in which R is given the value recommended to be used across the microphone for the particular application.

From Eq. (4), a family of curves has been computed showing the values of microphone efficiency as a function of output voltage per unit free wave sound pressure. These curves are shown in Fig. 2 and apply for a diaphragm area of one square inch. For any other diaphragm area, the value of efficiency may be obtained by dividing the value found on the chart by the actual diaphragm area in square inches.

Many will be startled to find, upon substituting representative constants on this chart, that the efficiency of many of the best commercially available microphones is extremely low (less than one percent). This indicates that there is still room for fundamental progress in the design of microphones. These improvements may be made from two avenues of approach; one, the mechanical impedance of the vibrating system should be made such that maximum acoustic energy may be taken from the sound field, and two, an efficient system should be employed for converting the absorbed sound energy into electrical energy. The improvement of either or both of these factors will result in a more efficient microphone.

The Degenerative Sound Analyzer

H. H. Scott
General Radio Company, Cambridge, Massachusetts
(Received March 29, 1939)

Measurement of Noise

In countless factories and laboratories the sound-level meter has become well established as an almost indispensable measuring device. With this instrument, engineering and production tests are carried on as easily as measurements of current and voltage, thus allowing the noise-producing characteristics of electrical and mechanical devices to be held within definite limits in much the same manner as other characteristics. Modern sound-level meters are designed to comply with the tentative standards which were formulated by the American Standards Association under the sponsorship of the Acoustical Society. Such meters provide a standardized means of noise measurement, applicable to all general types of sound and allowing engineers, manufacturers and consumers to express their noise specifications in units which are readily understood by all.

In all fields of measurement, as soon as it has become possible to obtain satisfactory data concerning certain characteristics of the phenomena being studied, the demand arises for equipment to make further measurements in order to investigate other phases of the phenomena. The sound-level meter provides a measure of over-all noise, and through the use of weighting networks the readings may be closely correlated with the estimate of an average person regarding the sound level. Such measurements are quite sufficient for many types of work, particularly for acceptance and production tests on finished products. To engineers who are trying to design quieter equipment, however, other types of data are frequently desirable, and, in particular, an analysis of the characteristics of the sound may provide many clues as to the sources of the most undesirable components. The result has been a persistent demand for a suitable sound analyzer, and, with this problem in mind, many types of devices have been tried. However, analyzers originally developed for other purposes have, in general, certain characteristics which limit their use for noise analysis.

Classification of Noises

The noises generated by machinery may be divided roughly into two classes. The first class includes sounds at the fundamental frequency at which the machinery is operating, or at some harmonic of this frequency. Sounds of this class are characterized by the harmonic relationship between the important components and are characteristic of most types of rotating or reciprocating mechanisms, particularly those operating at high speeds.

The second class of noises contains those components which are not definitely related in frequency to the fundamental speed of the machine and includes mainly those components caused by the vibration of various mechanical parts at or near their natural frequencies. Such noises are generally caused by shock excitation and result in a series of damped waves which, although they may recur at regular intervals depending upon the speed of operation of the mechanism, consist essentially of components corresponding with the natural frequency of the vibrating parts or harmonics of that frequency. The actual frequencies involved in such sounds are seldom clearly defined, since the effects of the shock excitation, the natural damping of the mechanical parts, the movement of the parts and the variation of forces impressed upon them cause frequency shifts of an appreciable order of magnitude.

Of course, the total noise made by any one machine generally consists of sounds falling in both classes, but in a large percentage of practical cases it will be found that all of the important components are in one class or the other. For example, the whine of a dynamo consists almost entirely of the fundamental and harmonics of the dynamo speed and thus falls into class one.

The noise made by a typewriter, on the other hand, may be considered as falling into class two since all of the important components are caused by shock excitation of the various parts of the mechanism. Sounds in class one are characterized by being rather sharply pitched, the pitch depending upon the machine speed, and containing mainly harmonics of that speed, and any variation in this speed will result in a corresponding percentage shift in frequency of all of the components of the sound. Noises falling in class two, in comparison, are characterized by being only approximately pitched and including many components which are not harmonically related. The frequency of the components in a class two sound is affected only to a small degree, if at all, by a change in the operating speed in the mechanism.

Analysis of Noise

The idea of analyzing sound by means of an electrical device is not new. Various types of analyzers have been developed for use on electrical wave forms, and, since a sound-level meter provides at its output terminals an electrical wave form corresponding closely with the acoustical wave form picked up by the microphone, it is only logical to attempt to use these analyzers for resolving the noise wave into its component frequencies. The average electrical analyzer, however, is of the heterodyne type, and a characteristic of this sort of analyzer is that the band width expressed in cycles remains constant, regardless of the frequency to which the analyzer is tuned. This response is the natural result of the type of circuit used in the heterodyne analyzer. In a device of this sort the tuned circuits or filters which provide the selectivity remain fixed, and the component being measured is heterodyned with another sinusoidal wave form, providing a beat note which passes through the filters.

This type of characteristic is, of course, entirely satisfactory for the applications for which these analyzers were originally designed. In measuring the wave form of power-line voltages, or in measuring distortion in amplifiers, etc. the actual wave form being measured is generally steady in frequency and absolutely recurrent. This is also the case with class one sounds of constant pitch, and for sounds of this type the heterodyne analyzer is quite satisfactory. For class one sounds of variable pitch, however, and for the unpitched sounds of class two the extreme selectivity of the heterodyne type of analyzer in the high frequency ranges makes accurate results impossible and in many cases makes it difficult to obtain any sort of measurements whatsoever.

Since few types of machinery operate at a sufficiently constant speed for satisfactory analysis of the high frequency sound components with a conventional type of heterodyne analyzer, various alternatives and modifications have been tried. Heterodyne analyzers have been made available with two or more band widths which are obtained by switching the filter circuits. This is an improvement, but obviously there will be a discontinuity in the readings at that point in the frequency range where the shift is made from one band width to the other, the extent of the discontinuity depending upon the pitch variations in the sound.

Other experimenters have abandoned the heterodyne analyzer entirely in favor of the tuned-circuit type, such as was in common use in electrical laboratories before the development of heterodyne analyzers. Since the band width of tuned circuits widens out as the frequency is increased, such an analyzer is, from this standpoint, inherently better for noise analysis than the heterodyne type, since the band-widening process may be continuous and automatic. The disadvantages of such analyzers are many, however, including undesirably large size and weight, caused mainly by the large coils and condensers required for operation at low audiofrequencies, susceptibility to magnetic interference, the difficulty of obtaining sufficient selectivity at low audiofrequencies and the fact that large inductances and capacitances cannot be made continuously variable. The use of the tuned-circuit type of analyzer has, accordingly, been restricted to only a few applications.

The Ideal Noise Analyzer

Most users of sound-measuring or sound-analyzing equipment are in agreement that, in the ideal noise analyzer, the band width or

selectivity curve should be proportional to the frequency to which the device is tuned. Obviously, for class one sounds of variable pitch this will provide the minimum error, since any attenuation caused by frequency modulation of the sound will be equal for all components, which will then remain in their true relative proportions. For the unpitched sounds of class two it is somewhat more difficult to determine an ideal characteristic, but it is apparent that the broader selectivity curve in the high frequency ranges of the constant-percentage-band-width analyzer, as compared with the conventional heterodyne type of analyzer, will provide a considerable improvement in the response to these high, unpitched components. In this connection it may be well to note that sounds falling in class two are generally considered more annoying by the average person than sounds of a similar level falling in class one, since class two sounds are generally what are referred to as rattles or clashes. It is these sounds of the most annoying character which it has not been possible hitherto to analyze satisfactorily.

The Degenerative Sound Analyzer

In an effort to produce an analyzer more suitable for the great majority of industrial noise applications, the Engineering Department of the General Radio Company has developed a device operating on the inverse-feed-back principle,[1] which combines many of the advantages of the heterodyne and tuned-circuit types of analyzer without the disadvantages of either. The degenerative analyzer consists essentially of a high gain amplifier and a feed-back network which is so designed that all frequencies except that to which the analyzer is tuned are fed back to the input of the amplifier with such a phase relationship as to produce degeneration and consequent cancellation of the gain. The maximum gain of the amplifier is obtained, therefore, only at the frequency to which the device is tuned, and the amplification decreases rapidly as the frequency of the impressed signal is varied away from this point. This arrangement is shown in Fig. 1.

[1] H. H. Scott, "A New Type of Selective Circuit and Some Applications," Proc. I. R. E. **26**, 226–235 (1938).

In this analyzer the feed-back network is of the parallel-T type, which balances to a sharp null at a frequency predetermined by the values of the circuit elements, in much the same manner

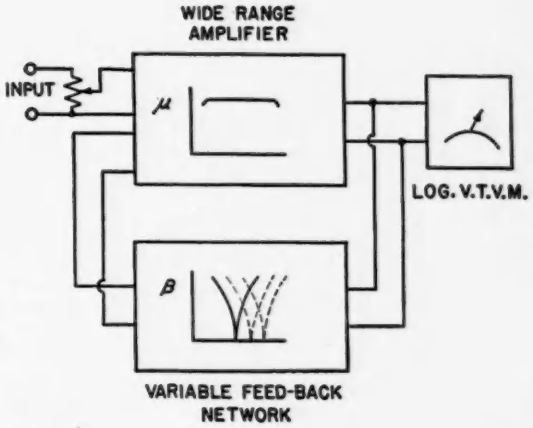

FIG. 1. Functional schematic showing principle of operation of the degenerative sound analyzer.

as a Wien bridge. This type of network requires only resistances and capacitances, and hence no coils whatsoever are required. This results in several advantageous features. Continuous tuning is accomplished by ganged variable resistors wound on tapered cards to give an approximately logarithmic frequency characteristic, and switching from one frequency range to the next is accomplished by means of a push-button switch. Since the main tuning dial may be rotated continuously in one direction, it is possible to scan the entire frequency range quickly and easily, while the push-button range control allows quick transfer between two widely separated frequencies. The elimination of all inductances from the circuit results in an appreciable reduction in weight and makes the instrument unsusceptible to magnetic pick-up.

In regard to stability of tuning, an analyzer operating on these principles is, of course, far superior to the conventional heterodyne type. In the latter the tuning depends on the high frequency oscillator, and a relatively small percentage shift in its frequency will result in a large percentage shift in the analyzer tuning. In the case of the degenerative circuit the selectivity is determined by the constants of the feed-back network, and, since these consist of

high quality mica condensers and wire-wound resistors, the analyzer possesses an inherently high degree of frequency stability. This is an important advantage since it eliminates the need of any adjustments for resetting the frequency

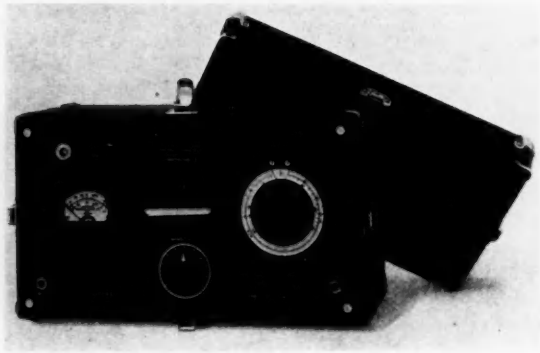

FIG. 2. The Type 760-A Sound Analyzer, which operates on the degenerative principle.

calibration, which in the case of heterodyne instruments generally have to be reset each time measurements are made.

The complete instrument, which is known as the Type 760-A Sound Analyzer, has been designed as a companion instrument for the Type 759-A Sound-Level Meter and, accordingly, is housed in a similar case of airplane-luggage construction. As a result of the circuit and mechanical design, the instrument is small and relatively light in weight when compared with other types of analyzers. The appearance of the new analyzer is shown in Fig. 2.

Another noteworthy feature of the new analyzer, which is entirely distinct from the selective circuit, is the vacuum-tube voltmeter used as an intensity indicator. The circuit for operating this meter was developed in order to provide as simple operation of the analyzer as possible. The output from the vacuum-tube voltmeter amplifier tube is rectified, and a part of the resulting direct voltage is fed into the grid circuit, providing an automatic volume-control action. Thus the complete intensity range over which the analyzer is usable may be read on the single meter scale without the aid of any multipliers. This feature speeds up noticeably the process of analyzing noises.

ACCURACY IN NOISE ANALYSIS

The accuracy of the results obtained in analyzing any particular sound do not, unfortunately, depend only upon the conventional accuracy ratings of the analyzer. The usual accuracy ratings for an electrical analyzer give the limit of error on frequency and voltage calibrations, but apply only so long as the measured component is of a constant frequency. This condition is seldom encountered in noise measurements. As has been pointed out, the selectivity characteristics of a conventional heterodyne type of analyzer are such as to produce serious errors, although the analyzer for many other applications might be entirely satisfactory. Disregard of the true seriousness of these errors has been the reason for the failure of many attempts to analyze noise and is probably one of the main reasons why the subject of noise analysis is avoided by many engineers who have the impression that it is generally unsatisfactory and, at best, involves complicated and expensive equipment.

Figures 3 and 4 are presented to show comparative performance characteristics of the degenerative type of analyzer as contrasted with the heterodyne type of wave analyzer, in order to show the relative magnitude of errors possible with the two types when used for noise analysis.

The selectivity curve of two analyzers is shown in Fig. 3. The solid line is for the new Type 760-A Sound Analyzer, and the most noticeable feature is that the constant-percentage

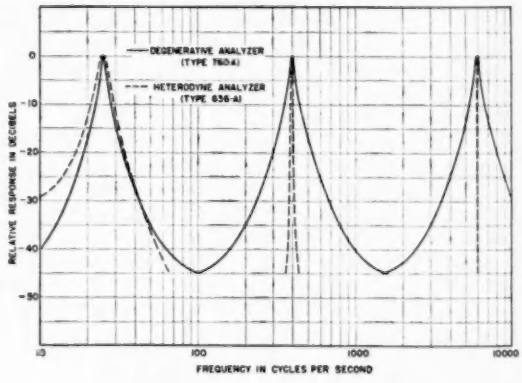

FIG. 3. Comparison of the selectivity characteristics of the degenerative analyzer and a typical heterodyne type of analyzer.

selectivity feature results in a selectivity curve which, when plotted to the conventional logarithmic frequency scale, remains the same throughout the entire range of frequencies.

The broken line represents the corresponding curve for an analyzer of the heterodyne type. This particular model uses a crystal filter and has proved very successful in many applications in the electrical and radio industries. The selectivity curves for the device, however, show readily why it is difficult to obtain satisfactory noise analyses with any device of this type. At 25 cycles the heterodyne analyzer is noticeably broader tuning than the degenerative type, making it more difficult to measure frequencies closely. At about 50 cycles the peaks of the two selectivity curves will be quite similar, but above that frequency the heterodyne analyzer becomes increasingly selective in terms of percentage of the frequency to which it is tuned, so that by the time 400 cycles is reached this device is quite unusable for many purposes unless the frequency is extremely stable. At higher frequencies the percentage selectivity curve becomes so narrow as to appear as a single straight line on the logarithmic chart. At 6000 cycles, for instance, a frequency shift of only 0.03 percent will throw the component being measured entirely outside of the band of the analyzer.

This figure shows quite clearly how difficult it is to tune an analyzer of the heterodyne type when measuring high harmonics which are varying in frequency. The inconvenience of this extreme selectivity is, however, considerably less important than the seriousness of any possible error if measurements are made with an analyzer of this type. In general, the most important characteristic of the noise which can be learned from the analysis is the relative amplitude of the various components. The problem of the response of an analyzer to sounds of varying frequency is extremely complicated, and no single set of conditions can be set forth which will clearly show the many possible variations in the results. The curves in Fig. 4 have been plotted, however, as being typical of a large number of such cases.

For purposes of simplification, it was assumed in plotting these curves that, after the analyzer had been tuned to the desired component, the frequency shifted by one percent, thus causing an amount of attenuation depending upon the selectivity curve of the analyzer. In actual practice, of course, the frequency would be shifting continuously back and forth, and the error would depend not only upon the extent of the shift, but on the frequency *versus* time characteristic. It is believed that Fig. 4, however, gives a rather good idea of the type of error caused by the variation in frequency and serves to point out that the error may be extremely serious. Since it is unpredictable with the equipment ordinarily at hand, the actual extent of the error is seldom known. This, of course, renders most measurements made under these conditions quite worthless.

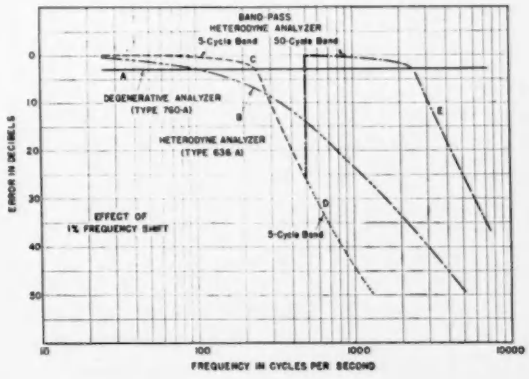

FIG. 4. The effect of one percent frequency shift on the accuracy of various types of analyzers.

Curve *A* shows the characteristics of the Type 760-A Sound Analyzer. For any given percentage frequency shift throughout its range it will be noted that the attenuation on all components is exactly the same. Accordingly, in the analysis the relative amplitudes of the components are not disturbed, and the absolute amplitudes are only slightly reduced. An analysis made with this instrument will, therefore, show actually what class one components are the most important from the standpoint of the amount which they contribute to the total noise.

Curve *B* in Fig. 4 illustrates what happens when a conventional type of heterodyne analyzer is used under the same conditions as outlined above for the feed-back analyzer. The error reaches 10 decibels at a frequency only a little above 300 cycles, and in the range from 1000

cycles to 2000 cycles, where the ear is most sensitive, the response of the analyzer is down by approximately 30 decibels. Obviously, these conditions will result in highly erroneous readings.

To minimize this difficulty, analyzers have been developed which use several band widths, usually related by factors of 10. Curve *C* shows the response of a typical analyzer having a 5-cycle band-pass characteristic with a sharp cut-off beyond that point. Curve *D* is a continuation of curve *C* into the higher frequency range and shows the extreme attenuation which would be obtained if only this single band-pass characteristic were employed. Curve *E* represents the response of the same analyzer with a 50-cycle band width. Under normal operating conditions, the error obtained with this analyzer would, therefore, be indicated by curves *C* and *E*. The large discrepancy falling at the cross-over frequency, in this case 500 cycles, should not be overlooked. An error of 25 decibels occurs at this point, which falls within the range of a large part of the energy of the average noise. If the 50-cycle band were used at lower frequencies in order to minimize this error, the selectivity would generally be insufficient to give satisfactory results because, even at the cross-over frequency of 500 cycles, the band width is ten percent of the frequency to which the device is tuned.

As previously mentioned, the actual results obtained with any given sound with the heterodyne types of analyzers may be better or worse than that shown in the diagram, depending upon the extent and other characteristics of the frequency shift. The unpredictability of the results and the possibility of such serious errors are probably the main reasons why the heterodyne type of analyzer has been generally abandoned for most purposes of sound analysis except in those few cases where the machinery speeds can be held within very close limits and where clashing and rattling sounds are not present.

This discussion of frequency shifts and the resulting errors is obviously more readily applicable to class one sounds than it is to class two sounds. The rattles and clashes falling in this latter class do not necessarily shift in frequency by the same percentage as the fundamental speed of the machine, and, accordingly, it is far more difficult to evaluate the performance of any analyzer for sounds of this character. In general, however, two characteristics may be said to be desirable. The first of these is a relatively wide band width compared to conventional heterodyne analyzers, so that the normal frequency range covered by any average component in these sounds will be included satisfactorily. The second is that the selectivity curve should have a rounded top, so that the analyzer may be tuned definitely to the component. In this connection band-pass filters are, of course, useful for locating these noises in certain parts of the frequency spectrum, but an analyzer having continuously variable tuning and a rounded-top selectivity curve is essential to locate the components with any particular degree of exactness.

It has been shown by actual experience that the type of selectivity curve present in the degenerative analyzer is well adapted for measuring these relatively unpitched sounds of class two. The curve is wide enough to provide satisfactory indications on all important components, and the shape is such as to allow definite tuning, thus giving an indication of the

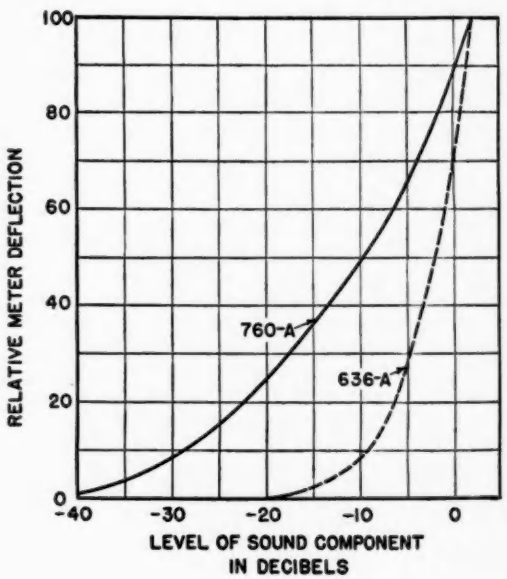

FIG. 5. Response of the approximately logarithmic vacuum-tube voltmeter of the Type 760-A Sound Analyzer, as compared to a conventional type of vacuum-tube voltmeter.

mean frequency of each component. An inspection of the curves in Fig. 3 will show readily why this type of analyzer is so much more satisfactory than the heterodyne type, while plotting additional curves similar to Fig. 4, but for various degrees of frequency shift, will make readily apparent the fact that any error generally encountered with the degenerative type of analyzer will be far less in magnitude than that encountered with the sharper-tuning heterodyne type.

Figure 5 has been included to show the relatively wide range available on the vacuum-tube voltmeter of the new analyzer, as contrasted with a vacuum-tube voltmeter of more conventional design. The inclusion of the complete operating range on a single-meter scale is a distinct advantage in regard to both accuracy and convenience. If the low level end of the scale is crowded so that multipliers must be used, the lower intensity components in the sound are frequently passed over without being noticed when an analysis is made. The type of meter used on the new analyzer provides a readily noticeable response for all components having an amplitude high enough to be of any importance in making up the total noise.

As a typical example of the type of analysis which may be obtained with the degenerative analyzer Fig. 6 is presented. This represents the actual noise made by a typical household refrigerator of standard make. The analysis was made with a Type 759-A Sound-Level meter and a Type 760-A Sound Analyzer. The 40-decibel weighting network was used on the sound-level meter, so the level of the components corresponds to their effect upon the average ear under normal listening conditions, where the noise from the refrigerator is noticeable but not loud.

It will be noted that there are strong components at the fundamental speed of rotation and various harmonics. There is also an appreciable hum from the motor field. Of all of the components shown, only this field hum and the lower frequencies can be measured satisfactorily with the conventional type of heterodyne analyzer. The strongest components are actually in the region between 1000 and 2000 cycles, and it is in this very range that the largest errors frequently occur with heterodyne analyzers. In this particular analysis there are several strong components in this region which represent roughly pitched whistling noises due to valves, etc. in the discharge line. The other components represent rattling or clashing sounds. When the analysis is made with a conventional heterodyne

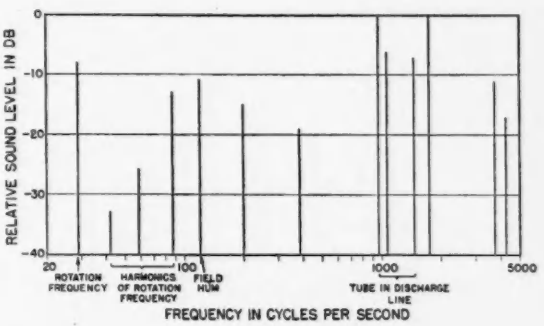

FIG. 6. Noise analysis of a domestic refrigerator as determined with the degenerative sound analyzer.

type of analyzer, all of the components above the 120-cycle field hum are greatly attenuated or do not show up at all.

A large number of field tests on many types of mechanical equipment, including typewriters, watt-hour meters, airplane propellors, office machinery and automobiles, have proved that analyses of this type as made with the degenerative analyzer do show up in their relative amplitudes the important components in a noise as heard by the ear. The accuracy of the instrument on sounds falling in both classes seems to be entirely satisfactory, and results have been obtained in many instances where all previous attempts at analysis had failed. In a surprising number of cases hitherto unsuspected components due to shock excitation were shown up by analyses made with the degenerative unit. Naturally, such data are invaluable to manufacturers, since it is only by knowing the source of a noise that they can take effective steps to eliminate it.

ADDITIONAL USES OF THE DEGENERATIVE ANALYZER

Because of its important features, such as continuous tuning at low frequencies, freedom

from magnetic pick-up, and stability, the Type 760-A sound analyzer is being used in many fields other than that for which it was originally designed. Of most importance, probably, is its use as a null detector in making bridge balances. The device may also be modified to function as a selective filter.

To meet the special requirements of certain other applications a null indicator and a low distortion oscillator[2] functioning on the same degenerative principle have been developed.

[2] The Type 707-A cathode-ray null detector and the Type 608-A oscillator are described in the April, 1939, issue of the General Radio *Experimenter*.

Conclusion

Of the many possible uses of the degenerative type of selective circuit, it is believed that its function as a noise analyzer is one of the most important, since it provides a much needed and hitherto unavailable type of selectivity characteristic. The ready acceptance of the new analyzer by engineers in many branches of industry and research indicates that it is filling a large demand for simple and effective noise-analyzing equipment. It is hoped that this new instrument will enable engineers to carry further their already noteworthy work of making this world a quieter place in which to live.

The Propagation of Shock Waves in Air. I

L. THOMPSON AND N. RIFFOLT
Naval Proving Ground, Dahlgren, Virginia
(Received June 19, 1939)

From a consideration of conditions at the boundary of a source of shock in air, and of conditions at great distances, a formula of the Riemann type has been derived for the velocity of propagation of a finite pulse. The formula includes an additional constant which provides the necessary flexibility to represent data obtained throughout the fields of sources consisting of detonating charges of explosives, and of other sources. The observations of wave displacements have been summarized in terms of an integral for "reduced" times, from which the constants of the function for velocity are immediately available. All distances are defined with reference to an equivalent dimension of the source, and the characteristics throughout the velocity field are obtainable from the characteristics of the source. A table is given for the velocity of a condensation pulse, for representative boundary velocities, at various distances from the source out to points at which the velocity has decreased approximately to its asymptotic value (the normal velocity of sound). Results obtained by Wolff and Burlot for very large sources are shown for comparison on a plot of reduced times. Preliminary results obtained with piezo-gauges of experiments to determine relative pressures at the head of the wave are given in comparison with theoretical gauge pressures obtained by formulas derived in Part II.

1.

RIEMANN'S formula[1] for the velocity of a finite pulse in air

$$V=a\left[\left(\frac{\rho'}{\lambda}\right)^{(\kappa-1)/2}\left(1+\frac{2}{\kappa-1}\right)-\frac{2}{\kappa-1}\right]$$

with ρ' maximum density, λ normal density, κ ratio specific heats, a normal velocity of sound, r distance from center of source, may be written for spherical waves, to second-order approximation,

$$V=a(1+K/r^2)^{\frac{1}{2}}$$

by means of the substitutions

$$\rho'=\lambda+b^2/r^2, \qquad K=((\kappa+1)/\lambda)b^2$$

and the binomial expansion. The quantity K depends with b on the initial condensation and on the changing characteristics of the wave during its propagation. Lacking means for predicting the function b and admitting uncertainty as to the appropriate value of κ, the formula is not particularly useful.

A function of the Riemann type can be given in a convenient form by taking advantage of the boundary conditions known to exist. It is known, for example, that the initial velocity of shock in air radiating from the surface of a detonating charge is in many cases quite accurately the velocity of the detonating wave in the solid explosive.[2, 3, 4] It is also known that at great distances the wave velocity is the normal velocity of sound. Following an earlier paper,[5] it has been found that introducing an additional constant φ in the Riemann formula would produce good fit of our observed velocities not only near the limits but throughout the field, provided the boundary condition is written

$$V=V_d \quad \text{for} \quad x=1$$

or

$$\frac{V}{a}=\left[1+\left(\frac{V_d^2-a^2}{a^2}\right)(\varphi+1)^2\frac{1}{(\varphi+x)^2}\right]^{\frac{1}{2}}$$

$$\equiv\left[1+\frac{C}{(\varphi+x)^2}\right]^{\frac{1}{2}},$$

of which x, the distance from the center of the source is measured in half-diameters of the equivalent spherical source. Note that $V=a$, the normal velocity of sound, for $x\to\infty$.

[1] Riemann, Abh. Konigl. ges. der Wiss. Göttingen **8**, 43 (1860); Wolff, Ann. d. Phys. u. Chem. **69**, 329 (1899).

[2] Perrott and Gawthrop, J. Frank. Inst. **203**, 103, 387 (1927).

[3] Payman and Woodhead, Proc. Roy. Soc. London **A163**, 575 (1937).

[4] E. Jouguet, Memor. de l'Artill. Franc. **21**, 259 (1927).

[5] L. Thompson, Phys. Rev. **49**, 421A (1936).

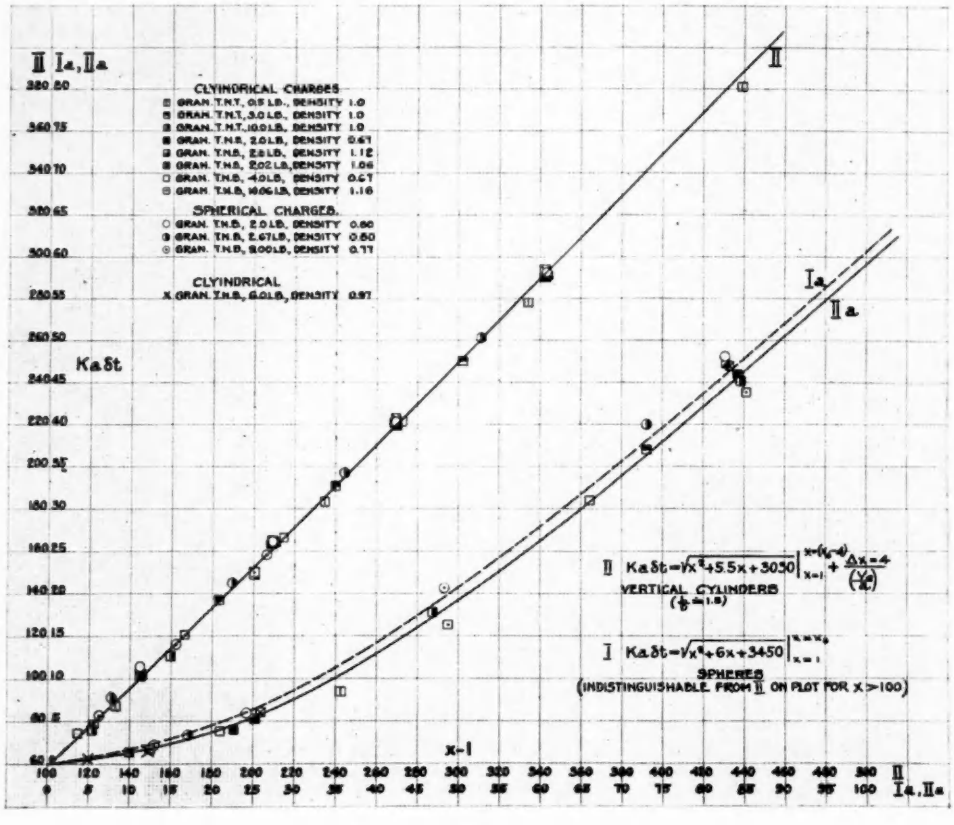

FIG. 1.

In summarizing the results of our experiments with shock waves from certain explosives which are described in Section 2 below, V_d is the velocity of the detonating wave in the solid explosive, but the value of V_d can be any boundary velocity.

We make then the following assumptions: (a) The wave surface advances as if it had proceeded from a point φ half-diameters farther removed than the actual center of the disturbance. The value of φ, which must be determined empirically, appears to be unique for sources of a given shape regardless of size. (b) The initial velocity of the wave in air is the velocity of the detonating wave in the charge, if the source is a detonating charge of an explosive of fairly high brisance. (c) Similar distances of displacement x are proportional to the diameters of "equivalent" spherical sources.

The introduction of a fictitious offset of the source is directly significant only as an effort to obtain greater flexibility in representing the full range of data for velocities of the finite wave. In effect, however, it identifies a dissipative function which represents well enough the decrease of velocity caused by loss of energy to the medium and change of wave form (over and above the attenuation by spherical divergence). The excessive rates of dissipation for high condensations are reflected in the sensitiveness of the velocity function to change of x for small x values. The numerical effect of these losses is everywhere identical with the effect of an additional spherical divergence corresponding to φ additional half-diameters of wave displacement.

The term $C/(\varphi+x)^2$ of the equation for velocity, which is identified below as (1.5), takes the place of Riemann's K/r^2 without introducing a variable analogous to K.

Instead of calibrating the velocity formula by means of observed values of velocity, which would entail numerical differentiation of the displacement data, it is convenient to refer to similar or "reduced" times $Ka\delta t$. By definition

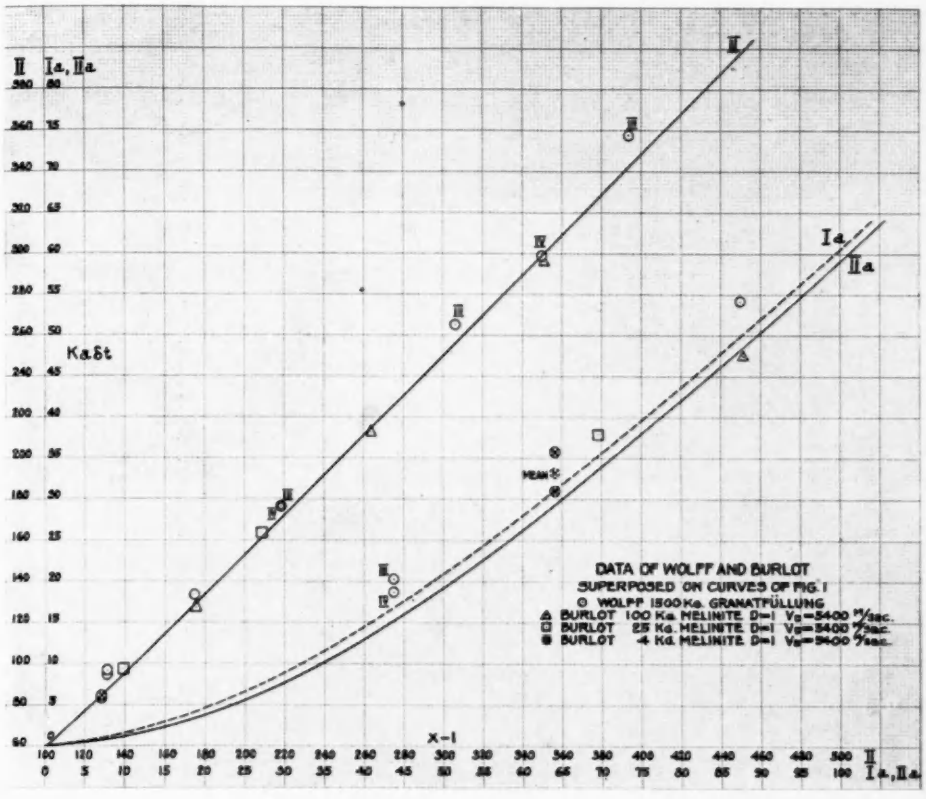

FIG. 2.

$$\delta t = \int_{x=1}^{x=Ks} \frac{dx}{KV(x)} = \frac{1}{Ka} \int_{x=1}^{x=Ks} \frac{(\varphi+x)dx}{(x^2+2\varphi x+C_1)^{\frac{1}{2}}}$$

or

$$Ka\,\delta t = (x^2+2\varphi x+C_1)^{\frac{1}{2}} \Big|_{x=1}^{x=Ks}$$

where K is now defined as $K=x/s$, s being distance in meters, V velocity in meters/second, and $C_1=C+\varphi^2$.

In the experimental work outlined in Section 2, shock waves were produced by detonating charges of high explosives. We have found that a single curve represents the reduced times for all sources of a given shape regardless of size. The data compiled in the tables of observations were plotted in Figs. 1 and 2. The best value of the constant φ was found from the distribution of observed δt and distance values (s), multiplied, respectively, by Ka and K to obtain similar times and similar distances, $Ka\delta t$ and x. The constant $\varphi=3$ represents all of the data with spherical charges, within the limits of experimental precision, and a slightly lower value ($\varphi=2.75$) is necessary for best fit with the data for cylindrical charges. In the latter case there is a narrow zone of width approximately $\Delta x=4$ in which the velocity of propagation in a direction normal to the axis of the cylindrical charge is of negligible attenuation. The formula II of Fig. 1, for cylindrical charges of length approximately $1.5d$, allows in this manner for a zone of nearly constant velocity as the only means of getting a sufficiently low sequence of $Ka\delta t$ values in the vicinity of $x=20$, with the proper characteristics elsewhere. This result appears to be in agreement with the data of Perrott and Gawthrop[2] who obtained either constant or increasing velocities in the air gap for a short distance close to a detonating cartridge. It is presumed that the reduced attenuation in the narrow zone adjacent to cylindrical charges represents a nearly cylindrical wave propagation near the charge. Perrott and Gawthrop with a constant velocity from the flat end zone of a

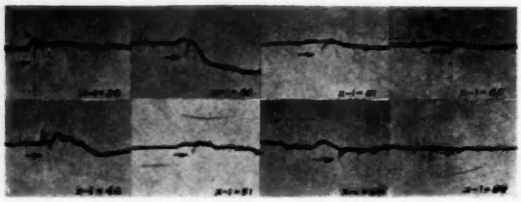

FIG. 3.

cartridge might similarly expect a plane wave for a very short distance. However, their results sometimes involved an increasing velocity in the air gap. A full explanation of this latter phenomenon probably includes recognition of the existence of a condensation in the products of detonation accompanying the wave in the solid which corresponds to a wave velocity in air greater than the detonating velocity in the solid. Thus at the boundary of the cartridge as the shock is transmitted to the adjacent layer of air the velocity in air must increase until the condition defined by Eq. (1.6) of Part II[6] is satisfied. The result of increasing velocity in the gap is characteristic of explosives having fairly low detonating velocities and not those used in the present experiments.

The formula for velocity which is given in Section 2 as Eq. (1.5), may be modified to include Jouguet's formula for V_d in a solid. According to Jouguet[7]

$$V_d=\frac{1.25}{1-\omega\Delta}(TV_0)^{\frac{1}{2}}.$$

with ω the co-volume, Δ the density of loading, V_0 volume of gaseous products of detonation l/kg at normal temperature and pressure, and T, temperature of explosion reaction.

An approximation for V_d may be had accordingly where no experimental values of V_d are available. It is best to alter the form by writing

$$V_d=f_1(\omega, \Delta)(TV_0)^{\frac{1}{2}},$$

and determine a suitable value for f_1 by substituting numerical results with other explosives having the same product $\omega\Delta$ and known detonating velocities for this condition. The definition of C_1 then becomes

$$C_1=(\varphi+1)^2\left[f_1^2(\omega, \Delta)\frac{TV_0}{a^2}-1\right]+\varphi^2.$$

2.

The reduced times of wave displacement are shown in Fig. 1 as a function of the distance from the source, the distance measured in units proportional to the diameter of an equivalent source. An equivalent source is defined either as a spherical charge of explosive of some standard density having the weight of the actual source, or merely as a spherical surface through which a wave is emitted with the given boundary velocity. Except for slight variations depending on shape, this function is unique in presenting the results of all of our tests, regardless of the size of the source. It will be noted in Fig. 2 that the curves also fit quite well the data for charges much larger than those we have used, extending up to Wolff's 1500 kilograms of *granatfüllung*.[1] In the experimental work of this paper the shock waves were produced by charges of high explosives detonated electrically. The formulas derived can be applied to other sources either in terms of their boundary characteristics or by obtaining measurements of velocity at two or more representative points in the fields.

An attempt has been made to measure pressures for the conditions in the "wave surface" itself, as distinguished from the pressure wave following the shock. Inasmuch as the time of condensation is remarkably small, in some cases less than 10^{-11} second, it is clear that any gauge used for the purpose, with the exception of optical systems which are not well adapted to use with our sources, must operate as a kind of ballistic unit. The deflections obtained with a cathode oscillograph for the rochelle-salt gauge of these experiments are taken, however, to be proportional to maximum pressures developed at the surface of the gauge during the condensation cycle. Somewhat better recording capacity might be had with an oscillograph of the Dufour type but it was not thought worth while to substitute this unit in view of the limitations in time resolution of pressure which are set by the gauge itself. The results of the work with

[6] Part II of this paper will be mentioned hereafter as II.
[7] Marshall, *Explosives* (Blakiston's, 1932), Vol. 3, p. 146.

pressures were difficult to interpret on an absolute scale because of inability to calibrate the gauge except by reference to theoretical pressures in the wave system. The records for one series of tests are shown in Figs. 3 and 4, and the relative gauge deflections are compared with relative gauge pressures calculated in II on the assumption of certain values for the ratio of the specific heats of air and the Rankine-Hugoniot equation of condition.

Details of Experimental Work

The data of Tables I to XII inclusive were obtained with the experimental arrangement shown in Fig. 6. Piezoelectric pressure gauges were placed as screens at convenient distances from the charges of explosive, the instant of arrival of the pulse being recorded on a moving film by a set of stiff oscillograph elements; a separate element was connected through an amplifier to each gauge. Time calibration was superposed on the film in the usual manner by means of a tuning fork. At points close to the source the piezo-gauges were replaced by sensitive contact units, to avoid damage to the gauges from the impinging gas jet. A new contact unit was required for each round. In certain instances this "rupteur" was also used in alternate positions with the piezo-gauge at the greater distances.

The mountings for the gauges were designed to prevent interference by the ground wave, and

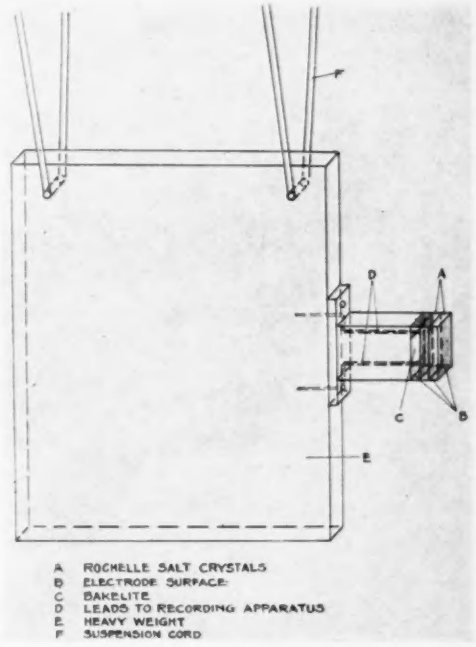

Fig. 5.

consisted of taut Y suspensions of rope securely tied in two planes approximately normal to each other. Careful tests were made to insure that no record was produced by disturbances passing over the rope.

Six screens were ordinarily set up, extending to a distance of about 50 feet, in addition to one placed at the surface of the charge. The latter was merely a fine wire wound tightly around the charge. The zero of time was accordingly the time at which the detonating wave reached the surface.

The detonation of the charges was initiated by electric detonators, of sizes No. 8 and No. 6.

The pressure records of Fig. 3 were taken with the rochelle-salt gauge shown in Fig. 5. It was necessary to use a single unit (here consisting of two crystals in a series connection) mounted, without a rigid clamp or housing. The gauges of Fig. 6, set up for displacement-time records, are enclosed in oil in a metal case, the pressure being

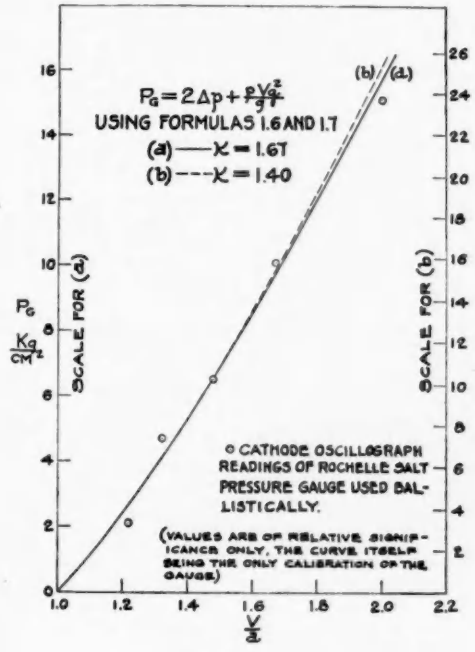
$P_G = 2\Delta p + \frac{\rho V_g^2}{g}$
USING FORMULAS 1.6 AND 1.7
(a) —— $\chi = 1.67$
(b) --- $\chi = 1.40$
(b)//(a)
SCALE FOR (a)
SCALE FOR (b)
P_G $\frac{Kg}{CM^2}$
© CATHODE OSCILLOGRAPH READINGS OF ROCHELLE SALT PRESSURE GAUGE USED BALLISTICALLY.
(VALUES ARE OF RELATIVE SIGNIFICANCE ONLY, THE CURVE ITSELF BEING THE ONLY CALIBRATION OF THE GAUGE.)
$\frac{V}{a}$

Fig. 4.

FIG. 6.

communicated hydrostatically through a diaphragm. Distortion and vibration of the case produced stresses great enough to mask the direct effect of the pulse communicated by the diaphragm, making some modification essential. Details of the mounting finally adopted for the pressure work are given in the Fig. 5. The two crystals were held on the Bakelite base by wrapping tightly with a strong thread. The amplifier by which the impulse was communicated to the cathode oscillograph was a three-stage resistance-coupled set of standard design. The cathode oscillograph used was one of the type 687-B made by the General Radio Company.

The time during which the principal shock pressure is applied at the surface of the gauge is small compared with the time required for the pulse to pass through the gauge crystal. But the maximum pressure at the boundary should be proportional to the maximum condensation or amplitude of stress propagated in the crystal. Accordingly, the almost-instantaneous deflections of Fig. 3 (those having no measurable time width) are taken to be proportional to maximum effective pressures at the gauge surface. The system is, of course, incapable of resolving the variations of pressure (to show values less than the maximum) which occur during the action of the pulse. Calibration of the outfit was tried in several ways but no satisfactory method could be found which was independent of the wave system, which did not alter the characteristics of the gauge system while being calibrated. In II the calculated gauge pressures, made up of two terms, one of which is the dynamic effect of the moving air in the finite wave, are used to provide the kind of calibration shown in Fig. 4. The measured values of deflection were given such a pressure equivalent as to make the curves agree at the mid point of the range; the extent of agreement of the observed and calculated pressures at either end of the range of observation was then noted in a consideration of the validity of certain velocity-pressure functions and of the appropriate ratio of specific heats.

The pressures plotted in Fig. 4 are the averages for one series of detonations, for which the atmospheric and circuit conditions were uniform during the period of observation which was about six hours. Some of these records are the ones reproduced in Fig. 3. Fifteen records were obtained altogether, in the five gauge positions used for this series. The mean variation among individual deflections of the oscillograph was about one part in seven, indicating a probable error of about 7 percent for the mean points plotted in Fig. 4. There has been a well-defined tendency for the relative deflections of this figure to recur in other series, when the conditions of the tests were favorable to good uniformity of results for any one distance of the gauge, but the results are at best subject to considerable variation. It will be noted that in the series of tests for which records are reproduced there was an irregular electrical disturbance in the circuit occurring before the shock wave reached the pressure gauge. Measurement of the time duration of the disturbance shows that this interval is closely equal to the time after closing the firing circuit required for the wave to travel from the

charge to the gauge. The true shock pulse is marked by an arrow, and the average magnitudes of these deflections are the ones plotted in Fig. 4. The motion of the photographic recording surface was opposite to the arrows.

Summary of Data. Observed Wave Displacements

The Tables I–XVI summarize the data of our experiments with charges of TNT and TNB (trinitrobenzene) up to 10 lb. and also include observations with large charges by Wolff[1] and

Table I. *Granular TNT (trinitro toluene); density $\gamma \doteq 1$; detonating velocity $Vd \doteq 5000$ m/sec.; charge vertical cylinder 4.54 kg; $K = 12.30$; $Ka = 4145$; $T = 10°C$; $W = -5.$ m/sec.*

Screen	Surface	(1)	(2)	(3)	(4)	(5)	(6)
s (meters)	R	.890	3.892	6.956	9.924	13.027	16.377
$x = Ks$	1	10.9	47.9	85.5	122.1	160.2	201.5
$1000\delta t_0$ obs. (sec.)	0	.35	4.31	10.97	18.46	26.91	36.39
$Ka\delta t_0$ (obs.)	0	1.45	17.86	45.47	76.52	111.5	150.8
$*Ka\delta t_c$	0	1.45	17.8	45.2	75.9	110.5	149.4

* Corrected to equivalent value for wind =0.

Table II. *Granular TNT (trinitro toluene). Charge vertical cylinder 1.36 kg; $K = 18.38$; $Ka = 6205$; $T = 11°C$; $W = +1.6$ m/sec. Density $\gamma \doteq 1$.*

Screen	Surface	(1)	(2)	(3)	(4)	(5)	(6)
s (meters)	R		4.032		10.025	13.128	16.490
$x = Ks$	1		74.1		184.3	241.3	303.2
$1000\delta t_0$ (sec.)	0		5.95		21.98	30.64	40.12
$Ka\delta t_0$	0		36.91		136.34	190.06	248.86
$Ka\delta t_c$	0		37.0		136.9	190.8	250.0

Table III. *Granular TNT. Charge vertical cylinder 0.23 kg; $K = 33.39$; $Ka = 11235$; $T = 9°$; $W = 0$. Density $\gamma \doteq 1$.*

Screen	Surface	(1)	(2)	(3)	(4)	(5)	(6)
s (meters)	R	1.097	4.014	7.068	10.034	13.167	
$x = Ks$		36.6	134.0	236.0	335.0	439.6	
$1000\delta t_0$ (sec.)		.77	7.77	16.23	24.78	33.87	
$Ka\delta t_0$		8.65	87.30	182.36	278.43	380.56	
$Ka\delta t_c$		8.6	87.3	182.4	278.4	380.6	

Table IV. *Trinitro benzene. Charge vertical cylinder 0.91 kg; density $\gamma \doteq 0.67$; $K = 21.04$; $Ka = 6965$; $T = -1°C$; $W = +.7$ m/sec.*

Screen	Surface	(1)	(2)	(3)	(4)	(5)	(6)
s (meters)		1.122	4.057	6.977	10.086	12.89	16.331
$x = Ks$	1	23.6	85.4	146.9	212.2	271.2	343.6
$1000\delta t_0$ (sec.)	0	.57	6.60	14.75	23.49	31.63	41.69
$Ka\delta t_0$	0	3.97	45.96	102.7	163.58	220.27	290.33
$Ka\delta t_c$	0	4.0	46.0	102.9	163.9	220.7	290.9

Table V. *Trinitro benzene. Charge vertical cylinder 0.91 kg; density $\gamma \doteq 1.12$; $K = 21.04$; $Ka = 7000$; $T = +2°C$; $W = 0$.*

Screen	Surface	(1)	(2)	(3)	(4)	(5)	(6)
s (meters)		1.253	3.978	6.919	10.013	12.866	16.359
$x = Ks$	1	26.4	83.7	145.6	210.6	270.7	344.2
$1000\delta t_0$ (sec.)	0	.74	6.76	14.86	23.41	31.61	41.75
$Ka\delta t_0$	0	5.18	47.32	104.02	163.87	221.27	292.25
$Ka\delta t_c$	0	5.2	47.3	104.0	163.9	221.3	291.2

Table VI. *TNB. Charge vertical cylinder 0.92 kg; density $\gamma \doteq 1.06$; $K = 20.97$; $Ka = 6950$; $T = 0°C$; $W = +1.1$ m/sec.*

Screen	Surface	(1)	(2)	(3)	(4)	(5)	(6)
s (meters)		1.283	4.011	6.943	10.037	12.917	16.395
$x = Ks$	1	26.9	84.1	145.6	210.5	270.9	343.8
$1000\delta t_0$ (sec.)	0	.87	6.75	14.63	23.59	31.98	42.23
$Ka\delta t_0$	0	6.05	46.91	101.68	163.95	222.26	293.50
$Ka\delta t_c$	0	6.1	47.0	101.9	164.4	222.9	294.4

Table VII. *TNB. Charge vertical cylinder 1.82 kg; density $\gamma \doteq 0.67$; $K = 16.69$; $Ka = 5565$; $T = 3°C$; $W = -2.9$ m/sec.*

Screen	Surface	(1)	(2)	(3)	(4)	(5)	(6)
s (meters)		1.317	4.020	6.940	10.034	12.899	16.383
$x = Ks$	1	22.0	67.1	115.9	167.5	215.3	273.5
$1000\delta t_0$ (sec.)	0	.70	5.60	13.46	21.88	30.08	40.13
$Ka\delta t_0$	0	3.90	31.16	74.90	121.76	167.40	223.32
$Ka\delta t_c$	0	3.9	31.0	74.4	121.0	166.2	221.6

TABLE VIII. *TNB. Charge vertical cylinder 4.56 kg; density $\gamma \doteq 1.16$; $K = 12.28$; $Ka = 4065$; $T = -0.5°C$; $W = 0$.*

SCREEN	SURFACE	(1)	(2)	(3)	(4)	(5)	(6)
s (meters)		1.106	4.054	7.029	10.07		16.410
$x = Ks$	1	13.6	49.8	86.3	123.7		201.5
$1000\delta t_0$ (sec.)	0	.41	4.03	10.8	19.24		36.93
$Ka\delta t_0$	0	1.67	16.38	43.90	78.21		150.12
$Ka\delta t_c$	0	1.7	16.4	43.9	78.2		150.1

TABLE IX. *TNB. Charge spherical, 0.91 kg; Density $\gamma \doteq 0.8$; $K = 21.04$; $Ka = 7040$; $T = 5.0°C$; $W = -1.6$ m/sec.*

SCREEN	SURFACE	(1)	(2)	(3)	(4)	(5)	(6)
s (meters)		1.198	3.978	6.949	10.003	12.881	16.362
$x = Ks$	1	25.2	83.7	146.2	210.4	271.0	344.2
$1000\delta t_0$ (sec.)	0	.85	6.85	15.04	23.42	31.53	41.68
$Ka\delta t_0$	0	5.98	48.22	105.88	164.88	221.97	293.43
$Ka\delta t_c$	0	6.0	48.1	105.5	164.2	221.0	292.1

TABLE X. *TNB. Charge spherical, 4.09 kg; density $\gamma \doteq 0.77$; $K = 12.75$; $Ka = 4275$; $T = 6.5°C$; $W = -1.4$ m/sec.*

SCREEN	SURFACE	(1)	(2)	(3)	(4)	(5)	(6)
s (meters)		1.097	3.865	6.846	9.900	12.79	16.25
$x = Ks$	1	14.0	49.3	87.3	126.2	163.1	207.2
$1000\delta t_0$ (sec.)	0	.51	4.85		19.46	27.26	37.12
$Ka\delta t_0$	0	2.18	20.73		83.19	116.54	158.69
$Ka\delta t_c$	0	2.2	20.7		83.0	116.1	158.2

TABLE XI. *TNB. Charge spherical, 1.21 kg; density $\gamma \doteq 0.8$; $K = 19.09$; $Ka = 6420$; $T = 8.0°C$; $W = 0$.*

SCREEN	SURFACE	(1)	(2)	(3)	(4)	(5)	(6)
s (meters)		.951	3.877	6.934	9.991	12.872	16.362
$x = Ks$	1	18.1	74.0	132.4	190.7	245.7	312.3
$1000\delta t_0$ (sec.)	0	.53	6.23	14.21	22.58	30.67	40.70
$Ka\delta t_0$	0	3.4	40.00	91.23	144.96	196.90	261.29
$Ka\delta t_c$	0	3.4	40.0	91.2	145.0	196.9	261.3

TABLE XII. *TNB. Charge, vertical cylinder, 2.72 kg; density $\gamma \doteq 0.97$; $K = 14.60$; $Ka = 4835$; $T = 0.2°C$.*

SCREEN	SURFACE	(1)	(2)
s (meters)	0	.335	.842
$x-1$	0	4.9	12.3
$1000\delta t_0$(sec.)	0	.11	.32
$Ka\delta t_0$	0	.54	1.54

TABLE XIII. *Burlot data.*[8]

SCREEN	SURFACE	(1)	(2)	(3)	(4)	(5)
Charge, 100 kg Melinite; density $\gamma \doteq 1.0$; $K = 4.39$; $Ka = 1515$; $T = 23°$.						
s(meters) $- R$	0	20	40	60	80	100
$x-1$	0	87.8	175.6	263.4	351.2	439
$1000\delta t_0$	0	31.36	84.19	140.18	195.4	252.7
$Ka\delta t_0$	0	47.5	127.5	212.3	295.9	382.8
Charge, 25 kg Melinite; density $\gamma \doteq 1.0$; $K = 6.96$; $Ka = 2400$; $T = 23°$.						
$s - R$	0	10	20	30		
$x-1$	0	69.6	139.2	208.8		
$1000\delta t_0$	0	15.8	40.7	68.2		
$Ka\delta t_0$	0	37.9	97.7	163.8		
Charge cylindrical, 4 kg Melinite; density $\gamma \doteq 1.0$; vertical axis; $K = 12.83$; $Ka = 4360$; $T = 15°$.						
$s - R$	0	5	10			
$X-1$	0	64.2	128.3			
$1000\delta t_0$	0	8.20 7.10	19.57 19.15			
$Ka\delta t_0$	0	35.77 30.97	85.36 83.53			

TABLE XIV. *Wolff data.*[1] *Charge 1500 kg granatfüllung (Mixture picric acid and TNT) $K = 1.75$; $Ka = 595$; $T = 11.4°$; 12.8°C.*

SCREEN	SURFACE	(1)	(2)	(3)	(4)	(5)	(6)
$s - R$	0	25	75	125	175	200	
$x-1$	0	43.7	131.2	218.7	306.2	350 393.7	
1000 t_0	0	31.5 34.2	159 162.3	296.5 296.4	434. 446.1	503.1 600.9	(Test IV) (Test III)

by Burlot,[8] which were plotted in Fig. 2 for comparison with the $Ka\delta t$ function derived from the present experiments. The data of Table XVI for flame propagation are measurements of Fig. 7, showing the progress of the flame surface as a function of time, which are plotted in Fig. 8.

The distances to the gauges, measured with a metal tape, have a probable error approximately 0.002 meter, and the probable error of the

[8] E. Burlot, Memor. de l'Artill. Franc. **19**, 935 (1926).

TABLE XV. *Payman and Shepherd data;[9] No. 6 detonator in 40-cm tube; diameter of tube 2.5 cm; take* $K=(1/R)=(1/0.0125)=80$; $Ka=26720$; $T=3.°C$; $V_0=1150$ *m/sec.*

δt (SEC.)	δt FOR $x=1$, TO $x=x_s$	s (METERS)	$x=Ks$	$Ka\delta t$ OBSERVED	$Ka\delta t$ CALCULATED $Ka\delta t=(x^2+2\varphi x+C_1)^{\frac{1}{2}}\Big\|_{x=1}^{x_s}-C_2+\frac{C_2}{(Vd/a)}$				
					$C_2=0$	1	2	3	4
0	0	0	1	0	0	0	0	0	0
.00011	.00010	.10	8.0	2.67	3.4	3.0	2.8	2.5	2.3
.00031	.00030	.20	16.0	8.02	9.3	8.8	8.3	7.8	7.4
.00055	.00054	.30	24.0	14.43	16.3	15.7	15.1	14.5	13.9

$V_d/a=3.44 \qquad \varphi=3$

$$C_1=\varphi^2+\{(1150/334)^2-1\}\cdot(\varphi+1)^2=183.$$

TABLE XVI.

DISPLACEMENT	SURFACE	(1)	(2)	(3)	(4)	(5)	(6)
Charge, 2.73 kg TNB. Data on flame displacement, Fig. (3). $K=14.59$; $Ka=4950$.							
$s-R$	0	.305	.610	.762	.920	1.521	1.655
$x-1$	0	4.45	8.89	11.12	13.43	22.19	24.15
$1000\delta t_0$	0	.095	.24	.34	.45	1.27	1.54
$Ka\delta t_0$	0	.47	1.19	1.68	2.24	6.29	7.63
Chage, 0.23 kg TNB. $K=33.4$; $Ka=11235$.							
$s-R$	0	.152	.305	.457	.548	.610	
$x-1$	0	5.09	10.18	15.27	18.32	20.36	
$1000\delta t_0$	0	.064	.146	.286	.43	.58	
$Ka\delta t_0$	0	.72	1.64	3.21	4.83	6.52	

observed times is from 0.00001 second to 0.00002 second. Corrections were applied for wind components in the direction of propagation, and the value of the normal velocity of sound a used in computing $Ka\delta t$ is that for the temperature of the experiment. The wind corrections were obtained from the ratio

$$\frac{\delta(Ka\delta t)}{Ka\delta t}=\sum_{x=1}^{x_s}\delta\left(\frac{1}{V(x)}\right)_\tau\Big/\sum^{x_s}\left(\frac{1}{V(x)_\tau}\right),$$

the changes δV in effective velocity $V(x)$ being

[9] Payman, Robinson and Shepherd, Safety in Mines Res. Bd. **18**, 29 (1926).

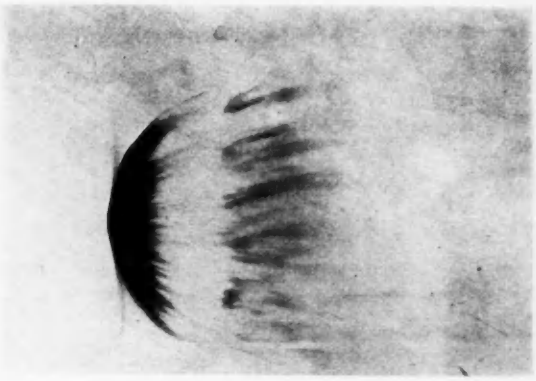

FIG. 7.

equal numerically to the range winds. Humidity variations were of negligible effect.

Table XV gives wave data by Payman, Robinson and Shepherd,[9] obtained in a study of propagation from the end of a tube of length 40 cm and diameter 2.5 cm. A comparison is included of the fit of these displacements by the formulas, assuming $\varphi=3$ and taking the value of K to be the reciprocal of the radius of the end of the tube. Fairly good agreement between observed $Ka\delta t$ values and the formula is found to occur with $C_2=3$. That is, the displacement-time data are so distributed in the observations as to correspond to a velocity nearly constant for a distance of about 3 half-diameters beyond the initial hemispherical boundary at the end of the tube, assuming that the given values of φ and K are applicable to the condition at the end of the tube. An independent check could be had regarding these quantities by substituting accurately measured values of the velocity, obtained at several points in the field, in the formula for velocity.

The close fit of the integral curves I and II, of Fig. 1 by all of the data obtained in the experiments with charges varying from 0.2 kg to about 4 kg, and the fair agreement of the observations by Wolff and Burlot for charges from 20 to 400 times the maximum of our series, indicate that the generalization is satisfactory. The average deviation of the observed reduced times, referred to the single curve representing charges of all magnitudes, is approximately 1.3 units of $Ka\delta t$, giving a probable deviation

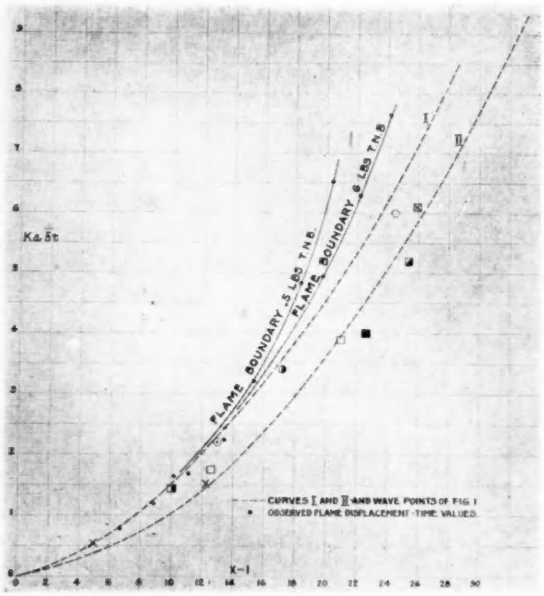

FIG. 8.

corresponding to 0.0001 to 0.0002 second, throughout the range. This result is equivalent to the statement that time intervals calculated by the formula will agree with time observations of wave displacements from sources of a wide range of magnitudes (as often as not), within 0.0001 second to 0.0002 second. Some of the data taken by Burlot and Wolff for large charges are of greater deviation (the probable value being about 0.0005 second). The deviations of the *means* of their sets of observations for charges of like condition average little more however, than is expected in view of the dispersions within the Wolff and Burlot groups for identical conditions, indicating merely a greater fluctuation of experimental origin. Also, the shapes and orientations of their charges were not identical with those used to calibrate the curves I, II of Figs. 1 and 2—factors which would affect somewhat the distribution of the points for x values less than 100. Another minor source of deviation in using these observations is introduced by the uncertainty regarding the correction required for effective wind. The data by Wolff and some of those of Burlot were taken with Le Boulenge and Schultz chronographs, and these instruments are usually not capable of measuring small intervals of time with much better uniformity than is shown in Fig. 2 with respect to the formula curves.

The dotted curves for velocity shown on Fig. 9 for comparison with our curve were computed to represent the Rüdenberg formulas[10, 11] for the velocity of finite waves:

$$\frac{V}{a}=\left(\frac{\kappa+1}{\kappa-1}\right)^{\frac{1}{2}}\left(1+C'\left(\frac{1}{x}\right)^{2}\right)^{\frac{1}{2}} \tag{1}$$

for points near the source.

$$V/a=(1+C_1'(1/x)^2)^{\frac{1}{2}} \tag{2}$$

for distant points, of which

$$C'=\frac{W_0^2-a^2}{W_0^2+2a^2/(\kappa-1)}\left(\frac{W_0}{a}\right)^2\cdot\frac{\kappa-1}{\kappa+1}.$$

$$W_0=\left(\frac{\rho_0'}{\rho_0}gE\right)^{\frac{1}{2}},$$

ρ_0', density of gases from explosive, standard conditions,

ρ_0, density of air, standard,

E, specific energy of explosive,

$$C_1'=\left(\frac{\kappa+1}{\kappa-1}\right)^2 C',$$

g, acceleration of gravity.

The formula (1) has the limit $V\doteq W_0$ for $x=1$ and $V=[(\kappa+1)/(\kappa-1)]^{\frac{1}{2}}a$ for $x\to\infty$, the latter being about $2.4a$ instead of the required value a. Formula (2) has the correct limit for $x\to\infty$, but is not satisfactory for intermediate values of x. It is clear from an examination of Fig. 9 that formula (1) above is not in good approximation for $x>10$, and that the time integrals based on either formula cannot represent well the observed fields of Figs. 1, 2, and 9. Following Rüdenberg, these curves were computed using the ratio of specific heats $\kappa=7/5$.

The photograph of Fig. 7 was taken with a camera having a rotating film and shows by the transverse dimensions of the image of the flame the position of the advancing flame surface at

[10] R. Rüdenberg, *Artilleristische Monatshefte*, May, June (1915), pp. 237, 285.
[11] C. Cranz, *Lehrbuch der Ballistik II* (J. Springer, 1926), p. 174.

successive instants. The positions for charges of 0.5 lb. and 6 lb. relative to the wave surfaces are plotted on the $Ka\delta t$ plot of Fig. 8.

The purpose of these latter tests was to find at what point the wave surface is definitely in advance of the expanding gases (flame). The records, which were obtained with spherical charges so placed that their horizontal diameters were accurately focused on the lower edge of the slit (in front of the moving film, with the film moving downward toward the edge) were sharp enough to show a distinct difference between the $Ka\delta t$ values for the flame and the wave values for the same distance (curve I, Fig. 1), at about 10 half diameters. There is no doubt, however, that with the explosives we have used, for which the detonating velocities are of the order of 5000 meters per second, the shock radiated from the boundary greatly exceeds in velocity the expanding gases, and the accompanying shock wave produced by those gases. The experiments of Lafitte,[4, 12] Perrott and Gawthrop,[2] and Payman and Woodhead[3] all show the shock proceeding from a charge across an air gap from these explosives to have velocities at least equal to the velocity of the wave of detonation in the charge, and the results of Payman and Woodhead with spark photography show the shock wave at an early phase of the disintegration cycle to be well in advance of the gaseous products. It is doubted that Audibert's residual combustion[4] has any effect in "supporting" the initial shock wave, provided the brisance of the charge is fairly high.[13] Rüdenberg's use of a much lower boundary velocity probably explains in part the failure of the Rüdenberg functions to represent very well the data for the *initial* shock wave.

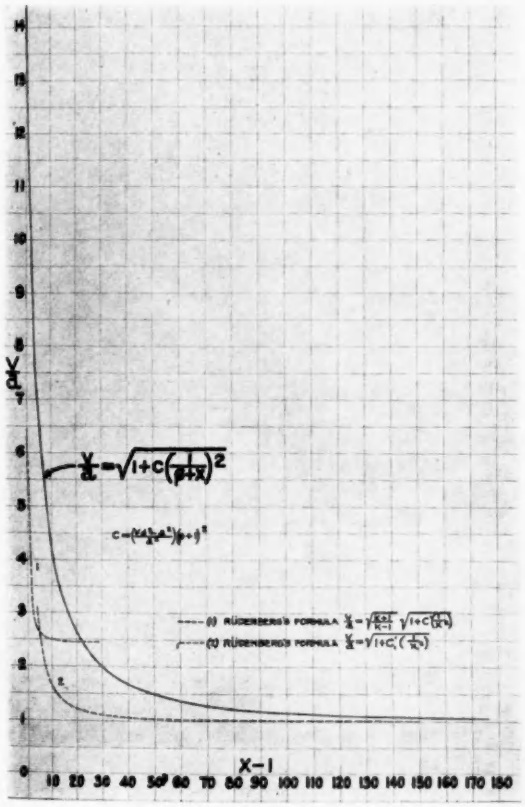

FIG. 9.

The curves of Figs. 1 and 9 may be used to calculate the velocity and time of displacement from the source, to any point in the field, for the wave generated by the detonation of any quantity of explosive. First obtain a value for

$$K = 12.3(M_0/M)^{\frac{1}{3}}.$$

The reference charge M_0 has been taken throughout as 4.54 kilograms. The magnitude of K is roughly but not exactly the reciprocal of the radius of the equivalent spherical charge of density unity. The agreement is sufficiently close to justify the use of $x=1$ as the boundary of the source. The constant of the formula for K could have been selected to make the equality exact, but there would have been no great advantage. The important consideration is merely that K shall be proportional to $M^{-\frac{1}{3}}$. Having obtained K, compute $x=Ks$ where s is the distance in meters of the point of interest from the center of the source. The curves will then give values of V/a and $Ka\delta t$ representative of the point for explosives having a detonating velocity of the order of 5000 meters per sec. when the density of loading is approximately unity. Divide $Ka\delta t$ by K times the normal velocity of sound (a) to get actual time of wave displacement δt. As

[12] Lafitte, Comptes rendus **178**, 1277, 2176 (1924).

[13] The conditions here are unlike those at the muzzle of a gun, for example. At the muzzle of a gun, as the powder gases first escape, a finite, "supported" shock wave is set up by the moving boundary of the jet. The apparent position of the "source" may change during a very short interval of time following ejection, depending on the curvature of the wave surface. This case is discussed in II. See Cranz, p. 447; also see Dayton C. Miller, *Sound Waves—Their Shape and Speed* (Macmillan, 1937).

TABLE XVII.

	$Ka\delta t$ (δt (SEC.) = TABULAR VALUES/Ka)						VELOCITY M/SEC.					
BOUNDARY VEL. M/SEC.	3000	4000	5000	6000	7000	8000	3000	4000	5000	6000	7000	8000
$x=$ 1	0	0	0	0	0	0	3000	4000	5000	6000	7000	8000
10	2.11	1.60	1.28	1.08	.93	.81	978	1273	1572	1875	2178	2483
20	6.65	5.17	4.21	3.54	3.06	2.68	620	722	932	1096	1263	1431
50	28.26	23.71	20.26	17.59	15.50	13.81	408	454	507	566	628	692
100	73.53	66.11	59.74	54.21	49.44	45.34	359	374	391	412	435	460
200	170.7	161.3	152.5	144.3	136.7	129.6	345	349	354	360	367	375
500	468.9	458.1	447.6	437.3	427.3	417.6	341	342	342	343	345	346
1000	968.3	957.0	945.9	934.9	924.0	913.3	340	340	341	341	341	342

shown by the plotted points of Fig. 1, the results will not be appreciably in error if the charge is compressed to a smaller volume, giving a larger density (and a correspondingly higher detonating velocity). It is true that the boundary velocity is then higher, sometimes as much as 25 percent, but the unit of distance (proportional to charge diameter) is also smaller. The results of Fig. 1 show that when the wave has reached the diameter the charge would have had at density unity, the velocity has decreased to the order of the boundary velocity for that density. On the other hand, if the boundary velocity V_d differs from 5000 meters per second by more than a few percent, for a density of unity, or for any equivalent source, then the values of velocity and time should be got directly from the formulas[14]

$$V/a=(1+C/(\varphi+x)^2)^{\frac{1}{2}} \tag{1.5}$$

(for cylindrical sources use $x=x_s-C_2$ and associate the velocity thus calculated with x_s; for $x=1$ to $x=C_2$ use $V=V_d$)

[14] The numbers given to the following equations are the designations used in II.

$$Ka\delta t=(x^2+2\varphi x+C_1)^{\frac{1}{2}}\Big|_{x=1}^{x_s-C_2}+\frac{C_2}{(V_d/a)} \tag{1.4}$$

for cylindrical sources;

$$Ka\delta t=(x^2+2\varphi x+C_1)^{\frac{1}{2}}\Big|_{x=1}^{x=x_s} \tag{1.3}$$

for spherical sources; $\varphi=3$ for spherical sources, 2.75 for cylindrical sources.

$$C=\left(\frac{V_d^2-a^2}{a^2}\right)(\varphi+1)^2, \quad C_1=C+\varphi^2.$$

V_d, boundary velocity of shock wave; equals detonating velocity in charge under certain conditions; note $V=V_d$ for $x=1$; $V=a$ for $x\to\infty$. a, normal velocity of sound; C_2, characteristic constant; $C_2=4$ for cylindrical charges for which length $\doteq 3/2$ diameter; $C_2=0$ for spherical charges. The above formulas are equivalent to those shown in Figs. 1 and 2.

Values of velocity and reduced time of wave displacement at representative distances x from the center are tabulated in Table XVII for spherical sources having boundary velocities from 3000 m/sec. to 8000 m/sec.

The Propagation of Shock Waves in Air. II

L. THOMPSON
Naval Proving Ground, Dahlgren, Virginia
(Received June 19, 1939)

Using the Rankine-Hugoniot equation of condition and Hugoniot's velocity of a discontinuity in a gas, formulas are obtained for density and pressure at the head of a shock wave which are referred to velocity of the wave as a parameter. Gauge pressures are defined in a form considered to represent the observations of pressure obtained in Part I. The function is used to calibrate the gauge, and a comparison of results by Rayleigh's pressure function is included. A discussion is given of the appropriate ratio of specific heats for condensation cycles so extremely short in duration as those of intense shock waves, with references to the literature bearing on the subject of the accumulation of molecular excitational energies in short intervals of time.

1.

THE conditions under which an intense wave of condensation can maintain itself in air without change of type have been discussed at length by Rayleigh.[1] He showed, for example, that some dissipative action, either as conduction of heat or the effect of viscosity, is necessary for the existence of a permanent regime. Earnshaw's condition for the stable propagation of a plane wave in a gas is given by the equation

$$p+m^2/\rho=p_0+m^2/\rho_0,$$

where the density at any point is ρ, the pressure p and

$$m=\rho_1(a-u_1)=\rho_0(a-u_0),$$

the mass-velocity of the wave; normal sound velocity a, and the finite velocity of air motion at the wave surface, u. With Rankine one may consider a gas being made to follow any prescribed law of variation of condition by the (analytically) simple expedient of transferring the right amount of heat at every stage in the propagation. The law derived by Rankine[2] and Hugoniot[3] for a finite condensation

$$p=p_0\frac{(\kappa+1)\rho-(\kappa-1)\rho_0}{(\kappa+1)\rho_0-(\kappa-1)\rho}, \qquad (1.1)$$

of which κ designates the ratio of the specific heats, does satisfy Earnshaw's condition. So it is plausible to assume that pressures and densities of intense shock waves in air follow fairly closely the relation defined by (1.1), particularly since it is known that shock waves of permanent status can be produced in air.

Perhaps one should hesitate to make imperfect gases go through an ideal transformation in a time interval as short as 10^{-11} second, which is the order of the time of condensation for a typical pulse, since pressures of very great magnitudes are reached in these intervals. Possibly there exists no unique function which actually represents the ratio of pressure to density as a function of temperature during all of the first part of a condensation cycle. The molecular motions are unidirectional, or nearly so for intense shock waves, and excessive "dynamic" temperatures are set up in the direction of flow.

However, in spite of circumstances which make an attempt to identify temperature and pressure within shock wave surfaces seem very arbitrary, there is a considerable amount of information to be had by methods which are in part obtained from Hugoniot. Rankine and Hugoniot in the development of (1.1) show why for hypothetical, ideal gas cycles the ordinary adiabatic law is not applicable to the region of the wave front.[4] The excess of work done per unit time on the gas entering an element of the surface over that on leaving exceeds the gain of kinetic energy; when this residual (per unit mass) is equated to the increment of internal energy, the pressure-

[1] Lord Rayleigh, Proc. Roy. Soc. London **484**, 247 (1910); for 1a, see pp. 263–64, 283.
[2] W. J. M. Rankine, Phil. Trans. II **160**, 277 (1870).
[3] H. Hugoniot, J. de l'Ecole Polytechn. **57** (1887); **58** (1889).
[4] H. Bateman, Bull. Nat. Res. Council, **84**, 545 (1931); P. S. Epstein, Proc. Nat. Acad. **17**, 532 (1931).

density condition (1.1) follows. This result of Hugoniot's and Rankine's is sometimes called the Hugoniot adiabatic-dynamic law.

The computations outlined in the present paper were made partly for the purpose of finding what densities and total pressures are properly to be associated with the wave surface of a shock wave in air having the velocities at various distances from a source defined by formula (1.5) below. This formula, which represents accurately the velocities at all points in the fields of certain sources of shock, was derived from the experiments of Part I[5] of this paper. It was shown there that the velocities can be calculated for a point in the field in terms of the characteristics of the source. Having values for velocity at any desired point, either by direct measurement or by Eq. (1.5) in terms of the dimensions of the source and its boundary velocity, it is possible to derive other characteristics of the wave by using velocity as a parameter, provided suitable equations are available between velocity and pressure and velocity and condensation.

The point of view adopted here is a kind of compromise, in which one accepts an ideal system as far as the equation of condition is concerned, but finds a more realistic concept of the mechanism of propagation.

To obtain the required equations we introduce in combination with Eq. (1.1) a result of Hugoniot's in his theory of the propagation of discontinuities in a gas. It is believed that a theory of shock based on the idea of a discontinuity traveling in the gas at characteristic velocities comes closer to actual mechanism than the procedure which derives a velocity function in the manner of Rankine and Rayleigh[1a] from the thermodynamics of slow transformations. The pressures and densities computed by the former procedure, taking into account the probable value of the ratio of the specific heats for the conditions prevailing during condensation, are compared below with Rayleigh's results and with some relative values for *gauge* pressures obtained experimentally.

The experiments of I were concerned with spherical waves propagated from charges of explosives at detonation. The results are applicable to other sources, and in general these waves are not of the kind whose form will remain unchanged. However, since Eq. (1.1) between pressure and density is presumed to define what happens in an (ideal) plane shock wave of permanent status, employing a cycle of condensation differing in no essential respect from the cycle in any specific period of the propagation of ideal spherical waves, there is perhaps no objection to the use of Hugoniot's law as a basic thermodynamic relation for the general system. In effect, the spherical wave is assumed to follow Earnshaw's condition in the sense that for distances large in respect to wave "thickness" (which is of the order of 10^{-5} to 10^{-6} cm),[6] the form does not change materially. An equivalent assumption was implied in Rayleigh's treatment of the conditions at the nose of a projectile traveling at supersonic velocities. Even with flat nose projectiles, the wave surface is clearly not plane; that is, in the region where the amplitude is finite.

The velocity of a discontinuity of the second order as propagated in a gas, which Hugoniot obtained from the differential equation of motion of the particles by means of his equations of compatability,[3, 7] is

$$V=(dp/d\rho)^{\frac{1}{2}}. \tag{1.2}$$

This definition is identical in form with the velocity for infinitesimal waves. But in the case of finite waves the function $p'(\rho)$ is not constant, as is obvious if the pressure follows the Rankine-Hugoniot equation of condition.

It was shown in I that the formula for velocity of a shock wave in air defines an integral function for reduced times of wave displacement $Ka\delta t$. The actual time of displacement δt observed at a given distance x measured in units proportional to the diameter of the equivalent spherical source, identifies the reduced time in accordance with the equations

$$Ka\delta t=(x^2+2\varphi x+C_1)^{\frac{1}{2}}\Big|_{x=1}^{x=x_\delta} \tag{1.3}$$

[5] L. Thompson and N. Riffolt, preceding paper. Part I will be mentioned hereafter as I.

[6] Bull. Nat. Res. Council, **84**, 548; Rayleigh, reference 1, 270, 281–2.

[7] Webster-Plimpton, *Partial Differential Equations of Mathematical Physics* (Teubner, 1927), p. 288; for 7a see p. 286, Eq. (195).

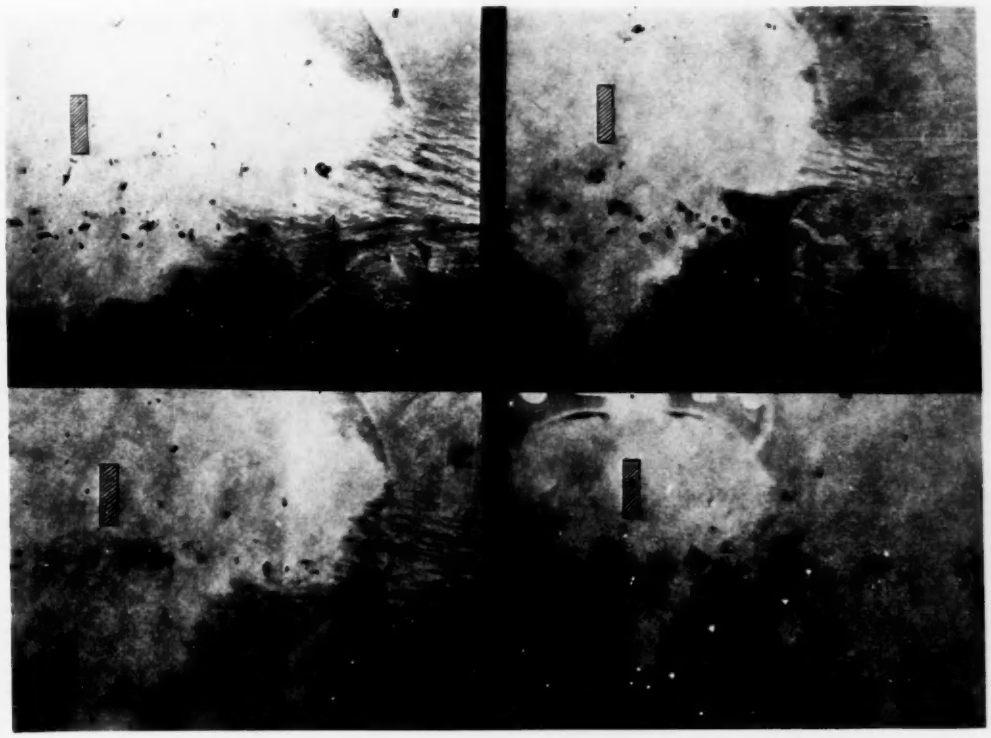

FIG. 1. Spark photographs by Lt. Col. H. H. Zornig, U. S. A. showing shock waves in field of exploded detonators. Positions of detonators indicated by hatched rectangles.

for spherical sources, and

$$Ka\delta t=(x^2+2\varphi x+C_1)^{\frac{1}{2}}\Big|_{x=1}^{x=x_s-C_2}+\frac{C_2}{(V_d/a)} \quad (1.4)$$

for cylindrical sources having a certain (approximate) ratio of length to diameter, where a=normal velocity of sound in air, $K=x/s=12.3(M_0/M)^{\frac{1}{2}}$ (for those sources which are charges of explosives), s=distance to center of source in meters, x=distance to center in units proportional to diameter of equivalent charge, M_0=reference charge 4.54 kg, M=weight of charge of explosive used as source, $C_1=C+\varphi^2$,

$$C=\left(\frac{V_d{}^2-a^2}{a^2}\right)(\varphi+1)^2,$$

V_d=velocity of shock wave at boundary of source, and φ, C_2 are general constants for sources of given (order of) shape. The velocity of propagation of the condensation pulse, which corresponds to the integrals (1.3) and (1.4), is

$$V=a\left(1+\frac{C}{(\varphi+x)^2}\right)^{\frac{1}{2}}, \quad (1.5)$$

a function somewhat similar to Riemann's formula[8] for the velocity of finite waves but having an additional constant and introducing a unit of distance defined by the characteristics of the source.

Referring to Fig. 1, to the papers of Payman and associates,[9, 10] and to Cranz's photographs,[11] it is evident that an explosion in free air produces an expanding gas bubble which is always preceded by a shock wave (provided the velocity of the gases exceeds the normal velocity of sound). When a gun is fired there is a condensation pulse in front of the jet of gases ejected from the muzzle, having the general form of the front

[8] B. Riemann, Abh. Konigl. ges. der Wiss. Göttingen **8**, 43 (1860).

[9] Payman, Robinson and Shepherd, Safety in Mines Res. Bd. **18**, 29 (1926).

[10] W. Payman and D. W. Woodhead, Proc. Roy. Soc. London, **A163**, 575 (1937).

[11] C. Cranz, *Lehrbuch der Ballistik II* (J. Springer, 1926), pp. 447–48.

of the jet, and this pulse produces momentarily the effect of a source "shot" from the muzzle, as Miller[12] described it. Here the shock wave does not immediately become a nearly spherical surface but travels out for a short distance with only moderate divergence. At this stage it is unlike the symmetric wave from a detonating charge in that it precedes a jet having high velocity only in the direction of the barrel. The regime is not permanent, however, in the sense of the wave preceding a bullet traveling at supersonic speeds and a wave field is soon produced because of the extremely dissipative nature of the gaseous system, which can be described by Eq. (1.5) for points not too close to the muzzle. The effective boundary velocity V_d may be had by measuring the velocity of the wave at two or more points in the field and substituting these values in (1.5).

The gas velocities are initially very high, both at the gun muzzle and at the boundary of detonating charges, of the order of 1500 or 2000 meters per second. The characteristics of a shock wave preceding the jet at such velocities must necessarily be rather extreme. The condensation in the bow wave of a projectile moving at half this speed is sufficient to produce a sharp "crack" as it passes. But when a charge of high explosive is detonated there is another agency for the production of a shock wave in air which may initiate still higher velocities. The detonating wave in the explosive is itself a condensation pulse and it communicates shock to the adjacent layer of air when it arrives at the boundary, or travels along the boundary. Although there is no obvious reason except chance combination of physical characteristics why the pulse propagated outward from the boundary should have the same velocity as the detonating wave in the charge, it is an experimental fact that the two velocities are nearly identical for common explosives of high brisance. The experiments of I require this conclusion for adequate representation of the observations of wave displacement, and a similar result has been obtained by Perrott and Gawthrop[13] and by Payman and others in the study of shock waves emitted from the ends of detonating cartridges. The result means merely that the condensation at the boundary in the gaseous products of disintegration actually corresponds to about the same stable velocity in air in accordance with Eq. (1.6) below. As was noted in I, the difference between the formulas of Rüdenberg[14] and the formulas of the present paper arises in part from Rüdenberg's not having taken the initial shock wave into account. In the case of the commoner high explosives, this shock precedes the wave accompanying the expanding gases and hence is the wave actually measured by chronographs in the field.

To obtain the required connections between velocity and density and velocity and pressure, differentiate Eq. (1.1) and note by (1.2) the identity

$$\delta(dp/d\rho) \equiv \delta(V^2),$$

from which

$$\frac{\delta(V^2)}{V^2} = 2(\kappa-1)\frac{\delta\rho}{(\kappa+1)\rho_0-(\kappa-1)\rho}$$

and, integrating

$$\rho = \frac{\rho_0}{V(\kappa-1)}[V(\kappa+1)-2a], \tag{1.6}$$

$$p = \frac{p_0}{a(\kappa-1)}[2\kappa V - a(\kappa+1)] \tag{1.7}$$

or

$$V = a\left[\frac{(\kappa-1)p+(\kappa+1)p_0}{2\kappa p_0}\right]. \tag{1.71}$$

The pressures by (1.7) are compared with Rayleigh's in Fig. 3. By means of (1.5), (1.6) and (1.7) the conditions within the wave surface with

[12] Dayton C. Miller, *Sound Waves—Their Shape and Speed* (Macmillan, New York, 1937). The explanation given by this reference for the abnormal velocities of sound from gun fire, for example on page 129, does not seem very clear. The idea is apparently to account for excess velocities near the muzzle of a gun without reference to the effects of finite condensation. But the motion of a source "shot from a gun," during the time a pulse is radiated, does not in itself imply a higher than normal velocity for the wave front in a medium which is at rest. The velocity will be normal unless the condensation produced is finite. Also, it is difficult to understand Miller's objection to the Riemann formula on the grounds that it gives infinite velocity at the time $t=0$. The time $t=0$ should be taken as referring to the boundary of the source, for which $r \neq 0$. The equivalent diameter of the source in the case of a gun muzzle would not be smaller than the bore of the gun.

[13] G. S. J. Perrott and D. B. Gawthrop, J. Frank. Inst. **203**, 103, 387 (1927).

[14] R. Rüdenberg, Artilleristische Monatshefte, May, June, 1915; pp. 237, 285.

respect to density and pressure can be computed on the assumption of a value for κ the ratio of the specific heats.

2.

The mean velocity V_g of flow of air particles at the wave surface, as the shock passes a given plane, may be calculated as follows. From the condition of continuity of flow, for plane waves, write[7a]

$$\frac{\rho}{\rho_0}=\frac{V}{V-V_g} \tag{2.1}$$

and combine this equation with the density-velocity equation (1.6). The error in using (2.1) for spherical waves is negligible even at points quite close to the source. The result is

$$V_g=2V\frac{V-a}{V(\kappa+1)-2a}. \tag{2.2}$$

The pressure by a plane-surface pressure gauge placed normal to the stream is then taken to be

$$P_G=2(p-p_0)+\rho V_g^2/g$$
$$=\frac{4\kappa p_0}{\kappa-1}\left(\frac{V}{a}-1\right)$$
$$+\frac{4\rho_0}{g}\frac{(V-a)^2}{(\kappa^2-1)-2(\kappa-1)a/V}. \tag{2.3}$$

The pressure recorded by the gauge is accordingly given as twice the excess pressure in the wave (at reflection)[15] plus the impulse pressure of the moving air. The flow of air is assumed to develop essentially parallel to the gauge plane after impact at these high, supersonic velocities.

If the ratio of the specific heats is taken to be $\kappa=7/5$

$$P_G=14p_0\left(\frac{V-a}{a}\right)+\frac{25\rho_0}{g}\frac{V(V-a)^2}{6V-5a}, \tag{2.31}$$

$$\rho=(\rho_0/V)(6V-5a), \tag{1.61}$$

$$V_g=5V(V-a)/(6V-5a). \tag{2.11}$$

[15] If the pressure-measuring technique is later improved sufficiently to permit precise comparisons with experimental results, it will probably be necessary to take into account a reflection coefficient modified for dissipative losses in accordance with the work of Hubbard and Herzfeld; see R. S. Alleman, Phys. Rev. **55**, 87 (1939).

TABLE I. $\kappa=5/3$.

V/a	APPROX. $x-1$ (FOR TNT, TNB)	$\frac{\rho}{\rho_0}$	$S=\frac{\rho-\rho_0}{\rho_0}$	$\frac{\Delta p}{p_0}=\frac{p-p_0}{p_0}$	$\frac{V_g}{a}$	$\frac{\rho V_g^2}{g}\left(\frac{KG}{CM^2}\right)$	$P_G\left(\frac{KG}{CM^2}\right)$ (GAUGE PRESSURE)
1	>200	1.0	0	0	0	0	0
1.1	130	1.2(7)	0.2(7)	0.5	0.24	0.11	1.14
1.2	85	1.5	0.5	1.0	0.4	0.36	2.39
1.5	50	2.0	1.0	2.5	0.75	1.72	6.88
1.7	39	2.2(4)	1.2(4)	3.5	0.94	3.0	10.3
2.0	30	2.5	1.5	5.0	1.2	5.4	15.8
2.5	22	2.8	1.8	7.5	1.6	10.9	26.4
3.0	17	3.0	2.0	10.0	2.0	18.3	39.0
4.0	11	3.2	2.2	15.0	2.8	38.2	69.2
5.0	8	3.4	2.4	20.0	3.5	64.5	106.0
10.0	2	3.7	2.7	45.0	7.3	300.0	393.0
20.0	—	3.8	2.8	95.0	14.8	1280.0	1480.0

TABLE II. $\kappa=7/5$.

V/a	APPROX. $x-1$ (FOR TNT, TNB)	$\frac{\rho}{\rho_0}$	$S=\frac{\rho-\rho_0}{\rho_0}$	$\frac{\Delta p}{p_0}=\frac{p-p_0}{p_0}$	$\frac{V_g}{a}$	$\frac{\rho V_g^2}{g}\left(\frac{KG}{CM^2}\right)$	$P_G\left(\frac{KG}{CM^2}\right)$ (GAUGE PRESSURE)
1	>200	1.0	0	0	0	0	0
1.1	130	1.45	0.45	0.7	0.34	0.26	1.7
1.2	85	1.83	0.83	1.4	0.57	0.89	3.8
1.5	50	2.67	1.67	3.5	0.94	3.6	10.8
1.7	39	3.0	2.0	4.9	1.14	6.1	16.2
2.0	30	3.5	2.5	7.0	1.43	10.9	25.3
2.5	22	4.0	3.0	10.5	1.87	21.3	43.0
3.0	17	4.3(3)	3.3	14.0	2.31	35.2	64.1
4.0	11	4.7(5)	3.7	21.0	3.16	72.0	115.0
5.0	8	5.0	4.0	28.0	4.00	122.0	179.0
10.0	2	5.5	4.5	63.0	8.18	560.0	690.0
20.0	—	5.7(5)	4.7	133.0	16.52	2380.0	2650.0

If the effective ratio is taken to be $\kappa=5/3$, then

$$P_G=10p_0\left(\frac{V-a}{a}\right)+\frac{9\rho_0}{g}\frac{V(V-a)^2}{4V-3a}, \tag{2.32}$$

$$\rho=(\rho_0/V)(4V-3a), \tag{1.62}$$

$$V_g=3V(V-a)/(4V-3a). \tag{2.12}$$

The data of Tables I and II were computed by using the formulas (2.3), (1.6) and (2.1), and the corresponding curves of Fig. 2 have superposed on them the average deflections of the rochelle-salt gauge described in I, at each of five points of observation. Approximately three records were obtained at each distance for the series recorded in the figure. The results for this group, the tests of which were carried out under weather conditions particularly favorable to uniform behavior of the gauge system, were reproduced in Fig. 4 of I. The readings are significant only as relative values since no calibration for the gauge was available except the calibration provided by

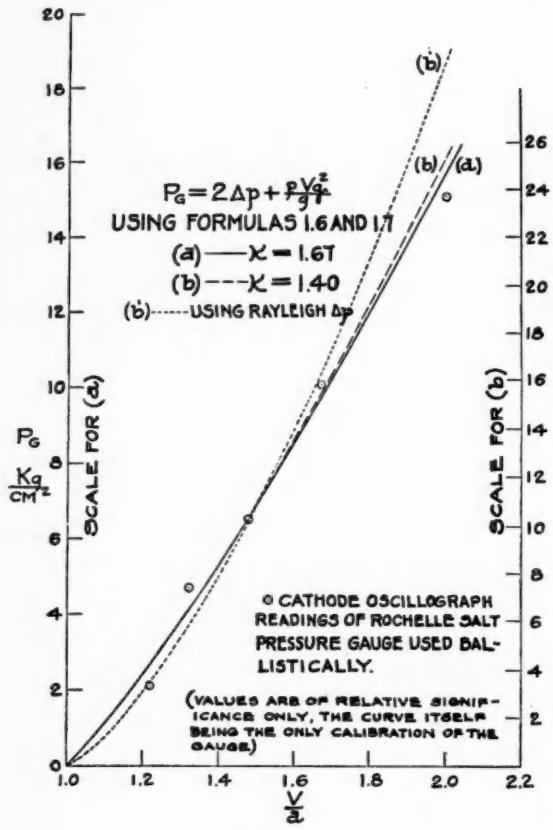
$P_G = 2\Delta p + \rho V^2$
USING FORMULAS 1.6 AND 1.7
(a) —— $\kappa = 1.67$
(b) --- $\kappa = 1.40$
(b)····· USING RAYLEIGH Δp
(b)
(b)
(a)
SCALE FOR (a)
SCALE FOR (b)
P_G $\frac{Kg}{CM^2}$
$\frac{V}{a}$
© CATHODE OSCILLOGRAPH READINGS OF ROCHELLE SALT PRESSURE GAUGE USED BALLISTICALLY.
(VALUES ARE OF RELATIVE SIGNIFICANCE ONLY, THE CURVE ITSELF BEING THE ONLY CALIBRATION OF THE GAUGE)

FIG. 2.

making the curves and observations pivot about the point for $V=1.5a$. It is clear, however, that the deflections do follow a function of the type of (2.3) in the region $V=a$ to $V=2a$. We are unable to use the gauge successfully at points closer to the source than $x=30$, for which $V \doteq 2a$, because of damage by the flame.

Rayleigh's function for pressure shown in Fig. 3, was used to compute gauge pressures P_G, as defined by Eq. (2.31), and these calculations are compared in Fig. 2 with gauge pressures by Eqs. (1.7) and (2.31). The experimental gauge pressures, which are superposed, were not presented in I as final results, though it is believed that the ballistic interpretation of the gauge readings from which they derive is essentially correct. Before obtaining confirmation of these results it is not justified to conclude that the curve based on Rayleigh pressures is definitely a poorer representation of actual pressures, but it does appear that the latter curve begins to deviate at velocities of the order of $2a$ by amounts well beyond the probable error of the mean gauge deflections. There is no difference in goodness of fit of Eq. (2.3), depending on the ratio of specific heats used, which distinguishes by these tests that one value of κ is preferred over the other. For the purpose of the present paper, in the absence of direct experimental confirmation, it is assumed that the ratio of specific heats which is correct for the principal range of conditions dealt with in the study of intense shock waves in air is approximately $5/3$, for reasons which are outlined below. The tables were computed with two values of κ, $5/3$ and $7/5$, since interpolation may be of interest in the case of application to waves of comparatively low velocity or to waves of extremely high velocity.

3.

The "thickness" of a shock wave has been defined as the distance in the direction of propagation from the intersection of the tangent (of maximum slope) at the wave front with the line of zero condensation, and a point on this line instantly beneath the point of maximum pressure.[6] The thickness so defined ranges from 10^{-5} cm to 10^{-6} cm. Taking account of velocities of these waves, the time intervals of condensation are therefore in the zone 10^{-10} second to 10^{-12} second. Accordingly, the average number of collisions per molecule during the period of condensation in shock does not differ greatly in order from unity. It is believed that all collisions even at ordinary temperatures and pressures probably produce rotational excitation,[16] though there would be insufficient time for any significant transfer of energy to vibration in the zone of the wave surface. But the finite motion of the molecules within the wave surface of a pulse of great condensation is extreme, both in amplitude and in velocity; the velocities extend from an average about equal to the normal velocity of sound for a wave velocity $1.5a$ to about ten times the normal velocity of sound for wave velocities of the highest values considered. These superposed motions lead very quickly, as the wave velocity increases, to a system which is unidirectional, in effect to the status of a one-

[16] E. Teller, opinion expressed in correspondence (1938); also see Landau and Teller, Physik. Zeits. Sowjetunion, **10**, 34 (1936).

dimension gas of relatively high temperatures and pressures.

Considering a one-dimension gas in which the velocities are assumed distributed normally not about zero but about $\bar{u} = V_g$ (the finite velocity of flow), it is calculated that the mean squared velocity is[17]

$$(u^2)_{Av} = (1/2hm) + V_g^2.$$

From this relation the effective dynamic temperature is $T_d = V_g^2 m/R$ where R and m have the usual significance. The dynamic temperature is measured by that part of the increment in the mean translational energy of the newly disturbed molecules, when the wave surface arrives at a given point, which occurs by virtue of the flow.

[17] $\Sigma u^2 = \int_{-\infty}^{\infty} u^2 e^{-hm(u-V_g)^2} du$; write $x = u - V_g$ $dx = du$

$$= \int_{-\infty}^{\infty} (x + V_g)^2 e^{-hmx^2} dx$$

$$= \frac{1}{2hm} + V_g^2 \equiv \overline{u^2}.$$

Note that the first term represents the energy which would obtain in the prevailing state of condensation if there were no flow; the modulus h by assumption corresponds to the temperature which would be recorded by a temperature gauge moving with the stream. Hence the first term measures the ordinary condensation temperature and the second term the dynamic temperature.

Taking the value 287×10^4 for R/m for air[18] the dynamic temperatures are found to range from about 300°K at wave velocities of $1.5a$ to about 20,000°K for wave velocities about $10a$. Total effective temperatures thus extend from 600° or 700°K for wave velocities about $1.5a$ to the extraordinarily high values of perhaps 25,000°K. It is an interesting thing that these excessive temperatures would not be recorded by a gauge moving with the wave stream, so that the stream is not so "hot" except to the molecules of a layer of air about to be penetrated by the wave surface, which up to the instant of arrival of the discontinuity are in a comparatively undisturbed state. However, even the condensation temperature is computed by Rüdenberg[19] to be about 6000°K for a wave velocity about $10a$. With effective temperatures (in the direction of propagation) as great as these, it is reasonable to suppose that vibrational energy may have more than a

[18] J. H. Jeans, *Dynamical Theory of Gases* (Cambridge, 1904), p. 113.

[19] C. Cranz, reference 11, p. 174.

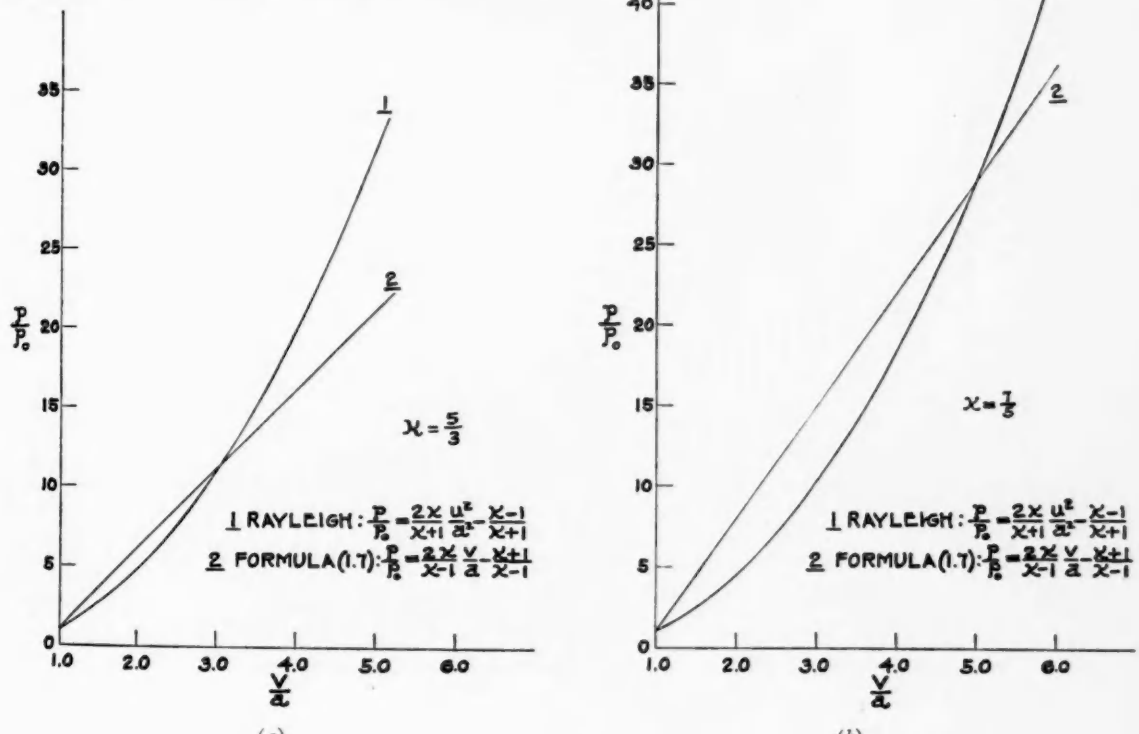

(a) (b)

FIG. 3.

negligible part in fixing the total heats. The investigations of Herzfeld and Rice,[20] Kneser,[21] Eucken[22] and others show that at ordinary temperatures the accumulation of energy in molecular vibrations is too slow to be a factor in the specific heats effective during the cycles of changes at supersonic frequencies. Dwyer[23] has recently confirmed by spectroscopic studies the long persistence of vibration, indicating that the process of attaining equilibrium in the vibrational degree of freedom is normally a gradual accumulation of that total energy which can be assembled during the average life of the excited state. Dwyer's experiments consisted in observing the duration of the absorption spectrum of a diatomic gas after excitation by shock but with the molecules in their normal electronic level. King and Partington[24] found evidence which would now be interpreted as showing vibrational heats beginning to be effective during the long periods of audible sounds, at temperatures less than 1000°. At ordinary temperatures and pressures only one collision in several million leads to an exchange of vibrational energy in the case of the O_2 molecule.[16] Even at the moderately high temperatures of a severe shock wave, where the equilibrium energy in vibration is considerable, the accumulation by exchange from translation is slow enough to be entirely negligible during the period of condensation. But if the rate is high, as it is for very high temperatures and pressures, the accumulation in the period of condensation may no longer be a negligible fraction of the total exchange.

While in air, at room temperatures, the necessary velocity for the transfer of energy from translation to vibration occurs only once in several million collisions, a tabulation of the probability function[25] shows that the same requisite velocity is exceeded at 1000°K in a notably increased proportion of impacts. The proportion is defined by the limit

$$x=(hm)^{\frac{1}{2}}u_0\doteq\sqrt{0.3}x_{(300°\mathrm{K})},$$

where $x_{(300°\mathrm{K})}$ is the value of the parameter for room temperature (the modulus of the velocity distribution h being proportional to the reciprocal of T°K) but the increase is not great enough to make vibrational energy an important factor. About one collision in a number of the order of 200 to 300 will involve transfer of energy in vibration at 1000°K. So in spite of an equilibrium heat of about 1 cal./mol. at this temperature, for vibration, there should be no significant effect of the vibrational degree of freedom on the total heat until long after the condensation cycle of the single shock pulse has been executed. At 3000°K the result is not quite the same; the frequency of exchange is high enough to develop during the condensation an appreciable fraction of the total vibrational energy for equilibrium. And the total accumulated at 3000° is relatively high[26] with respect to rotation and translation. At temperatures in excess of 10,000°K the proportion is so high that it is believed justified to admit vibrational heat in the order of its equilibrium value. Waves of great condensation have these excessive dynamic temperatures in the direction of wave motion. The equilibrium heat for vibration at very high temperatures is about 2 cal./mol. This value would be used, then, for wave velocities greater than about 5 or 6 times the normal velocity of sound, and the total heat C_p for a diatomic gas with only one degree of freedom in translation would then be 7; the ratio κ would be 7/5. The rotational degrees of freedom are assumed to be fully developed at all temperatures of interest, since all impacts are supposed to involve some degree of rotational excitation. Equilibrium as here defined should then be attained in periods as short as 10^{-11} or

[20] K. F. Herzfeld and F. O. Rice, Phys. Rev. **31**, 691 (1928).

[21] H. O. Kneser, Ann. d. Physik **16**, 337 (1933); V. O. Knudsen, J. Acous. Soc. Am. **6**, 199 (1935).

[22] Eucken, Mücke and Becker, Naturwiss. **20**, 85 (1932).

[23] Robert J. Dwyer, J. Chem. Phys. **7**, 40 (1939).

[24] J. R. Partington and W. G. Shilling, Phil. Mag. **45**, 416 (1923); King and Partington, Phil. Mag. **60**, 1020 (1930).

[25] E. Czuber, *Wahrscheinlichkeitsrechnung* (Teubner, 1932), p. 445. For three dimensions the formula for N_1, the number of molecules having velocity greater than u_0, is

$$N_1=N\left(1+\frac{2}{\sqrt{\pi}}x_0e^{-x_0^2}-\frac{2}{\sqrt{\pi}}\int_0^{x_0}e^{-x^2}dx\right),$$

where $$x_0^2=hmu_0^2=\frac{mu_1^2}{2RT}.$$

See C. N. Hinshelwood, *The Kinetics of Chemical Change in Gaseous Systems* (Oxford, 1933), p. 25. For 1 dimension, here considered, use

$$N_1=N\left(1-\frac{2}{\sqrt{\pi}}\int_0^{x_0}e^{-x^2}dx\right).$$

[26] P. S. Epstein, *Textbook of Thermodynamics* (Wiley, 1937), pp. 303–309.

10^{-10} second, nearly all molecules having in that time taken part in at least one transfer of energy in rotation; no further accumulation can occur, presumably, and it is statistically plausible that a cross section will show a partition of energy more or less characteristic of true equilibrium at any time after an average of one or a very few collisions per molecule have occurred in a great aggregate for which all combinations of translational and rotational energy states are possible after each impact. Experimental evidence of the absence of dispersion has not been obtained for intervals less than about 10^{-6} second.[27] But it is believed necessary to reduce intervals below 10^{-10} second to suppress the rotational energy in air at normal temperatures.[27a] During an initial period after collision which is one order smaller than a period of oscillation characteristic of the excitation, perhaps 10^{-3} or 10^{-2} times the period of condensation, there should be no excitational heats of any sort. The displacements produced by collision will as yet not have progressed far enough to disclose whether an atom has initiated a simple translation, a rotation or a vibrational movement; a gas should therefore be kinetically monatomic in appearance, regardless of the number of atoms in a molecule, during intervals immediately after exposure to shock which are small with respect to whole periods of oscillation. These intervals are only negligible fractions of the period of condensation for typical shock waves in air, and before the condensation has developed appreciably the effective heat should, it appears, have about the full rotational component.

The ratio of specific heats for air which is taken to be applicable to the region of the wave surface for wave velocities only slightly in excess of the normal velocity of sound is 7/5. It is assumed that the ratio becomes 5/3 as soon as the molecular trajectories become essentially unidirectional, that is for wave velocities much in excess of $1.5a$. At velocities in excess of $3a$ the vibrational energy seems not to be entirely negligible. Therefore, the value of κ decreases slowly again from 5/3 toward 7/5 as the shock wave increases in sharpness and amplitude. In the range of principal interest the ratio is taken to be approximately 5/3.

It is interesting to note one difference between the status of a single shock pulse in air and the conditions existing in the recurring cycles of supersonic waves. The latter waves develop a pseudo-steady state corresponding to some mean temperature representative of the typical cycle. In the single pulse of moderate intensity the energy accumulated in vibration may not approach the equilibrium value for a mean temperature by several orders of magnitude.

Supposing the condition of a shock wave to be as outlined above, there are implications which may seem inconsistent with well-known characteristics of waves of detonation in gases. The rates of propagation of the zone of reaction are in certain instances equal to the velocities of shock of very great intensity. Since it seems quite likely that energy transfer to vibration is an important vehicle in this ultra-rapid progress of the region of dissociation, it is well to consider whether a mechanism is available which can be reconciled with the idea that vibrational energy builds up relatively slowly for the conditions of a pulse of moderately high velocity.[28] One alternative is that the "center" of the zone of reaction actually lags at some fixed distance behind the surface of shock which it supports; that is, behind the detonating pulse, with the rate of reaction tapering off rapidly from this point toward the pulse boundary. The distance separating the pulse from the center would then correspond to the time required to develop important concentrations of vibrational energy. In any case, the velocities ("temperatures") of detonating shock are high enough to make such a space lag relatively small.

We desire to acknowledge indebtedness to Professors Teller, Loeb and Hubbard and to Mr. Milton Lipnick for helpful discussions of excitation phenomena and supersonic results, and to Mr. E. L. Welch for assistance in conducting the experiments. We are also under obligation to Lt. Col. H. H. Zornig, U.S.A., for permission to use the spark photographs of Fig. 1 (Part II) showing shock waves in the fields of exploding detonators.

[27] H. O. Kneser and M. Wallmann, Naturwiss. **22**, 510 (1934); Rose and Roy, Proc. Roy. Soc. London, **A149**, 511 (1935). (a) Kneser and Wallmann state a frequency of at least 10^8 cycles is probably necessary for rotational dispersion to be observable.

[28] L. B. Loeb, Comment outlined in correspondence (1938).

News of the Society

Members

THE following new members have recently joined the Acoustical Society:

Lee Bartholomew,
Celotex Limited,
North Circular Road,
Stonebridge Park,
London, N. W. 10, England.

Rudolph William Buntenbach,
Bell Telephone Laboratories,
463 West Street,
New York, New York.

Claude Stonecliffe McGinnis,
129 Washington Lane,
Wyncote, Pennsylvania.

Garrett Mott, Jr.,
17 Wayside Lane,
Scarsdale, New York.

Jay Harry Prager,
65 East Gun Hill Road,
Bronx, New York.

Andre Salmont,
30, Blvd. de la Saussaye,
Neuilly, S/Seine,
France.

Notice has been received of the death of H. A. Groskamp, Amsterdam, Netherlands, and of J. G. M. Rietbergen, Copenhagen, Denmark.

The total membership is now 706.

The Iowa Meeting

The fall meeting of the Acoustical Society will be held at the State University of Iowa, in Iowa City, November 3–4. Aside from the events announced in the July issue of the Journal, other features have been scheduled. Thursday evening, November 2, Mr. Homer Dudley of the Bell Telephone Laboratories will give a public demonstration-lecture on the Vocoder. Friday morning, as part of the symposium on "Speech and Vocal Music," Dr. J. C. Steinberg will present the first report of the current work at the Bell Laboratories on vocal cord photography and sound track analysis. There will be two special luncheons on Friday: one for local and visiting musicians, at which Professor F. A. Saunders and Professor Arnold Small will speak on acoustical studies of the violin; and the other for dramatic arts people, at which Mr. Harold Burris-Meyer will discuss "Sound in the Theatre." At the dinner Friday evening, Professor F. A. Firestone will offer "A Demonstration of How One Person Can Give a Public Speech or Sing a Quartet Without Using His Vocal Cords." A midwest group of speech experts, under the chairmanship of Dr. Grant Fairbanks, will hold a research conference in Iowa City at the time of the meeting. They will participate in two of the regular sessions and will, in addition, hold two roundtables which may prove of interest to some of the members of the Society. One roundtable discussion will deal with experimental phonetics as related to speech disorders, and the other will be concerned with phonograph recording. Participants in the discussion on recording will include Dr. F. V. Hunt, Dr. Milton Cowan and Mr. E. D. Peterson. The addition of these features to the previously announced symposia on "Architectural Acoustics" and "Hearing Defects" should provide for a program of rather wide appeal.

John Redfield

THOSE who attended the early meetings of the Acoustical Society of America will be particularly sorry to hear of the death of John Redfield, whose remarks on subjects pertaining to music enlivened many a meeting. He died rather suddenly on February 26th of pneumonia and is survived by Mrs. Vada P. Redfield, 43-09 40th Street, Long Island City, New York. Mr. Redfield's book entitled *Music, a Science and an Art* (Alfred A. Knopf) is very stimulating reading.

Book Reviews

A Table Relating Frequency to Cents. ROBERT W. YOUNG. Pp. 23. C. G. Conn, Ltd., Elkhart, Indiana, 1939. (Price: 100 cents, 1 semitone.)

For the purposes of music the cent (hundredth part of a semitone) is a most satisfactory logarithmic unit of measure of frequency ratio, and of frequency level above some arbitrary standard frequency. Both uses of the unit have been made in several tables[1] published since Ellis introduced this unit interval in 1884. These tables illustrated the convenience of the use of the cent, but they were not complete enough for general use.

This pamphlet contains notes on the use of the tables, a comparison of staveless notations, a principal table and four minor tables. The latter express the following: the ratio equivalent of integral cent values up to 100; the ratios of the intervals in the equally tempered scale; the cent equivalents of some just scale ratios; and cent equivalents for a large number of selected ratios.

The principal table of the pamphlet tabulates frequencies corresponding to cents deviation from notes occurring in the equally tempered scale (based on $A_4=440$ cycles per second). This table is rather complete, and has a novel arrangement which seems logical to a musician. A range is covered extending from the lowest C on a piano keyboard to the C seven octaves above it. The number of the piano key corresponding to each note is included in the table for the convenience of instrument-tuners. The zero frequency level used is a logical choice and corresponds to the frequency $C_0=16.352$ cycles per second, which is precisely 57 semitones below standard A_4, and is near the lower frequency limit of audibility.

This set of tables makes possible the general use of a logical, convenient, practical unit. Furthermore, its use should lead in the direction of a standard staveless notation.

DANIEL W. MARTIN
University of Illinois

[1] E. M. von Hornbostel, Zeits. f. Physik **6**, 29 (1921); A. T. Jones, *Sound* (Van Nostrand, 1937), p. 434.

Complex Variable and Operational Calculus. N. W. MCLACHLAN. Pp. 355. University Press, Cambridge, and Macmillan Company, New York, 1939. Price $6.50.

The operational calculus may be thought of as a set of rules and a short-hand procedure for the solution of the type of linear differential equation with constant coefficients with which we have to deal in mathematical-physics and technology. As practiced by Heaviside, the central problem of this calculus is that of finding the response of the system under the action of a stimulus (impressed force) which is zero up to zero time and unity thereafter ("unit function"). When this solution has been found the response to forces which are arbitrary functions of time can be found by integration, in accordance with Duhamel's theorem. The problem of finding the unit solution can be approached in two ways. The first method, emphasized by Carson, is based on the Laplace transform and involves the solution of an integral equation or the use of tables of known definite integrals. The second method involves the Bromwich contour integral over a complex path. The two methods are related by the Mellin-Fourier inversion theorem.

The present book on this subject by N. W. McLachlan emphasizes and is chiefly concerned with the second method, involving the Bromwich integral, although a mixture of both methods is recommended and frequently employed. The book is divided into four parts (I) Complex Variable, (II) Operational Calculus, (III) Technical Applications and examples to be worked out by the reader, (IV) Appendices and list of references. Part I is devoted to the technique of complex integration, a subject which receives little attention in the average course in engineering mathematics. In Part II the relation of the Laplace transform and the Bromwich integral are pointed out by means of the Mellin theorem. In Part III numerous applications are made to the solution of problems in aeroplane dynamics, electrical circuits, loudspeakers, electric wave filters, submarine cables, diffusion of heat and the absorption of moisture. A formal statement and proof of the Mellin theorem are given in the Appendix.

Dr. McLachlan's book contains ample evidence of scholarly preparation and his treatment of the difficult subject of complex integration is especially to be recommended. The treatment is perfectly straightforward and will appeal to technical readers who demand ample rigor but prefer their fare served simply without the distracting small-epsilon sauce of the serious mathematician. Whether or not one is able to share Dr. McLachlan's enthusiasm for the Bromwich integral method it is difficult to resist some misgivings as to whether the average engineer will have the time or inclination to acquire the difficult technique of complex integration which is required for the practice of this method, especially when in most cases the solutions may be found in other and easier ways. For those who do wish to become more familiar with the somewhat neglected contour integral method, however, this book can be recommended as a dependable guide.

STUART BALLANTINE
Ballantine Laboratories

Ultrasonics and Their Scientific and Technical Applications. LUDWIG BERGMANN, Professor of Physics at the University of Breslau. (Translated by H. Stafford Hatfield from the German work *Ultraschall*, published by VDI-Verlag, Berlin). Pp. 264, Figures 148, Tables 24. John Wiley and Sons, Incorporated, New York, 1938. Price $4.00.

The field of ultrasonics has increased rapidly and has become of great importance in many unexpected ways since the pioneering work a dozen or more years ago of Boyle, Cady, Pierce, and Wood and Loomis. Until the appearance of the present translation there had been no book on the subject in English, though the German original has been available for two years. It was preceded by the very complete chapter on the subject by E. Grossmann in the *Handbuch der experimental Physik*, and by the compre-

hensive review by E. Hiedemann in the *Ergebnisse der exakten Wissenschaften* in 1935.

The present book is a very exhaustive and impartial, if somewhat uncritical summary of the work done until early in 1937. A section on television has been added by the translator and to the original bibliography of nearly five hundred titles has been added a group of more than ninety titles of papers which appeared after the publication of the German edition, but to which no reference is made in the text.

The text has been divided into five chapters. The first treats in great detail the mechanical, thermal, magnetostrictive and piezoelectric generation of ultrasonic waves. The second gives a similarly complete account of their detection and measurement. These chapters are well illustrated by diagrams of apparatus and circuits and reference is made to practically every paper on these subjects up to the time of writing the German edition. They should be especially helpful to anyone considering the application of the methods of ultrasonics to his problems. Many American readers will welcome the very full discussion, amounting to forty-five pages, of optical methods of studying ultrasonics, an aspect of the subject largely neglected in this country.

Chapter Three, on the measurement of velocity and absorption of sound in liquids and gases necessarily is somewhat repetitious, since the availability of apparatus and methods already discussed is considered with reference to specific problems. The part on liquids gives a well-balanced treatment of interferometric and optical methods and contains very complete tables of numerical results. A sketch of the theory of molecular dispersion of sound in gases is given and is followed by a discussion of results obtained up to 1936. The method developed by V. O. Knudsen for the measurement of acoustic absorption in gases is credited by the author as being the most accurate thus far developed: it would have been helpful to have had a diagram illustrating it.

Chapter Four treats of the measurement of the velocity of sound in solids and the determination of their elastic and elasto-optical constants, a subject to which the author himself has largely contributed. Chapter Five gives a very interesting account of further applications of ultrasonics such as the ultrasonic stroboscope, application of ultrasonics to television, testing of materials for flaws or lack of homogeneity, dispersive, colloidal and coagulative effects, and miscellaneous effects of physical, chemical and biological interest. In both these chapters will be found much material for consideration by those interested in applied physics. The figures are excellently captioned and in nearly every case reference is made to the source. An especially valuable feature is the bibliography, already mentioned, and the name and subject indices are well done.

The author is to be commended for making so thorough and impartial a survey of a field in which developments have been so rapid that critical judgments must necessarily be held somewhat in abeyance for the present. This book should prove to be invaluable to students and to those actively working in the subject as well as to all who may be interested in widening their knowledge of the experimental resources for the study of the properties of matter.

J. C. HUBBARD

Supersonics: The Science of Inaudible Sounds. The Charles K. Colver Lectures given at Brown University in 1937. R. W. WOOD. Pp. 158, Figs. 42. Brown University, Providence, Rhode Island. Price $2.00.

General interest in ultrasonics and its applications to various physical, chemical and biological problems dates from the publication in 1927 of the work of Wood and Loomis. Their contribution resulted from a happy combination of imagination, resourcefulness, and technical equipment, of a kind which is seldom equaled. This book by Professor Wood, the first to be written in English on the subject, is therefore especially welcome.

The historical background is traced, reference being made to early work on the determination of the frequency limits of audible sounds, the piezoelectric effects, the experiments of Langevin, and the studies by Cady, Van Dyke, Dye, and Pierce of the properties of the piezoelectric resonator and its applications. Next is a very full account of the physical and biological effects discovered by Wood and Loomis, and of later experiments, especially of those by Gaines and by Chambers. The optical effects, beginning with the behavior of a sound field as a diffraction grating for light, found independently by Debye and Sears and by Lucas and Biquard, are described and a notably clear and nonmathematical treatment of the underlying mathematical theory is given. Acoustic interferometry, begun by Pierce, and measurements of sound velocity and absorption in liquids and gases are discussed, a feature being an explanation without mathematics of molecular absorption of sound in gases. A very adequate bibliography of the most important papers is appended. The book is most interestingly written and must surely stimulate a desire for further knowledge on the part of the student and the general reader to whom it may especially be recommended as an introduction to the subject.

J. C. HUBBARD
Johns Hopkins University

Current Publications on Acoustics

F. A. FIRESTONE

147 East Physics Building, University of Michigan, Ann Arbor, Michigan

Reviews of Contemporary Papers

MEMBERS who have occasion to translate important papers from foreign journals will be doing a real service to those members who do not read the foreign languages easily, if they will prepare a review of such articles for publication in this section.

These reviews should be of the nature of a lengthy abstract (500 to 1500 words) rather than a critique or appraisal, and should attempt to set forth in this limited space as much of the original author's contribution as possible. One or two figures may be included if desired.

Acoustical Properties of Especially Fine Toned Violins. H. MEINEL, Akustische Zeits. **4**, 89 (1939).—This paper presents the results of subjective and objective measurements made on violins in an effort to determine what acoustical properties especially high quality violins possess and to point out how these properties may be obtained in new instruments by advance design. In order to establish which violins from a group are especially fine, it is necessary that the violin be put to subjective proof by a jury of listeners in such a manner that all the different qualities of the violin are brought in. A testing committee composed of skilled violin makers, of artists, and of professors of music was assembled to pass judgment on seventy new instruments as compared to recognized high quality instruments. About half of these were then tested physically.

In making subjective measurements a suitable comparison violin was selected which was unanimously judged to be one of superior tone quality; all others being tested in comparison to it. Chromatic scales or a similar succession of tones over all frequency ranges, and under some circumstances, different bowing techniques, were used to prevent the jury from basing its judgments on the composition presented or on the dexterity of the artist. The physical measurements included the obtaining of sound pressure and loudness *vs.* frequency curves for the violins. For the most part, the amplitude of the fundamental of each of the tones was measured to get the response of the violin up to about 3000 c.p.s., while above that it was necessary to measure the amplitudes of the lower overtones in order to complete the curve out to 8000 c.p.s. Thus all strings are represented in one curve. It is also possible in much the same manner to obtain a separate curve for each string from a conventional harmonic analysis, and thus to study the resonant properties as dependent on the string being played. Loudness curves were obtained simultaneously by using a sound-level meter employing suitable weighting networks.

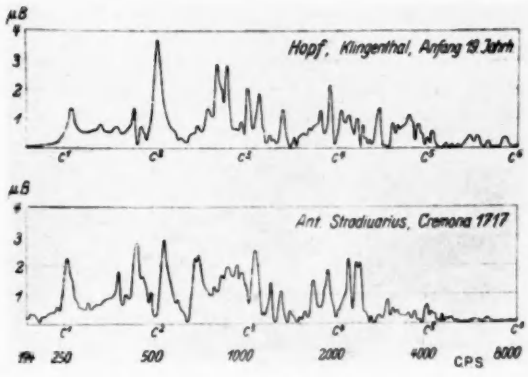

FIG. 1. Frequency curves of violins of different tone quality.

Figure 1 shows the frequency curves of two violins of quite different quality; the Stradivarius being judged far superior. In general the first resonance peak of all violins lies in the vicinity of c^1 and is the well-known air-chamber resonance. The second, and chief, resonant region lies in the vicinity of c^2 and Meinel says that almost always it is composed of two or three peaks in the case of high quality violins or of one peak in the case of mediocre violins, such as the Hopf. For the Stradivarius, it is seen that the sound pressure amplitudes below d^3 are larger for the most part than those of the poorer violin. This too is a property of most high quality violins. In the region of a^3 to d^4 the Stradivarius has higher sound pressure amplitudes than the Hopf. Above d^4 the amplitudes of the tones are definitely higher in the case of the mediocre violin. This is a significant fact on account of the large number of harmonic components of any note that lie in this region, and on account of the high sensitivity of the ear at these frequencies. Strong high harmonics in general are not desirable because they bestow on the tone a roughness which can be easily perceived by the ear. The high amplitudes of the lower harmonics of the Stradivarius as compared to those harmonics higher in frequency give to the violin a mellow, finished tone. The resonance conditions obtaining in the case of the superior instrument could not have come altogether from Stradivarius himself. In his time the tuning was a half-tone lower than today, and perhaps the resonance maxima have further been increased through constructional changes such as longer neck, new sound post, new bridge, new strings and perhaps changes in the

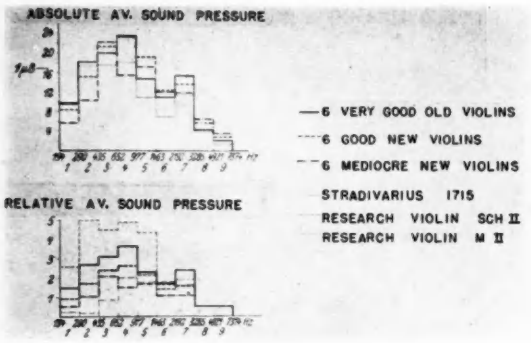

FIG. 2. Simplified frequency curves of violins.

wood itself. Large resonant amplitudes in the higher frequency regions are always to be avoided. One cause of such resonances is traced to a high arching of the violin body,[1,2] and the violins of Jacobus Stainer are given as examples.

The graphs shown in Fig. 2 were prepared from tests made on three groups of six violins each. The first group (solid line) was composed of three Stradivarii, a Guarnerius del Gesu, a Sancto Seraphin and a Testore, all of which were judged fine violins. The second group (dotted) consisted of violins chosen by testing committees as being the best of new German violins. The third group (dot-dash) was composed of new German violins of mediocre quality. In the graphs the frequency scale is divided off into nine regions and the ordinate for each region is chosen as the mean sound pressure as determined by the integration of the pressure amplitude *vs.* frequency curve in that region. A planimeter was used for the integration. In the first, second, and fourth regions (Fig. 2, upper) the pressure amplitudes of the old violins are undoubtedly higher than those of the mediocre violins. These high amplitudes mean that the fundamental tones of the old violins are much stronger than those of the new violins. The reversal of affairs in the third region is due to the single *vs.* double resonance peaks mentioned before. Meinel judges the differences in the fifth, sixth and seventh regions as not being large enough to be of any very basic significance. However, in regions eight and nine the mean amplitudes of the old violins are considerably less than those of the new violins. This agrees with the subjective tests in which it was decided that: "Small amplitudes at very high frequencies are a necessary characteristic of superior toned violins."

The lower graph of Fig. 2 was obtained by plotting the ratio of the sound pressure amplitude in each of the bands to the combined sound pressure of regions eight and nine as a function of frequency. One significant fact was drawn from this set of curves: For violins of superior tone quality, the ratio of the mean of the amplitudes of the fundamental to the numerous harmonics which lie above three thousand cycles is greater than this ratio for violins of poorer tone quality. If this ratio is too large, the violin will also be judged as bad. The curve of a special test violin (Sch II) is shown lightly dotted in the lower graph. Subjective tests on it gave the result that it sounded dull and "barrel-like." The other test violin (M II) was judged as being piercing, nasal, and hard in tone.

Practically, these curves may be used as criterions of the goodness of any violin, though the tolerances (±20 percent) should be borne in mind. Meinel says that *all violins whose curves lie significantly outside the tolerances and above the mean value curves for the group of the best violins, or below the curves for violins of mediocre quality are sufficiently mediocre to be designated as bad.* As for other violins, they may be classified according to the curves to which they come closest.

Similar results to those shown in Fig. 2 were arrived at for curves made on cellos, violas and for plucked instruments (zither and guitar). Comparisons between upright and grand pianos lead to the same sort of curves as between mediocre and very good violins.

Another recognized property of violins is the so-called "carrying power." The carrying power of a violin is its ability to make itself heard at the remote parts of a concert hall even when not being played loudly. According to the artists most violins made by the old masters are especially good in this respect. Meinel says that in most present-day concert halls the higher frequencies are more strongly absorbed, so that the essential reason for the differences in carrying power is that: Of the tones of a good violin, fewer will be absorbed than those of a bad violin. This follows directly from the discussion of Fig. 2 wherein for old violins the ratios between the amplitudes of the low and high harmonics are greater than those of mediocre violins and the amplitudes at high frequencies are considerably smaller.

A further necessary property of good violins, namely, the ease of playing is explained as being based on this same fact. If one gradually diminishes the bow pressure during bowing, one can observe the fundamental oscillation having one node, turn over first into the second harmonic, then the third and so on. Raman has offered a theory to explain this phenomenon.[3] Conversely, in setting up vibrations on the string the higher harmonics must be set into vibration first, passing on to the lower ones and finally setting the fundamental into vibration. If the high frequencies are not radiated, then the transient will consist of lower tones only

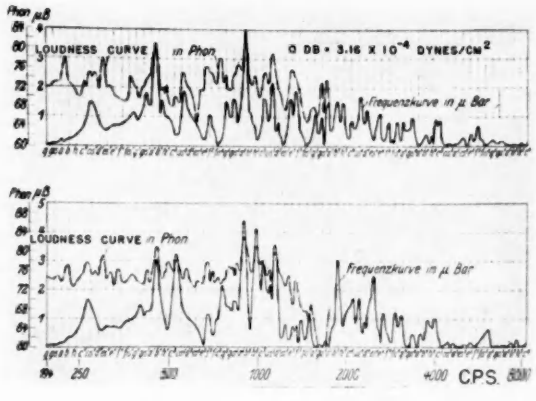

FIG. 3. Loudness balance of two violins.

and will be exceptionally short. This agrees with the subjective impression that, "The sound appears immediately and is characterized by a lack of higher harmonic response in the build up of the tone. The violin speaks out clearly and softly, with no bow noise."

Another important consideration of a violin is its "balance." By balance one means the greater or lesser uniformity of loudness and tone quality as one changes from one note to another on the same string or as one changes from one string to another. For good tonal balance the tone quality must be even for all notes. This condition is not satisfied in the case of mediocre violins. In Fig. 3 examples of violins having different degrees of loudness are shown. The one violin (lower curve) is very well balanced in loudness, the violin above less so. Significant features of the lower curve are that the maxima and minima are less pronounced and octave intervals between resonance maxima are avoided. Besides one often finds that at an octave or 12 note interval above a maximum (or a minimum), a minimum (or maximum) frequently occurs. Both of these violins were tested by the committee and its judgment agreed fully with experiment. Meinel finds little difference between the balance of old violins and the best new violins.

In Fig. 4 sound pressure curves for each of the strings are plotted. Some differences in sound output are observed as one transfers from one string to another noticeably in the regions of a^2 and c^4. Meinel states that transfers from one string to another are significant in causing changes in the harmonic content of the note. This serves as a confirmation of the subjective tests that notes having equal amplitudes but played on different strings are in general brighter and more piercing on the higher strings than on the lower ones.

It is not to be supposed, of course, that a new violin cannot sometimes be found which embodies the properties of the best old ones. However, Meinel states, such a violin does not represent the standard of present day violin construction in Germany. It seems that the best masters only give their violins a large ratio of fundamental to high overtone amplitudes. The curve for test violin Sch II shows, however, that it is possible to build violins which have even a higher ratio of fundamental to higher overtones than the best old Italian violins. This violin was constructed from extraordinarily thin wood. A comparison between the frequency curves of Sch II and M II (thick wood) is proof that with decreasing wood thickness the normal frequency of the violin decreases and that thereby the ratio between fundamental and high overtones is always larger. Also earlier investigations[1, 4] have shown that the body and sound pressure amplitudes increase in large degree for equal bowing conditions as the thickness of the wood decreases. It therefore follows that present-day masters have not attained the perfection of the old Italian masters because they have employed wood of too great a thickness. The only difficulty with this logic is that whereas the requirements on the acoustical output for a good violin are not rigid, the variations in wood thickness which will change the violin from a very good one to a very poor one are exceedingly small. It is not stated in general as to how thick the wood of a violin should be. However, Meinel says that the method of testing and the conclusions arrived at in this article allow one to know, at least, in which direction changes should be made to improve present-day violins, and to test the results brought about by these changes. So satisfactory did the comparisons between physical tests and subjective judgments seem to be that a recognized artist (formerly somewhat skeptical) is quoted as having said, "I am convinced that in the near future no valuable old Italian violin will be purchased without such curves."—L. BERANEK.

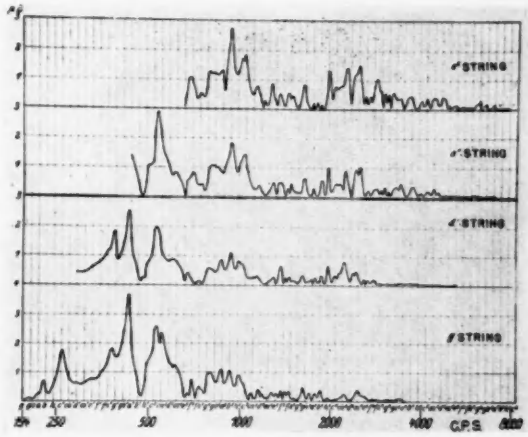

FIG. 4 Resonant properties as dependent on the strings of the violin

[1] H. Meinel, Akustische Zeits. **2**, 22 (1937).
[2] F. A. Saunders, J. Acous. Soc. Am. **9**, 81 (1937).
[3] C. Raman, Ind. Assoc. Sci. Bull. **15**, 62 (1918).
[4] H. Meinel, Elektr. Nachr.-Techn. **14**, 119 (1937).

Piezoelectric Measurements on the Absolute Auditory Threshold for Bone Conduction. G. V. BÉKÉSY, Akustische Zeits. **4**, 113 (1939).—Previous experiments[1] made on the absolute auditory threshold for bone conduction have not been as accurate as the corresponding measurements for air-borne sounds. The method employed was to press an oscillating body against the head and to record the amplitude of vibration at which perception begins. Since the properties of the skin are variable it is difficult to state the amplitude of vibration of the skull bones themselves. Measurements made by Békésy show that the thickness of a layer of skin decreases for constant pressures applied to it as a function of time and that Young's modulus for it increases by a factor of ten if the pressure is varied from 0.1 to 2.0 kg per cm^2. For accurate measurements, therefore, either the amplitude of vibration of the bone structure itself at the point of application or the pressure acting on it must be measured in order to define the true excitation of the bone structure. The first method was reported earlier[2] and the second is described in this paper.

The equivalent circuit of the vibrating system, including the bone conduction unit, skin, and the mass of the skull is

shown in Fig. 1. The lower circuit is of the type suggested by Firestone[3] wherein the masses go over into condensers, the springs into inductances, forces into currents, and velocities into voltages. If one can assume that the skin can be replaced by a simple dissipative spring then it is only

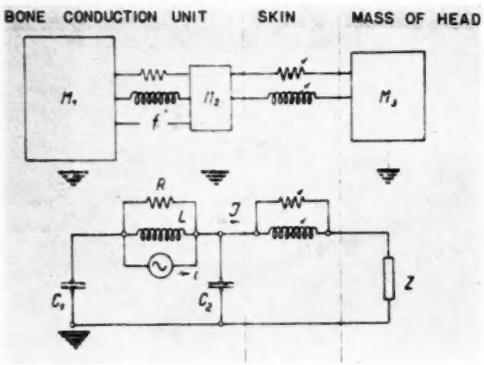

FIG. 1. Equivalent circuits of the mechanical system.

necessary to measure the pressure exerted by the unit upon the area of contact with the skin (current J) in order to obtain the pressure upon the skull.

Figure 2(a) shows one arrangement used for the measurement of the pressure exerted by the bone conduction unit on the area of contact. Here, m_1 is the mass of a quartz crystal having a piezoelectric constant d_1; m_2 is the mass of a similar crystal having a piezoelectric constant d_2; M_1 and M_2 are the masses of two electrodes, the open end of the first being covered by an aluminum foil which is fastened to the outside aluminum tubing for good contact and efficient shielding. This measuring cell is intended to be

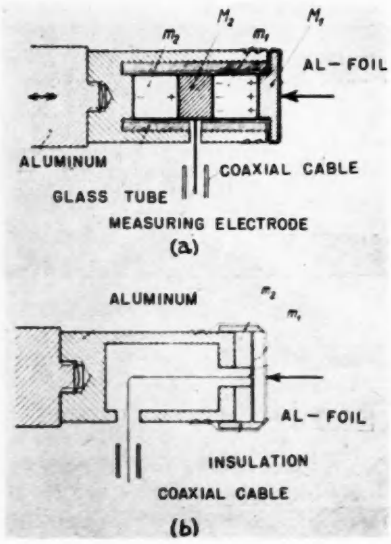

FIG. 2. Alternating pressure measuring cells.

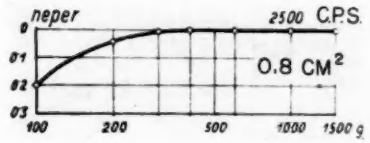

FIG. 3. Sound transmission through skin (2.5 mm thick) as dependent on static pressure.

connected between the end of the driving rod of the bone conduction unit and the head.

If the cell were attached to a large mass so that it was unable to move bodily then the voltage produced by a force acting on the movable end electrode would be given simply by

$$V = 2d \cdot P/C,$$

where d is the piezoelectric constant, P is the pressure and C is the capacity between the electrodes including that of the external wiring. However, if the cell is permitted to move then additional undesired potentials occur due to the

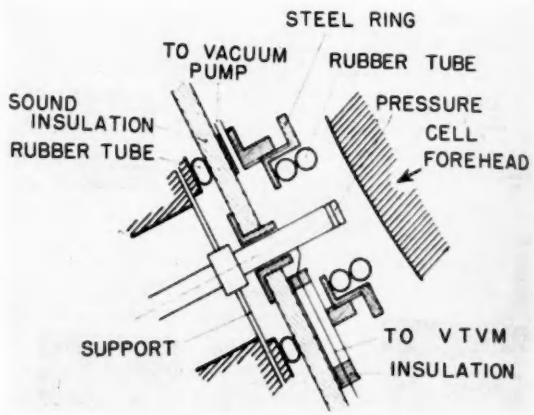

FIG. 4. Construction of the bone conduction unit.

inertia of the crystals and of the metal electrodes. It is shown that these disturbing voltages can be reduced to a minimum by making $m_1 = m_2$, $M_2 = 2M_1$, and $d_1 = -3d_2$. This means that the left quartz plate must be reversed in polarity and its sensitivity diminished by a factor of three, thus diminishing the sensitivity of the combined cell by one-third. Utilizing these relations, the cell of Fig. 2(a) with quartz plates 4 mm in diameter and 2 mm thick and an aluminum cover of 7 to 10 mm diameter gave e.m.f. outputs due to the impressed force many times greater than those resulting from self-motion. Further reduction in these unwanted potentials was obtained by using thin aluminum electrodes as shown in Fig. 2(b).

By placing one of the pressure units described above on one side of the layer of skin between the thumb and forefinger and a condenser microphone on the other side, it was possible to determine the sound transmission through skin as a function of both static pressure and frequency.

Fig. 3 shows that the alternating pressure was independent of steady pressures whose values were above about 400 grams per cm². (Loudness tests made in comparison to air-borne sounds also proved this statement.) The sound transmission was found to be unattenuated and phase shifts between the pressure on the two sides of the skin was noticed only above 8000 c.p.s. This is proof that the skin can be considered equivalent to a dissipative spring.

A sketch of the bone conduction unit used in these experiments is shown in Fig. 4. The pressure-measuring cell is located at the end of the driving rod. To provide more constant pressure between the head and the driving mechanism, the air space intervening was often evacuated. The capacitance C of the pressure cell was determined by adding external capacitance and finding the change in output. The vacuum tube voltmeter was calibrated by inserting a known test voltage in series with the pressure cell. All measurements of auditory threshold were made in the middle of the forehead since the results obtained there were more reproducible than those obtained on the side of the head though the sensitivity was about one-third as large.

An auditory threshold curve is shown in Fig. 5 for both open and closed ear canals. In the latter case the ear canal was tightly closed by a very light rubber membrane. Below 2000 c.p.s. the loudness increased when the canal was closed. The rather small rise of the auditory threshold below five hundred cycles seemed striking and at first overtones were thought to be responsible. This possibility was ruled out after measurements were made using both mechanical and electrical low-pass filters with no change in results. The following explanation of the closed canal curve is offered. If the forehead bone is excited into vibration at a low frequency, the whole mass of the skull oscillates through parallel displacements. Only the lower jaw remains at rest, through its inertia, because it is not directly connected to the other bones. Since the joint of the lower jaw is located very close to the ear canal the canal will be compressed and, if the canal is closed, pressures will be built up in the air column which in turn act upon the eardrum. If the mass of the skull is subjected to a constant pressure, its amplitude of vibration decreases in inverse proportion to the square of the frequency, and hence the pressure in the ear canal decreases similarly. From the frequency curve of the auditory threshold for air-borne sound it is known that the sensitivity of the ear increases at the low frequencies as the 2.77 power of frequency. However, since the sound pressure in the ear canal decreases with increasing frequency, only the 0.77 power of frequency

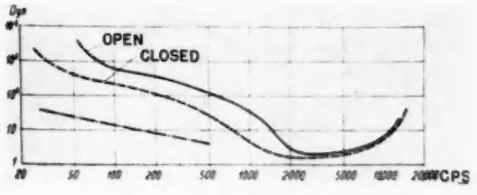

FIG. 5. Threshold curve for bone conduction with open and closed ear canals.

is left for the increase in sensitivity of the auditory threshold for bone conduction. The dot-dash curve of Fig. 5 has this slope and is seen to be essentially parallel to the curve directly above between 50 and 500 c.p.s.

The large rise in sensitivity around 2000 c.p.s. is probably connected with the resonance of the bones of the inner ear, since it is lacking in the case of people whose ear drums, hammers, and anvils have been removed surgically without otherwise impairing the nerve sensitivity (Fig. 6).

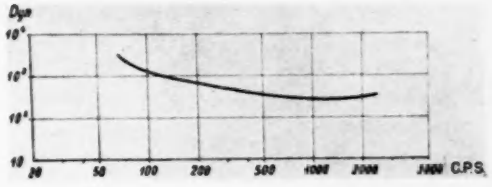

FIG. 6. Threshold curve for subjects without eardrum and inner ear bones.

Furthermore, it is seen that the rise in the threshold curve below five hundred cycles is only slight.

This method of measurement is suitable for the absolute calibration of tuning forks as used by ear specialists for bone conduction tests.—L. BERANEK.

[1] Knudsen and Jones, Arch. Otolaryng **13**, 489 (1931); N. Watson, J. Acous. Soc. Am. **9**, 294 (1938).
[2] G. V. Békésy, Ann. d. Physik **5**, 11, 227 (1931).
[3] F. A. Firestone, J. App. Phys. **9**, 373 (1938).

Inhomogeneity of the Magnetic Field of a Dynamic Loudspeaker. W. REINHARD, Akustische Zeits. **4**, 137 (1939).—This paper presents a method of determining nonlinear distortion arising in the output of a dynamic loudspeaker due to variations in the field strength outside the boundaries of the pole pieces. A simple measuring technique to determine the effective force acting on the voice coil at all points of the air gap is described.

For distortionless reproduction the force k must at all times be directly proportional to the current i.

$$k = B \cdot l \cdot i, \tag{1}$$

where B is the magnetic flux density and l is the length of wire cutting this flux density. In practice this is usually not the case and a more general expression must be written:

$$k = i \int^{l_1} B_a \cdot dl, \tag{2}$$

where k is now a summation of infinitesimal terms $B_a \cdot dl \cdot i$ and the integration must be carried out over the total length of wire l_1. Consider now a voice coil of length $2a_1$ as being situated in an air gap and constrained to move axially along the abscissa a with the origin of coordinates being at the longitudinal center of the gap or rest position of the coil. The wire length l varies in direct proportion to the abscissa a.

$$l = \alpha \cdot a.$$

Where α is the factor of proportionality and is independent of a. The force equation can now be written as a function of the abscissa a alone.

$$k = i\alpha \int_{a-a_1}^{a+a_1} B_a da. \tag{3}$$

The experimental set-up consisted of a single turn voice coil whose position could be varied in the dynamic loudspeaker field being tested. In addition, this coil was fastened to a mechanical driving system vibrating with a negligibly small amplitude and at a frequency of about 1000 c.p.s. When vibrated, a voltage was induced in the voice coil which was dependent on the location a and of magnitude given by,

$$u = B_a l_m v \cdot 10^{-8} \text{ volt},$$

with

$$v = A_m \omega \cos \omega t.$$

From this,

$$u_{\text{r.m.s.}} = B_a l_m A_m \omega (10^{-8}/\sqrt{2}) \text{ volt}, \tag{4}$$

where u is the induced voltage, B_a the flux density at position a, l_m the length of winding of the voice coil, and A_m the amplitude of vibration. If the frequency and amplitude are held constant during the measurements then,

$$B_a = \text{const.} \cdot u_{\text{r.m.s.}},$$

i.e., the curve of induced voltage along a gives also the flux density.

A typical curve taken with this apparatus is shown in Fig. 1. By means of Eq. (3) the force k for any given coil displacement can be calculated for any coil form and width. This integration is most easily done graphically and, since only the ratio of the force at any coil position a to the force at the rest position is necessary to determine the nonlinear distortion, the computation can further be simplified by writing (3) in ratio form.

$$\frac{k_a}{k_0} = \frac{i\alpha \int_{a-a_1}^{a+a_1} \text{const.} \cdot u_{\text{r.m.s.}} \cdot da}{i\alpha \int_{-a_1}^{+a_1} \text{const.} \cdot u_{\text{r.m.s.}} \cdot da} = \frac{\int_{a-a_1}^{a+a_1} u_{\text{r.m.s.}} \cdot da}{\int_{-a_1}^{+a_1} u_{\text{r.m.s.}} \cdot da}. \tag{5}$$

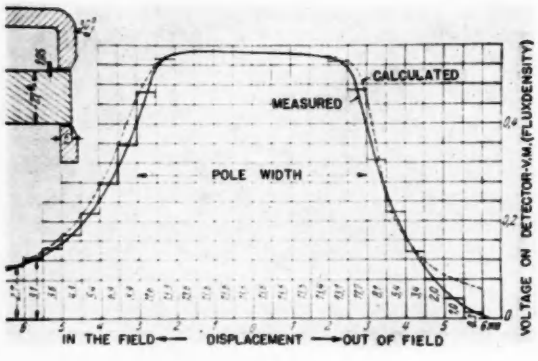

FIG. 1. Variation of flux density in the air gap.

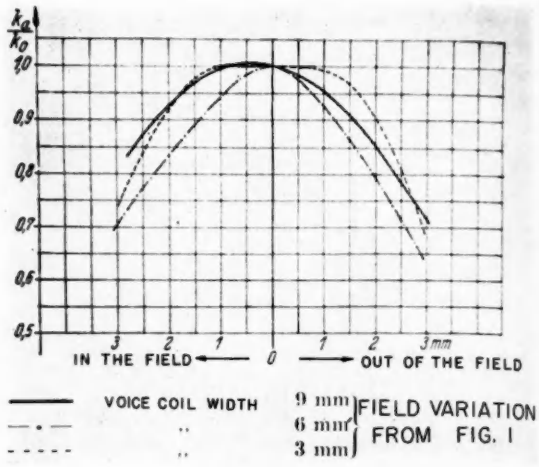

FIG. 2. $k_a/k_0 = f(a)$ for different voice coil widths.

Figure 2 shows results obtained by graphical integration of the curve of Fig. 1 for three different widths of voice coils, namely, broader than, equal to, and less than the width of the pole face of the magnet. From these curves it is seen that for amplitudes up to about 2 mm the smallest distortion will be obtained for coils small compared to the width of the magnetic field. In comparison to this, the curve for a very broad coil is only slightly less favorable, and for large amplitudes is even more satisfactory. The worst possible situation is obtained for a coil having a width equal to that of the pole face.

In the appendix an analytical determination of the curve shown in Fig. 1 was discussed, given the assumptions outlined above and the construction of the magnetic field (shown in cross section in Fig. 1). The calculation was based on the method of conformal representation, and led to the dotted curve of Fig. 1.—L. BERANEK.

Supersonic Phenomena. WILLIAM T. RICHARDS. Rev. Modern Physics, **11**, 36–64 (1939).—A critical study of recent advances. Especial attention is given to the theory of plane waves of sound in media in which the time of adjustment of internal energy states of the molecule must be taken into account. Experimental methods and results for velocity and absorption of sound are considered with critical evaluation of the results by interferometry and by optical methods. Valuable and constructive criteria are advanced for the interpretation of interferometric results, especially with respect to the purity of gases being investigated and the necessity for the removal of the last traces of moisture from the apparatus. The paragraphs on the results of measurement of the dispersion of sound in gases should be noted by any one undertaking work in this field. A closing section treats of the effects of sound waves of large amplitude, consideration being given a great variety of phenomena of interest to the physicist, chemist, engineer and biologist. The classified bibliography of 348 titles should prove of real assistance to any worker in this field.—J. C. Hubbard.

References to Contemporary Papers on Acoustics

MOST of the titles of papers appearing in other languages than English have been translated; Abstracts in English of many foreign papers have appeared or soon will appear in Science Abstracts, Section A. Where references are made to Science Abstracts, the reference is to the volume number and abstract number. The abbreviations of the names of journals are those used in Science Abstracts and can be found in any annual index to those abstracts.

The numbers appearing at the head of each entry are the numbers which identify the subject headings in the Cumulative Index of this journal which is to appear soon.

Compiled with the generous assistance of F. E. Orton, Physics Librarian, University of Michigan.

---

2. Architectural Acoustics

2.3 **Celotex Products are Utilized to Sound-Proof the Perisphere.** Refrigerating Engineering **37**, 264 (1939).

2.4 **Propagation d'ondes Sonores Planes au Voisinage d'un Plan Absorbant.** (Propagation of Plane Sound Waves in the Vicinity of an Absorbent Plane.) J. Brillouin. Rev. d'Acoustique **8**, 97–109 (1939). (See also 11.3.)

2.7 **Distribution of Eigentones at Low Frequencies** R. H. Bolt. Phys. Rev. **55**, 420 (1939). (Abstract only.)

2.7 **Über die Eigentöne von Bäumen mit Nichtebenen Wänden und die Diffuse Schallreflexion.** (Natural Frequencies of Rooms with Irregular Walls and Diffuse Reflection.) E. Skudrzyk. Akustiche Zeits. **4**, 172–186 (1939).

2.10 **La Transmission der Son a Travers les Glaces Simples et les Glaces Doubles.** (The Transmission of Sound Through Single and Double Windows.) L. Renault. Rev. d'Acoustique **8**, 12–46 (1939).

3. Books and Bibliographies

3 **Akustisches Schrifttum in Zeitschift Endes Jahres 1938.** (Acoustical Bibliographies in Periodicals for 1938.) K. Patermann. Akustische Zeits. **4**, 191–207 (1939).

3.0 **Bibliography.** Rev. d'Acoustique **8**, 117–119 (1939).

4. Ear and Hearing

4.1 **Resonance in the External Auditory Meatus.** N. Fleming. Nature **143**, 642–643 (1939).

4.12 **The Construction of a Timbre Test.** Don Lewis. Psychological Record **3**, 115–135, June (1939).

5. Instruments and Apparatus. Applied Acoustics

5.1 **Flammes Excitratrices Pour Signal.** (Sensitive Flames.) Z. Carriére. Rev. d'Acoustique **8**, 47–78 (1939).

5.1 **Construction, Performance, and Design of the Acoustic Air-Jet Generator.** J. Hartmann. Journ. Sci. Instruments **16**, 140–149 (1939).

5.2 **Amplitude Limiters and Auto-Regulating Systems in Communication Technique.** M. Nuovo. Ricerca Scientifica 10th yr. 261–270 (1939).

5.2 **Wave-Shape Plots for Checking Amplifier Distortion.** QST **5**, 50–51 (1939).

5.2 **Reflexed Amplifiers.** S. J. Watson. A. W. A. Techn. Rev. **4**, 35–50, Jan. (1939).

5.8 **Sound Diffusers in Loud Speakers.** J. de Boer. Philips Techn. Rev. **4**, 144–148 (1939).

5.8 **A Loudspeaker System for High-Quality Broadcasting.** S. A. Waite. Communications **19**, 12–13; 45 (1939).

5.8 **Electroacoustics.** Phys. Soc., Proc. **51**, 359–375 (1939). Sci. Abs. **A42**, 2173 (1939).

5.9 **Combination Oscillations and Dying-Out Processes of the Carbon-Microphone Diaphragm.** K. Braun. T.F.T. **28**, 104–109 (1939). Abs. Wireless Engineer **16**, 2816 (1939).

5.9 **Piezoelectricity in Electro-Acoustics.** C. Crescini. Radio e Televiscone **3**, 236–245 (1939). (In Italian.)

5.10 **An Integrating Altimeter for Aerological Soundings.** J. Lugeon. Comptes Rendus **208**, 1327–1329 (1939).

5.13 **Lagoon of Nations Sound System.** Electronics **12** No. 7, 26–28 (1939).

5.13 **Absorption Limits for Interference Nodes in Rooms.** M. Rettinger. Soc. Mot. Pict. Engineers, J. **32**, 518–526, May (1939).

5.15 **Equipment for Automatic Measurement of Audio-Frequency Circuits Developed by the Columbia Broadcasting System.** I. R. E., Proc. **27**, Sup. 2 (1939).

5.16 **Some Brief Experiments on the "Almite" Gramophone Record.** A. Miyata. Japanese Journ. Phys. Transactions and Abstracts. **13** Abstract p. 3 (1939).

5.16 **New Reproducing System.** I. M. R. C. Duotrac. El. Rev. **124**, 607 (1939).

5.16 **Lateral Disc-Recording for Immediate Playback with Extended Frequency and Volume Range.** H. J. Hasbrouch. I. R. E., Proc. **27**, 184–187 (1939).

5.16 **A New System of Sound Recording and Reproduction, and Sound Reproduction on Paper.** Internat. Marine Radio Company: Skvortsov. Electrician **122**, 556; 567 (1939).

5.16 **Semi-Professional Recorder.** M. P. O'Hara. Radio News **21**, 37–39 (1939).

5.16 **Acoustic Spectra Obtained by the Diffraction of Light from Sound Films.** D. Brown. Phys. Soc., Proc. **51**, 549 (1939).

5.16 **Synthetic Sound.** J. F. Schouten. Philips Techn. Rev. **4**, 167–173 (1939).

5.16 **Electric Gramophone.** M. G. Scroggie. Wireless World **44**, 432–436 (1939).

5.16 **A Simple Apparatus for Sound Recording.** K. de Boer and A. Th. van Urk. Philips Techn. Rev. **4**, 106–113 (1939).

5.16 **A Sound-Track Projection Microscope.** G. M. Best. Soc. Mot. Pict. Engineers, J. **33**, 198–202 (1939).

5.16 **Further Improvements in Light-Weight Record Reproducers, and Theoretical Considerations Entering into Their Design.** A. L. Williams. Soc. Mot. Pict. Engineers, J. **33**, 203–223 (1939).

5.16 **A 16 mm Studio Recorder.** R. W. Benfer. Soc. Mot. Pict. Engineers, J. **32**, 534–539 (1939).

5.16 **New Sound Recording Equipment.** D. R. Canady and V. A. Wellman. Soc. Mot. Pict. Engineers, J. **32**, 544–549 (1939).

5.16 **New Piezoelectric Devices of Interest to the Motion Picture Industry.** A. L. Williams. Soc. Mot. Pict. Engineers, J. **32**, 552–557 (1939).

5.16 **Report on Recent Activities of the Research Council Committee on Standardization of Theatre Sound Projection Equipment Characteristics.** J. K. Hilliard. Soc. Mot. Pict. Engineers, J. **32**, 610–630 (1939).

5.16 **Sound Picture Recording and Reproducing Characteristics.** D. P. Loye and K. F. Morgan. Soc. Mot. Pict. Engineers, J. **32**, 631–647 (1939).

5.16 **Analysis and Measurement of Distortion in Variable-Density Recording.** J. S. Frayne and R. R. Scoville. Soc. Mot. Pict. Engineers, J. **32**, 648–673 (1939).

6. Musical Instruments and Music

6.1 **Orchestral Pitch.** B. van der Pol and C. C. J. Addink. Wireless World **44**, 441–442 (1939).

6.1 **Analysis of Musical Sounds.** A. Dammann. Comptes Rendus **208**, 1283–1285 (1939).

6.1 **International Standard of Concert Pitch.** G. W. C. Kaye. Nature **143**, 905–906 (1939). Sci. Abs. **A42**, 2965 (1939).

6.7 **An Experimental Electronic Violin.** L. H. Stauffer. J. of Applied Physics **10**, 96–100 (1939).

7. Noise

7.1 **Noise at Telephone Locations.** D. F. Seacord. Bell Lab. Record **17**, 306–308 (1939).

7.7 **Eliminating Wind Thresh; Use of Rubber in Automobiles.** Automobile Engineer **29**, 98–100 (1939).

8. Standards

8.1 **Progress Reported in AIEE Conference on Sound Measurement.** Electrical Engineering **58**, 220–221 (1939).

9. Speech and Singing

9.6 **Synthetic Speaker.** H. Dudley, R. R. Riesz and S. S. A. Watkins. Frank. Inst., J. **227**, 739–764 (1939). Sci. Abs. **A42**, 2963 (1939).

10. Supersonics. (Ultrasonics)

10.1 **Supersonics.** Electrician **122**, 411–12; 445–6; 477–8; 507–8; 543–4 (1939).

10.1 **Generation of High Power at Ultrahigh Frequencies by Means of Back-Coupling.** M. Kobayashi and H. Nisio. Nippon Elect. Comm. Eng. **14**, 493–498 (1938). Sci. Abs. **B42**, 1240 (1939).

10.2 **Influence of Supersonic Vibrations on Rotatory Power of High-Molecular Substances. Part I. Gelatin Solutions.** N. Sata. Kolloid Zeits. **87**, 186–190 (1939). Sci. Abs. **A42**, 2962 (1939).

10.2 **Supersonic Dispersion and Infra-Red Radiation.** Richardson. Nature **143**, 638–639 (1939).

10.2 **Diffraction of Light by Supersonic Waves. Part I.** K. N. Rav. Indian Acad. Sci., Proc. **9A**, 422–446 (1939). Sci. Abs. **42A**, 2960 (1939).

10.2 **The Fresnel Diffraction Phenomenon with Supersonic Waves and Its Evaluation by Mascart's Method.** F. Mahler. Ann. d. Physik **34**, 689–716 (1939).

10.4 **Effect of Ultrasonic Waves on the Discharge Potential of Hydrogen.** R. Piontelli. Atti Della Reale Accademia Nazionale dei Lincei. Pendiconti, Classe d'Scienze, Fische, Mathematiche e Naturali. **27**, 1–75 (1938).

10.4 **Absorption of Sound in CO_2 and Mixtures.** A. van Itterbeek, P. de Bruyn and P. Mariëns. Physica **6**, 511–518 (1939). Sci. Abs. **A42**, 2966 (1939).

10.4 **Supersonic Velocity in Gases and Vapors. V. Heat Capacity of Vapors of Acetone, Benzene, Cyclohexane, Hexane and Methyl, Ethyl and Propyl Ethers.** S. K. Kulkarni Jatkar. Indian Inst. of Science, J. **22A**, 19–37 (1939).

10.4 **Supersonic Velocity in Gases and Vapors. VI. Specific Heats of the Vapors of Alcohols and Ethyl Acetate.** S. K. Kulkarni Jatkar. Indian Inst. of Science, J. **22A**, 39–58 (1939).

10.4 **Remarks on the Anomalous Damping of Ultrasonic Waves.** O. Halpern. Phys. Rev. **55**, 881 (1939).

10.4 **Measurement of the Absorption of Supersonic Waves in Air and Argon, and Application of Töpler's Method to the Measurement of Supersonic Absorption in Air.** Dadaian and Pumper. Korolev. Comptes Rendus (Doklady) de l'Acad. des Sciences, U. S. S. R. **20**, 539–542; 545–46 (1938). (In French and English.)

10.5 **Dispersion of Supersonic Velocity in Liquids.** K. G. Krishnan. Indian Acad. Sci., Proc. **9A**, 382–385 (1939). Sci. Abs. **42A**, 2959 (1939).

10.5 **Über die Dispersion des Ultraschalls in Flüssigheiten** (Dispersion of Supersonics in Liquids). F. Matossi. Phys. Zeits. **40**, 294–297 (1939).

10.5 **Absorption of Supersonic Waves in Water and in**

Aqueous Suspensions. G. K. HARTMAN AND A. B. FOCKE. Phys. Rev. **56**, 217(A) (1939).

10.5 **Supersonic Velocity and Adiabatic Compressibility of Liquids.** S. BHAGAVANTAM AND C. V. J. RAO. Indian Acad. Sci., Proc. **9A**, 312–315 (1939). Sci. Abs. **42A**, 2958 (1939).

10.6 **Zur Werkstüchprüfung mittels Ultraschalls** (Metal-Testing by Supersonics). F. KRUSE. Akustische Zeits. **4**, 153–168 (1939).

10.6 **The Ultrasonic Method for the Determination of the Elastic Properties of Solids.** H. LUDLOFF. Phys. Rev. **55**, 593–594; 681 (1939) (Abstracts).

10.6 **The Dispersion of Supersonic Wands in Cylindrical Rods of Polycrystalline Silver, Nickel and Magnesium.** S. K. SHEARARD AND A. B. FOCKE. Phys. Rev. **56**, 217(A) (1939).

10.6 **Supersonic Method of Measurement of Certain Elastic Adiabatic Constants of Crystals.** E. BAUMGARDT. Comptes Rendus **208**, 1280–1282 (1939).

10.9 **Absorption of Supersonic Waves in Human Tissues and Its Variation with Frequency.** R. POHLMAN. Phys. Zeits. **40**, 159–161 (1939). Sci. Abs. **A42**, 2169 (1939).

11. WAVES AND VIBRATIONS

11.3 **Absorption of Sound in Strong Electrolytes.** M. LEONTOVICH. Journal of Experimental and Theoretical Physics (USSR) **8**, 40–51 (1938).

11.3 **Periodic Variation of Temperature Caused by Sound Waves.** T. HAYASHI. E. T. J. **3**, 103–106 (1939). Sci. Abs. **A42**, 2957 (1939).

11.3 **Propagation d'ondes Sonores Planes au Voisinage d'un Plan Absorbant.** (Propagation of Plane Sound Waves in the Vicinity of an Absorbent Plane.) J. BRILLOUIN. Rev. d'Acoustique **8**, 97–109 (1939). (See also 2.4.)

11.3 **Die Wahre Schallgeschwindigkeit in Luft.** (True Velocity of Sound in Air.) H. KENSER. Ann. d. Physik **34**, 665–668 (1939) .Sci. Abs. **A42**, 2167 (1939).

11.3 **Propagation of Sound in Disperse Systems.** S. M. RYTON *et al.* Journal of Experimental and Theoretical Physics (USSR) **8**, 614–621 (1938).

11.5 **Zur Deutung der Knallwellen-Ausbreitung an der Trennschicht Zweier Medien.** (Explanation of the Propagation of Explosion Waves at the Boundary between Two Media.) G. JOSS AND J. TELTOW. Wireless Engineer **16**, 2642(A) (1939).

11.6 **Le Tuyau Acoustique Comme Filtre Passe-Hant.** (The Acoustic Tube as High Pass Filter.) L. BRILLOUIN. Rev. d'Acoustique **8**, 1–11 (1939).

11.7 **Combination Tones in Sound and Light.** W. H. BRAGG. Roy. Inst., Proc. **30**, 424–433; Nature **143**, 542–545 (1939). Sci. Abs. **42A**, 2587 (1939).

11.7 **Periodic Analysis of Seismic Waves, and Problems Connected Therewith.** P. CALVI. Ricerca Scientifica 10th yr. 275–290 (1939).

11.7 **Sine Wave Oscillations with the Habann Tube.** K. LÄMMCHEN AND L. MÜLLER. E. N. T. **16**, 37–42 (1939).

11.7 **Damping of Flat Impulses of Small Amplitude.** I. M. SHMUSHKEVICH. J. Techn. Phys. **8**, 2168–2174 (1938), (In Russian). Wireless Engineer **16**, 2812(A) (1939).

11.7 **Excitation of Chladni Figures.** L. SIBAIYI. Indian Journ. Phys. **12**, 407–408 (1938). Sci. Abs. **A42**, 2165 (1939).

11.7 **Reseaux Filtrants a Cellules Indefiniment Croissantes ou Decroissantes.** (Filters with Openings Indefinitely Increasing or Decreasing.) J. BRILLOUIN. Rev. d'Acoustique **8**, 70–96 (1939).

11.7 **Eigenschwingung und Dämpfung von Gasblasen in Flüssigkeiten.** (Natural Frequencies and Damping of Gas Bubbles in Liquids.) E. MEYER AND K. TAMM. Akustische Zeits. **4**, 146–52 (1939).

11.7 **Ultradynamische Lissajous-Figuren.** (Anharmonic Lissajous Figures.) H. E. HOLLMANN. Hochfrequenztechn. u. Elektroakustik **54**, 19–30, July, 1939.

THE AMERICAN INSTITUTE OF PHYSICS

INCORPORATED

ADMINISTRATIVE STAFF

HENRY A. BARTON, *Director*

MADELINE M. MITCHELL, *Publications Manager*

Offices: 175 Fifth Avenue, New York, New York

JOURNALS

THE PHYSICAL REVIEW
REVIEWS OF MODERN PHYSICS
JOHN T. TATE, *Editor*
J. W. BUCHTA, *Assistant Editor*

JOURNAL OF APPLIED PHYSICS
ELMER HUTCHISSON, *Editor*

THE JOURNAL OF THE OPTICAL SOCIETY OF AMERICA
THE REVIEW OF SCIENTIFIC INSTRUMENTS
F. K. RICHTMYER, *Editor*

JOURNAL OF THE ACOUSTICAL SOCIETY OF AMERICA
FLOYD A. FIRESTONE, *Editor*

THE JOURNAL OF CHEMICAL PHYSICS
HAROLD C. UREY, *Editor*
JOSEPH E. MAYER, *Assistant Editor*

THE AMERICAN PHYSICS TEACHER
DUANE ROLLER, *Editor*

GOVERNING BOARD

For The American Physical Society:

JOHN T. TATE, *Chairman*
University of Minnesota

GEORGE B. PEGRAM, *Secretary*
Columbia University

KARL T. COMPTON
Massachusetts Institute of Technology

For The Optical Society of America:

E. C. CRITTENDEN
National Bureau of Standards

A. C. HARDY
Massachusetts Institute of Technology

W. B. RAYTON
Bausch & Lomb Optical Company

For The Acoustical Society of America:

FLOYD A. FIRESTONE
University of Michigan

HARVEY FLETCHER
Bell Telephone Laboratories

WALLACE WATERFALL
The Celotex Corporation

For The Society of Rheology:

WHEELER P. DAVEY
Pennsylvania State College

MELVIN MOONEY
United States Rubber Products, Inc.

R. L. PEEK, JR.
Bell Telephone Laboratories

For The American Association of Physics Teachers:

PAUL E. KLOPSTEG
Central Scientific Company

FREDERIC PALMER, JR.
Haverford College

F. K. RICHTMYER
Cornell University

The American Institute of Physics is a membership corporation of which five societies are the founding members. These five societies are the principal national societies devoted to pure and applied physics in America. Their names, and those of their representatives who form the Governing Board of the Institute, are given above. The principal work of the Institute is the publication of journals sponsored by the societies or by itself. The names and the editors of the journals are also listed above.

The broad purpose of the Institute is to represent, in all matters of wide or common interest, the five thousand or more members and subscribers associated with the Founder Societies and the journals. It aims to advance the science and profession of physics, and to promote cooperation between pure research, the applied sciences and the industries. To achieve these aims, it is greatly in need of an endowment and is empowered by law to administer grants and funds of any kind.

This number of THE JOURNAL OF THE ACOUSTICAL SOCIETY OF AMERICA
was issued October 11, 1939

LANCASTER PRESS, INC., LANCASTER, PA.